Evaluation of Active Acoustic Methodology in Diagnosis of Pleural Effusion

by
Hamed Minaei Zaeim

Thesis presented in fulfilment of the requirements for the degree of Master *of Engineering in the Faculty of Engineering at Stellenbosch University*

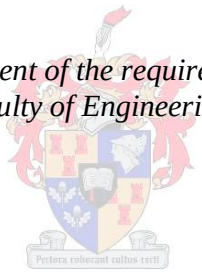

Supervisor:
Prof. Cornie Scheffer
Dr. Mike Blanckenberg

March 2013

Declaration

By submitting this thesis electronically, I declare that the entirety of the work contained therein is my own, original work, that I am the sole author thereof (save to the extent explicitly otherwise stated), that reproduction and publication thereof by Stellenbosch University will not infringe any third party rights and that I have not previously in its entirety or in part submitted it for obtaining any qualification.

Signature:.....

H. Minaei Zaeim

Date: .....March 2013.....

Abstract

Pleural effusion is a common respiratory condition that is characterized by an abnormal collection of fluid in the lung cavity. In this study, an innovation using the transmission of sound into the respiratory system as a novel tool to detect fluid in the lung was developed. First, the method was evaluated on a phantom model of a lung. Based on the results of this test model, the appropriate technique was used in a clinical study. This method has several advantages, such as that is non-invasive, low cost, and easy for clinical review.

Two techniques, including analysis of the frequency response of the model and the transient time of transmitted sound in the lung, were evaluated in the phantom models of the human lung. Two phantom models with similar geometry to the human lung, including a healthy model (without fluid in the model) and a pleural effusion model (with bulk of fluid in the model) were developed. These models have acoustical properties similar to the lung parenchyma. To obtain the frequency responses of the model, a sine sweep signal was transmitted into the model and the frequency response of the model was then calculated using the fast Fourier transform. The transient time of the transmitted sound was calculated using a cross correlation method. The results show that the locations of fluid in the model were detectable using both techniques. However, the transient time technique is better than the frequency response technique because it is simple, fast, and has potential for use in a clinical enviorment.

Based on the results obtained from the phantoms, the transient time method was performed on both 22 healthy participants and four patients diagnosed with pleural effusion. To perform this technique on human subjects, a data acquisition system was developed. Two types of sound, including a complex chirp sound and a polyphonic sound, were transmitted into the respiratory systems of the participants. The time delay between a reference microphone, located on the trachea of the subject, and eight microphones attached to the chest was computed using a cross correlation method, and the effect of inhalation and lung size on the transient time of transmitted sound on the healthy subject was evaluated. The results show that using transmission of sound in the lung is a promising technique in the diagnosis of pleural effusion.

Opsomming

Pleurale effusie is ’n algemene respiratoriese toestand wat gekenmerk word deur ’n abnormale versameling van vloeistof in die longholte. In hierdie studie is ’n innoverende manier ontwikkel om vloeistof in die long met behulp van die transmissie van klank te bespeur. Die metode is eers op ’n fantoommodel van ’n long geëvalueer. Op grond van die resultate van hierdie toetsmodel is die geskikte tegniek in ’n kliniese studie gebruik. Hierdie metode het verskeie voordele, soos dat dit ingreepsvry is, nie duur is nie en kliniese evaluering moontlik maak.

Twee tegnieke, naamlik ontleding van die frekwensierespons van die model en die oorgangstyd van versende klank in die long, is in die fantoommodel van die menselong geëvalueer. Twee fantoommodelle met soortgelyke geometrie aan die menselong, met inbegrip van ’n gesonde model (sonder vloeistof in die model) en ’n pleurale-effusie-model (met ’n massa vloeistof in die model), is ontwikkel. Hierdie modelle het akoestiese eienskappe soortgelyk aan die longparenchiem. Om die frekwensieresponse van die model te verkry, is ’n sinuskrommesein tot in die model versend. Die frekwensierespons van die model is met behulp van die vinnige Fourier-transformasie bereken. Die oorgangstyd van die versende klank is deur ’n kruiskorrelasie-metode bereken. Die resultate toon dat die ligging van die vloeistof in die model met albei tegnieke bespeur kan word. Die oorgangstyd-tegniek is egter beter as die frekwensierespons-tegniek, aangesien dit eenvoudig en vinnig is en maklik in ’n kliniese omgewing gebruik kan word.

Op grond van die resultate wat van die fantome verkry is, is die oorgangstyd-metode op 22 gesonde deelnemers en vier pasiënte wat met pleurale effusie gediagnoseer is, uitgevoer. ’n Dataverkrygingstelsel is ontwikkel ten einde hierdie tegniek op proefpersone uit te voer. Twee soorte klank, naamlik ’n komplekse tjirpgeluid en ’n polifoniese klank, is na die respiratoriese stelsels van die deelnemers versend. Die tydvertraging tussen ’n verwysingsmikrofoon in die tragea van die proefpersoon en agt mikrofone wat aan die bors vasgeheg is, is met ’n kruiskorrelasie-metode bereken, en die uitwerking van inaseming en longgrootte op die oorgangstyd van versende klank op die gesonde proefpersone is geëvalueer. Die resultate toon dat die gebruik van transmissie van klank in die long ’n belowende tegniek vir die diagnose van pleurale effusie is.

Acknowledgements

I would like to express my sincere thanks to the following people:

- My parents for all their love and encouragement over the course of my studies.
- My sister and my brother for all their support through the tough times.
- Prof. Cornie Scheffer, my supervisor, for his unfailing leadership and support during the entire project and Dr. Mike Blanckenberg, my co-supervisor, for all his sound advice, patience and guidance throughout the project.
- Dr. Kiran Dellimore for his advice and support during the project

Dedication

To my lovely parents

Contents

List of figures

List of tables

Nomenclature

Abbreviation	Description
AAM	Active acoustic methodology
AIDS	Acquired immunodeficiency syndrome
BMI	Body mass index
CCF	Cross correlation function
CORSA	Computerized respiratory sound analysis
CT	Computer tomography
EC	European community
FFT	Fast Fourier transform
FIR	Finite impulse response
HPF	High pass filter
HRC	Human research committee
IDW	Initial deflection width
LPF	Low pass filter
PAM	Passive acoustic methodology
RLS	Recursive least square
SNR	Signal to noise ratio
TB	Tuberculosis
TDW	Total deflection width
VRI	Vibration resonance imaging
WTO	World health organization
2CD	Two-cycle duration

Symbol	Description
C	Capacitor
Co_2	Carbon dioxide
dB	Decibels
Hz	Hertz

mm	Millimetre
ms	Millisecond
O_2	Oxygen
R	Resistor
S	Second
V	Volt
Λ	Forgetting factor
µ	Micro (10^{-6})
σ	Input variance

1. Introduction

1.1 Background

Auscultation, which is the term for listening to the internal sounds of body is one of the oldest techniques used to diagnose diseases [1] . Before the invention of the stethoscope in 1819 by Laennec, auscultation was performed by physicians by placing their ears directly on the patient's chest or abdomen [2]. From 1819, stethoscopes have been used to examine cardiovascular [3], respiratory [4] and gastrointestinal systems [5]. In the past, stethoscopes have been used as an initial instrument for diagnosis, after which, respiratory diseases are confirmed by methods such as x-ray, computed tomography (CT) scans, spirometry and blood pressure measurement. These are more accurate diagnostic techniques.

Although stethoscopes are used widely, this technique has several limitations, one of which is that physicians listen to many auscultation points on the chest of a patient's body using stethoscopes. At each of the auscultation points, physicians ask patients to perform inhalation and then exhalation. Patients may try to hide their disease by forcing themselves to breathe normally in order to convince the physician that they are healthy [6]. Another problem with stethoscopes is that they can sometimes cause misdiagnosis of diseases because of variability in physicians, auditory training. Furthermore, variable techniques in applying a stethoscope to the patient and variability of respiratory sounds between points greatly affect the sound perceived by the physicians [7].

Over the past few decades, electronic stethoscopes have been developed to measure the lung sounds on a computer. One of the advantages of using multiple-digital electronic stethoscopes is that respiratory sounds from different locations of the chest wall can be analysed, monitored and recorded in the computer instantaneously. These sounds can then be played back or analysed by signal processing techniques to diagnose different types of disease. Currently, multiple-digital electronic stethoscopes are used to diagnose cardiovascular and pulmonary diseases [8].

Generally, capturing lung sounds using multiple- digital stethoscopes can be divided into two main categories: passive acoustic methodology (PAM) and active acoustic

methodology (AAM). In PAM, several electronic stethoscopes are attached to the chest of a patient. Lung sounds are recorded during the procedure. PAM is a dynamic method and it can show the functional properties of diseases [9, 10]. The method has been performed in several studies to aid in the monitoring and diagnosis of respiratory disease. In AAM, which is the subject of this study, low frequency sound (normally below 1 KHz) is transmitted into the respiratory system by a loudspeaker introduced into a patient's mouth, for detection on the chest surface. In this technique, the time delay and frequency response of the lung are calculated to better understand the sound propagation into the respiratory system, as well as the static or even dynamic properties of lung parenchyma [11].

1.2 Problem statement

Sound propagation through the respiratory system is complex, because of the complex structure of the respiratory system, in which there exist several pathways to the thoracic cage wall [12]. Propagation of sound in the parenchyma tissue is also complicated; the parenchyma can be represented as a homogenous mixture of gas and tissue [13], and the density of parenchyma tissue changes during the inspiration and expiration. In this study, the evaluation of the transmission of sound through the respiratory system of the lung was performed as a novel technique for detecting pleural effusion (fluid in the lung), using multiple-digital electronic stethoscopes on the patient's chest.

Since the AAM is a novel technique for the diagnosis of pleural effusion, several challenging problems need to be addressed. The main challenges of this research are to investigate the best technique as well as the best data analysis method to detect fluid in the respiratory system by performing the AAM on human subjects. Another challenge in this study is to overcome the high attenuation level of the propagation sound wave in the lungs.

1.3 Clinical motivations

Pleural effusion is a common respiratory condition which is characterized by the abnormal collection of fluid (between 30 ml and 2500 ml) in the pleural cavity [14]. Each year over one million patients are diagnosed with pleural effusion in the United States [15]. The most frequent causes of pleural effusion in the USA are, in order of frequency, congestive heart failure, pneumonia and cancer [16]. However, the most common cause of

pleural effusion in developing countries is tuberculosis (TB), followed by congestive heart failure [17]. South Africa has one of the highest incidences of tuberculosis and HIV in the world [18]. According to the World Health Organization (WHO), South Africa ranked 9th on the list of 22 countries affected by TB [19]. Moreover, pleural effusions are frequently encountered in patients with Acquired Immunodeficiency Syndrome (AIDS). One hospital study showed that plural effusion could be found in 27% of patients with HIV in the hospital [20]. Furthermore, pleural effusion has a high rate of mortality, which varies between 10% and 40%, depending on the causes [21].

Typically, pleural effusion is diagnosed using a combination of medical history and physical examination, and confirmed by posteroanterior and lateral chest radiographs, chest x-ray, computed tomography or ultrasonic examination. However, most of these techniques are expensive and are impractical in rural areas. Using the AAM to detect pleural effusion has several advantages, including being non-invasive, low cost, simple, safe, easy to operate for routine check ups and suitable for use in low resource (e.g. rural) settings.

1.4 Objectives

The objective of this thesis is to investigate the diagnosis of pulmonary diseases by using sound transmission into the lungs. Evaluating AAM in the diagnosis of pleural effusion by using multiple-digital electronic stethoscopes is the main goal of the study. To achieve this, additional aims included:

- Development of a phantom model of the human lungs based on the acoustic characteristics of the human lung to investigate the hypothesis on the model, as well as to find the best range of frequencies for transmission.
- Development of the experimental apparatus used to perform sound transmission into the lung.
- Using AAM to find parameters which can be used in the diagnosis of pleural effusion by testing at least four patients who have been diagnosed with pleural effusion and are currently undergoing treatment, and 22 healthy patients who have been examined and classified as healthy and have no respiratory disease.

- Development of techniques to use in the detection of fluid in the lungs in clinical trials. The technique should be non-invasive, simple and suitable for use in low resource (rural) settings.

1.5 Thesis outline

A brief background to auscultation and current techniques using multiple digital stethoscopes in respiratory sound analysis is presented in Chapter one. The problem statement, clinical motivations and objective are also provided.

Chapter two contains the literature studies into the pathology of pleural effusion as well as current methods of diagnosis and treatment. This is followed by detailed research into current methods of passive acoustic methodology in the diagnosis of respiratory diseases, especially in diagnosis of pleural effusion. Detailed research into active acoustic methodology over the last few decades as well as all previous studies which used this method of diagnosis of disease, are also discussed in Chapter two.

In Chapter three, the development of the phantom model of the human lungs is presented. The evaluation of using frequency responses as a technique to aid detection of fluid in the model, which includes the methods, data analysis, results and discussion are described. The innovation of using the transient time of applied sound in the lung as a tool to aid to detect fluid, which is also followed by methods, data analysis and discussion, are presented.

Chapter four contains an evaluation of the use of active acoustic methodology in clinical trials. The development of data acquisition systems for use in clinical trials is also presented. Furthermore, the test locations used for the obtaining data and in clinical trials and data acquisition procedure are discussed. Chapter four continues with a data analysis method to calculate the time delay, and the effect of inhalation and the size of the lung on the time delay. A case study using active acoustic methodology in diagnosis of effusion is presented.

Chapter five concludes the thesis with the significant results and finding of this study as well as recommendations for future research.

2. Literature review

2.1 Overview of the anatomy of the human respiratory system

Since pleural effusion affects the respiratory system, it is essential to understand the anatomy and physiology of the human respiratory system, as well as the pathophysiology of pleural effusion. This information is necessary to better understand the origin of lung sounds as used by physicians in the auscultation procedure.

The major function of the respiratory system is to supply oxygen to the blood and to expel waste gases, of which carbon dioxide is the main constituent, from the body. The supply of O_2 and removal of CO_2 is achieved by a mechanical process known as the respiration process, which has two parts: Inspiration (inhalation of atmospheric air into the lung via the nose and mouth) and expiration (exhalation of carbon dioxide). Moreover, the respiratory system has a major role in controlling normal blood pH and body temperature.

During inspiration, air enters into the respiratory system through the mouth and nose. From the pharynx, the air passes to the larynx, commonly called the voice box, to enter the trachea (windpipe). After the air moves from trachea, it passes to the left and right bronchi, which are divided into increasingly smaller branches called bronchioles. Bronchioles also further divide into alveolar sacs, which contain alveoli. In humans, the two lungs contain approximately 700 million alveoli, representing a total surface area of over 70 m^2 [22]. The anatomy of the respiratory system is shown in Figure 1.

Gas exchange occurs by diffusion between the alveoli and a capillary network within the alveolar wall. The walls of alveoli are extremely thin (approximately 2 µm). Consequently, the oxygen molecules and carbon dioxide can diffuse through the wall. After inhalation, the concentration of oxygen molecules increases rapidly in the alveoli. The oxygen diffuses from the alveolus to the bloodstream, moving from a region of higher concentration to a region of lower concentration. The carbon dioxide also diffuses in the opposite direction, from the capillary to the alveoli [22, 23].

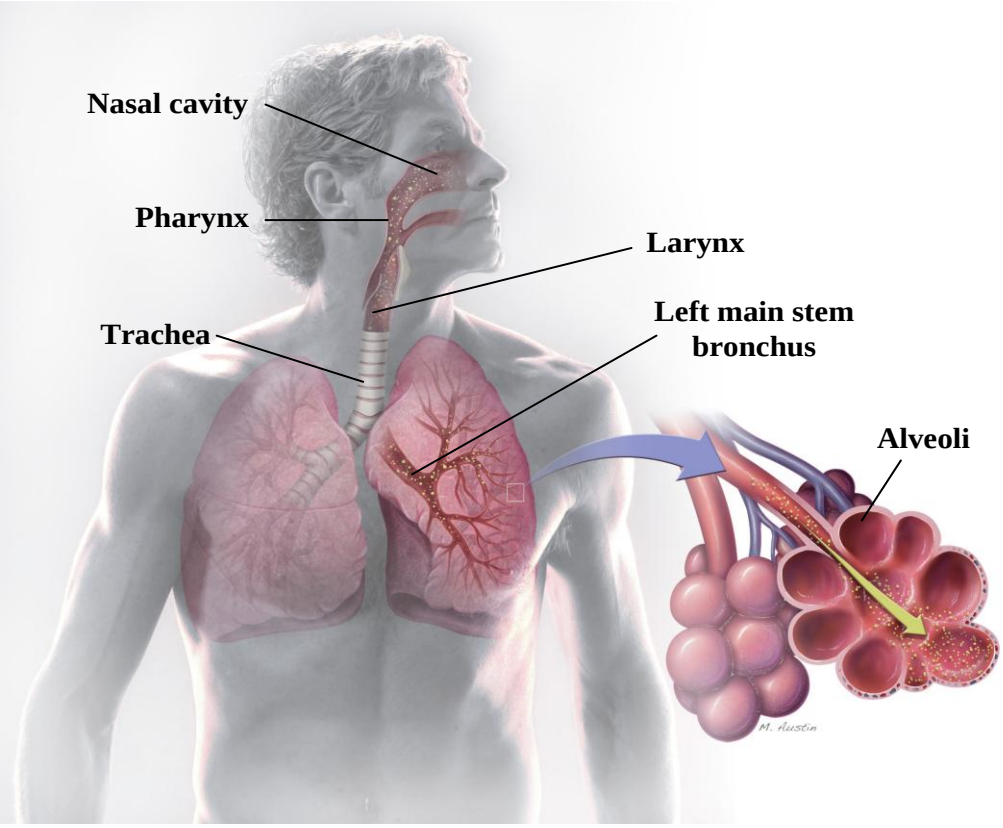

Figure 1. Anatomy of respiratory system, ©Mike Austin, medical illustrator [24]

The pleura is the serous membrane that covers the lung parenchyma, the mediastinum, the diaphragm and the rib cage. The pleura is divided into visceral pleura and parietal pleura. Visceral pleura covers the entire surface of the lung and the parietal pleura covers the entire surface of the thoracic cage. The pleural cavity is the thin space between two pleural layers and it normally contains pleural fluid. The thin layer of fluid acts as a lubricant and allows the visceral pleura to slide along the parietal pleura during the respiration movement. The total amount of fluid in a non-smoking person is 0.26± 0.1, ml/kg which is expressed per kilogram of body mass [25, 26]. The thickness of the pleural space varies from 5 to 27 µm [23]. The anatomy of the pleura is displayed in Figure 2.

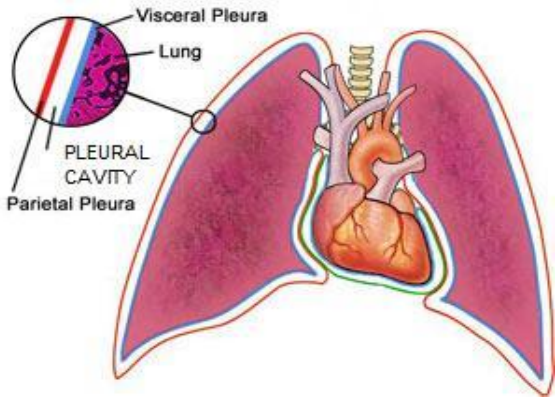

Figure 2. Anatomy of pleura [27]

2.3 Overview of pleural effusion

This section provides of an overview of pleural effusion, including the pathology, symptoms, etiology, and current treatment. Pleural effusion is an abnormal collection of fluid in the pleural space. In a healthy person without any respiratory diseases, a small amount of fluid (0.01 ml/kg/h) constantly enters the pleural space from capillaries, and exactly the same amount of fluid is absorbed by the lymphatic system in the parietal pleura. However, in the person diagnosed with pleural effusion, the rate of pleural fluid formation exceeds the rate of plural fluid absorption. Therefore, the pleural fluid accumulates in the pleural space.

2.3.1 Pathology of pleural effusion

Pleural effusion can broadly be classified into two types: transudative pleural effusion and exudative pleural effusion. Transudative pleural effusion is caused by an imbalance between hydrostatic and oncotic pressure [1][26]. Therefore, fluid leaks from blood vessels into the pleural space. The most common cause of transudative pleural effusion is congestive heart failure, cirrhosis, and pulmonary embolism. By contrast, the exudative is an inflammation fluid which is leaking between cells. Pleural effusion occurs because of alterations in the local factors that influence the formation and absorption of pleural fluid, such as those caused by lung infections, tuberculosis, bacterial pneumonia, pulmonary embolism, breast cancer and lung cancer [26, 28]. A summary of the causes of pleural effusion is shown in Table 1.

[1] osmotic pressure is exerted by proteins in the blood plasma, and usually tends to pull water into the circulatory system.

Table 1. Summary of causes of pleural effusion [26]

Trasudative pleural effusion	Exudative pleural effusion
congestive heart failure	lung infections
cirrhosis with ascites	tuberculosis
pulmonary embolism	bacterial pneumonia
peritoneal dialysis	pulmonary embolism
superior vena cava obstruction	breast cancer
early mediastinal malignancy	lung cancer

2.3.2 Symptoms

The symptoms of pleural effusion are neither sensitive nor specific and some patients may have no symptoms [29]. However, the common symptoms of pleural effusion are:

- Cough**:** Many patients with a pleural effusion have a dry, non-productive cough, a consequence of inflammation of the pleurae or compression of the bronchial walls
- Dyspnea: (shortness of breath) is a common symptom of pleural effusion. Dyspnea occurs because of a combination of a restrictive lung defect, a ventilation perfusion mismatch, and a decrease in cardiac output.
- Chest pain**:** occurs because of the irritation of pleural lining of the lung. The pain is usually described as a sharp pain, worsening with a deep breath. As the pleural effusion increases in amount, the pain may increase.

2.3.3 Current diagnostic approach

Diagnosis of pleural effusion is normally accomplished by a combination of medical history and physical examination, confirmed by posteroanterior and lateral chest radiographs, chest x-ray or computer tomography (CT) scan. If the accumulated fluid is more than 300 ml, there are usually detectable clinical signs in the patient, such as decreased movement of the chest on the affected side, a stony dullness to percussion over the fluid, diminished breath sounds on the affected side and decreased vocal resonance. Usually, to confirm the presence of pleural effusion, posteroanterior and lateral chest radiographs are used. However, if doubts exist, chest x-ray or ultrasound or a computer tomography (CT) scan will be used to

differentiate pleural fluid from pleural thickening [30]. An X-ray picture of a person with pleural effusion is shown in Figure 3.

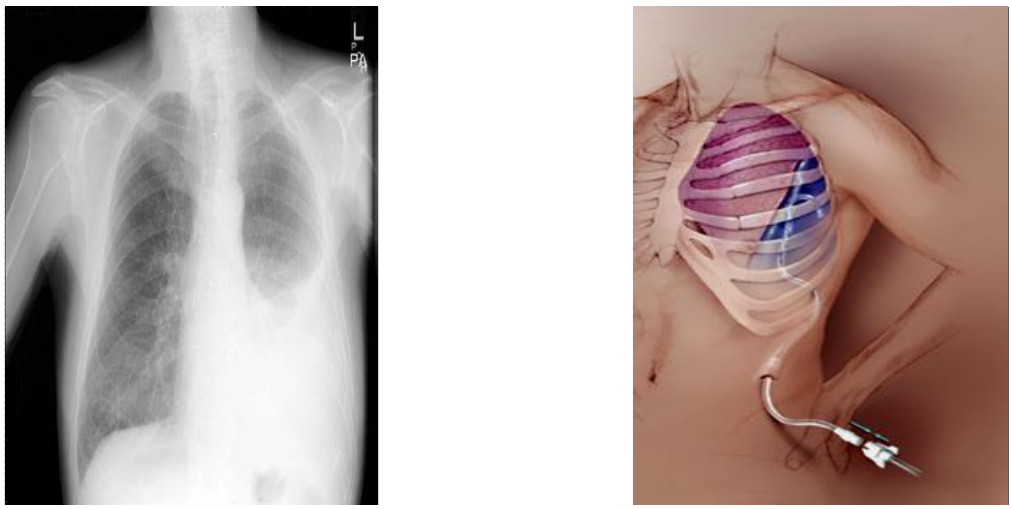

Figure 3. (a) The X-ray of a person with pleural effusion on the left lung - (b) treatment of pleural effusion using the thoracentesis process, © Christy Krames, medical illustrator [31].

2.3.4 Treatment

The treatment of pleural effusion depends on the underlying cause of the effusion, for example, antibiotics for pneumonia, chemotherapy or radiotherapy for cancers. To determine the cause of pleural effusion, pleural fluid is drawn out from the pleural spaces in a process called thoracentesis, as shown in Figure 3. In a thoracentesis process, a needle is inserted through the back of the chest wall in the sixth, seventh, or eighth intercostal space on the midaxillary line, into the pleural space to obtain a sample of pleural fluid and to drain large amounts of fluid for therapeutic purposes. The fluid then will be analysed to find the causes of effusion.

2.4 Overview of electronic respiratory sound analysis

Lung sounds contain a lot of information which can be used in the diagnosis of pulmonary diseases. To capture lung sounds from the chest wall and mouth, multiple-digital stethoscopes have been used in several studies. Generally, monitoring of lung sounds by multiple digital stethoscopes is divided into two main categories, mainly: respiratory sound analysis (passive method) and sound transmission into lung (active method).

In the passive method, respiratory sounds are recorded by multiple digital stethoscopes over the chest wall during respiratory cycles. However, in the active method, an acoustic signal, normally with a frequency of less than 20 KHz, is transmitted via the mouth by a speaker and received by the multiple digital stethoscopes attached over the chest wall. The received signals in both the active and passive methods are analysed by signal processing methods to obtain information. This information can then be used to monitor and diagnose a patient.

2.5 Standardization of electronic respiratory sound analysis

Since the field of respiratory sound analysis is still relatively new, there are no fixed guidelines for the acquisition, data storage and processing of lung sound recordings. To develop guidelines for performing research and for clinical practice in the field of respiratory sound analysis, a European Community (EC) project for computerized respiratory sound analysis was conducted by Sovijärvi et al. [32]. This project was run in seven European countries including Belgium, the Netherlands, Britain, France, Finland, Germany and Italy [32].

The authors reviewed 1672 research papers in the field of respiratory sound analysis in order to establish guidelines aimed at curbing the variety of instruments, testing conditions and methods used by researchers around the world [33]. Although these standards are not compulsory, the guidelines have been used extensively by researchers and engineers who conduct research and publish papers in the field of respiratory sound analysis. Therefore, this project will also follow these guidelines as set in the European respiratory review of 2000 [32].

2.6 Passive acoustic methodology (breath sound analysis)

The passive acoustic methodology (breath sound analysis) is one of the oldest techniques used to diagnose respiratory diseases. Pulmonary diseases affect the respiratory sounds. Traditionally, these sounds have been used for the preliminarily diagnosis of respiratory disease by a physician using a stethoscope. Over the past 30 years, the use of electronic respiratory sounds has been developed to aid in monitoring and diagnosing respiratory diseases.

Although this study is focusing on sound transmission into the lungs, a brief review of respiratory sounds, as well as previous studies in the use of passive acoustic methodology in diagnosis of pleural effusion are useful to better understand the acoustic properties of the human lungs. The following section provides a review of the categories of respiratory sounds. It includes the terminology and an explanation of the physiological origin of respiratory sounds used by medical practitioners. Furthermore, it looks at previous studies that attempt to detect and characterize these sounds by using signal processing techniques. An overview of the standardization of electronic respiratory sounds and of the relevant previous studies in breath sound analysis to detect pleural effusion, are also presented.

2.6.1 Categories of lung sounds

Respiratory sounds are classified into two major groups: normal lung sounds and adventitious lung sounds. The normal lung sounds have distinctive characteristics that can be differentiated from abnormal lung sounds. Furthermore, normal lung sounds differ in the different locations of the chest area and vary with ventilation cycles [34]. Normal lung sounds are subdivided as tracheal, bronchovesicular, and vesicular sounds [35]. Generally, adventitious lung sounds relate to respiratory diseases or conditions such as an obstruction in the airway passages or a pulmonary disease. According to the origin and the nature of adventitious sounds, they are sub-divided into two main categories: wheezes and crackles. Wheezes and crackles also are divided into sub-categories. The categories of lung sounds are shown in Figure 4.

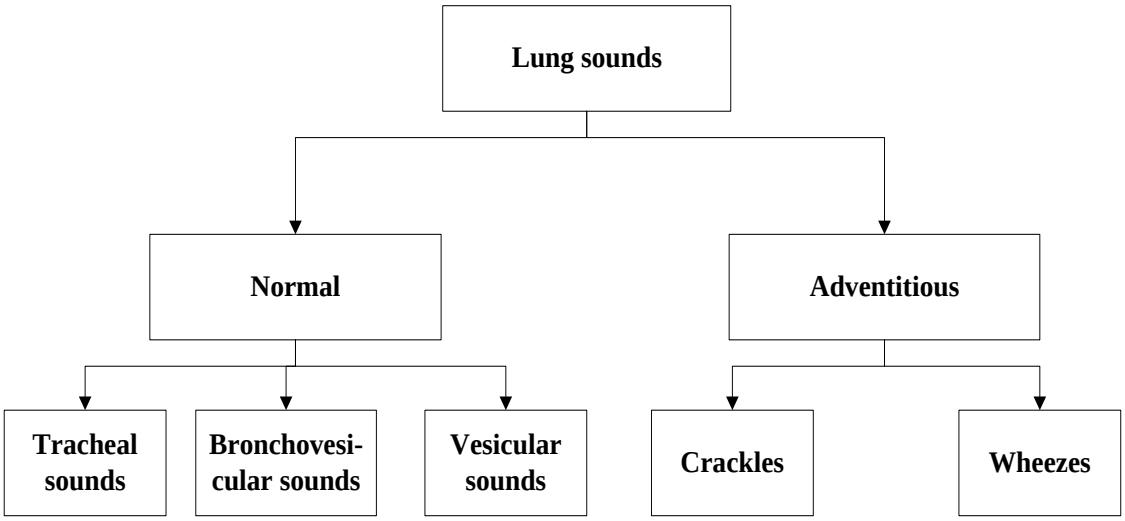

Figure 4. The categories of lung sounds

Normal lung sounds are described by Laence as “a distinct murmur corresponding to air into and out of air cells” [36]. The human lung sounds’ frequency is in the frequency range of 50 to 2500 Hz. The lung sounds with a frequency below 100 Hz are not easily distinguishable from muscle and cardiovascular sounds. The chest wall acts as a low pass filter. The amplitude of normal lung sounds drops sharply above 200 Hz [11], but it is still detectable in a quiet room. Normal respiratory sounds recorded over the lung have a frequency band of between 200 and 250 Hz, which is also shared with cardiovascular sounds. The discrete peaks cannot be detected in normal lung sounds, and it is not a musical sound.

The mechanism of lung sound generation is not completely clear. Air turbulence generates lung sounds in the frequency range above 300 Hz. However, the mechanism of the generation of sounds at the lower frequencies is not clear [34, 37]. Although lung sound amplitude differs between people and between locations, it primarily varies with air flow [37, 38]. Normal respiratory sounds have a soft character and an inspiration phase that is longer than an expiration phase. A ratio of the inspiration to the expiration is 2:1 during tidal breathing. Breathing sounds are nearly silent during expiration [34]. Moreover, respiratory sounds differ across the chest wall. Sound intensity also has regional variations. At the apex, the sound is less intense during inspiration. On the other hand, at the base, the intensity of sound is less at the beginning of the inspiration and gradually increases to reach the maximum at about 50% of vital capacity [39].

A wheezing sound is one of the most common sounds that can be heard in several respiratory diseases [32, 37]. According to the new definition presented by computerized respiratory sound analysis (CORSA), a wheezing sound is defined as continuous adventitious lung sounds (musical sounds) with a frequency domain greater than 100 Hz and a duration of longer than 100 ms. A wheezing sound is a periodical sound which must include at least 10 successive vibrations. A wheeze is called monophonic when it contains only a single frequency and it is termed a polyphonic wheeze when it contains several frequencies [37]. The spectrogram of the wheezing sound recorded over the trachea and below the right lung of an 11 year old girl with acute asthma [40] is shown Figure 5.

The pathophysiologic mechanisms of wheeze generation are not completely clear. It may be generated because of the movement of airway secretions. The flutter of airway walls

also plays a significant role in producing the wheeze [37].A wheezing sound is generated in the following pathologies [37]:

- Infections such as croup (infection that generally affects infants of branchitis less than three years), whooping cough, laryngitis, acute tracheobronchilis
- Laryngo-, tracheo-, or bronchomalacia
- Laryngeal or tracheal tumours
- Tracheal stenosis
- Emotional laryngeal stenosis
- Foreign body aspiration
- Airway compression
- Asthma: wheeze detection in asthma, identification of nocturnal asthma

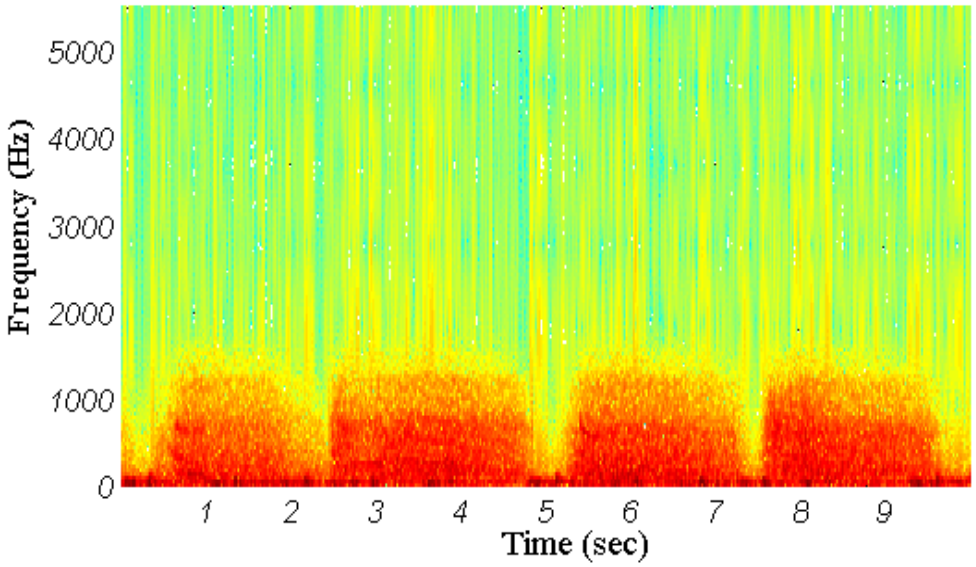

Figure 5. The spectrogram of a wheezing sound recorded over the trachea and below the right lung of an 11 year old girl with acute asthma [40]

Crackles are discontinuous, non-musical, and explosive sounds of less than 20 μs in duration, with a spectrum of frequencies between 100 and 2000 Hz. The crackles appear generally during the inspiration phase. Crackles can be divided into two groups: fine crackles and coarse crackles. Fine crackles are associated with high frequency components, while coarse crackles are associated with low frequency components.

The occurrence of crackles in lung sounds is associated with pulmonary disorders such as lung infections, pneumonia and pulmonary oedema [37, 41, and 42]. Crackles occur at the end of the inspiration phase or during the closing of the glottis. One of the important factors of concerning crackles is the position of the occurrence of crackles in the respiratory cycle. The shape of the waveform also contains significant pathological information [37]. Figure 6 shows a typical crackle. The normal shape of a crackle begins with a width deflection, followed by a long and damped sinusoidal wave as shown in Figure 6. Initial deflection width (IDW) corresponds to the duration between the beginning of the crackle and the first deflection. Two-cycle duration (2CD) is defined as the duration from the beginning of the crackle to the time at which the waveform has completed two cycles. Total deflection width (TDW) is defined as the total duration of the signal crackle. Crackles can be found in the following pathologies [34, 42]:

- Pulmonary fibrosis (2CD < 8 ms, frequency around 200 Hz)
- Asbestosis (crackles' duration around 10 ms)
- Bronchiectasis (2CD > 9 ms, they generally appear late in the inspiratory cycle and have a relatively long duration compared to the respiratory phase)
- Chronic obstructive pulmonary disease (COPD) (2CD > 9 ms, generally starting early in inspiration and ending before the mid-point of inspiration)
- Heart failure (2CD > 10 ms)
- Pneumonia (2CD between 9 and 11 ms), they appear at the mid-point of inspiration)
- Sarcoidosis.

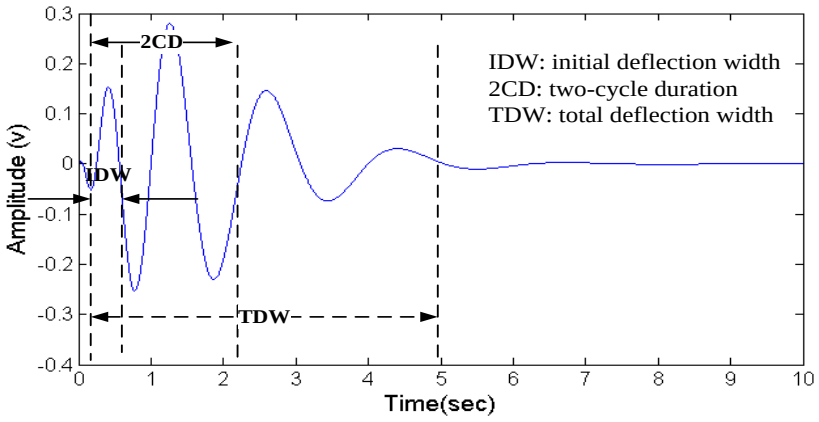

Figure 6. Typical crackle

2.6.2 Relevance of respiratory sound analysis to pleural effusion

A few studies have been performed to diagnose and monitor pleural effusion by using the analysis of lung sounds. The pleural friction sound is described as coarse crackles generated by the parietal and visceral pleura rubbing against each other. This sound is a sign of the inflammatory processes of the pleura and usually precedes the beginning of pleural effusion and disappears when the fluid is formed [43].

One of the earliest studies of a quantities assessment in the diagnosis of pulmonary diseases such as chronic bronchitis, bronchial asthma, pneumonia, bronchiostasis and pleural effusion was conducted by Chowdhury and Maiumder [44]. They investigated the frequency analysis of adventitious sound in four groups of subjects which were classified based on adventitious sounds. The details of each group are shown in the Table 2.

Table 2. Details of participants in the Chowdhury and Maiumder's study [44]

Group	Number of patients	Diseases	Adventitious sound
Healthy (Normal)	5		
Patients	7	Chronic bronchitis, bronchial asthma, pneumonia	Wheeze
Patients	8	Localized fibrosis, bronchiostasis, lobar pneumonia	Rales
Patients	5	Pleural effusion, emphysema, dry pleurisy	Pleural friction rub

The authors calculated the frequency response at the four discrete frequencies. Their results showed that by using respiratory sound analysis, various categories of pathogenic lung sounds could be visually distinguished from one another. Furthermore, they found that wheezes could only be detected significantly in certain regions of the chest wall, and that a pleural friction rub is significant in patients suffering from pleural effusion emphysema and dry pleurisy [44]. However, they did not investigate the frequency responses over a wide range of frequencies.

Currently, vibration resonance imaging (VRI) is used to monitor and diagnose lung diseases. The VRI machine has forty active piezoelectric contact sensors and two inactive

contact sensors connected to the chest skin with vacuum coupling to record the lung sounds. The recorded signals are analysed to produce a grayscale image of the lung.

Dellinger et al. [45] conducted research on the evaluation of VRI systems to monitor pleural effusion and other respiratory diseases. They measured the lung sounds of five healthy subjects, four patients with pleural effusion, four patients with unilateral central airway obstruction, three patients with acute asthma and two mechanically ventilated subjects. The signals were analysed by using an algorithm to convert respiratory sounds in the frequency range of 150–250 Hz to a dynamic image and quantitative assessment of respiratory sounds distribution. Their results showed that the images of healthy subjects have similar breath sound distribution and the images of subjects with respiratory illness differ from the images of healthy subjects. Moreover, the results show that each respiratory disease has its own different sound distribution image patterns [45].

A feasibility study of vibration response imaging in the detection of pleural effusion was carried out by Anantham et al. in 2008 [46]. In that study, respiratory sounds were recorded from 56 patients who had been diagnosed with pleural effusion using VRIxp^{TM}(Deep Breeze TM , Or Akiva, Israel) to produce VRI images of the lung. VRI images were evaluated by a physician, who was unaware of the patients' clinical history, physical examination or chest X-ray images, to make a quantitative report on the presence of any pleural effusion in the left or right hemithorax. Furthermore, the physician classified the pleural effusion based on the size of the effusion into none, small and moderate/large. The VRI recordings were compared to upright chest X-rays, bedside ultrasound examinations and volume of fluid drained via thoracentesis. The results showed that VRI recording correctly predicted the diagnosis in 80% of patients (45/56) as compared to chest X-rays which can be used in the diagnosis of pleural effusion [46].

Another study in this area was conducted by Ram Mor in 2007 [47] to determine whether there are differences between the respiratory sounds distribution maps of patients with pneumonia and pleural effusion. They recorded respiratory sounds of 20 patients with pleural effusion and 20 patients with pneumonia and 60 healthy patients for control, using VRIxp^{TM}(Deep Breeze TM , Or Akiva, Israel) to produce a grayscale image of the lung. The images of 40 patients and 40 controls were interoperated by the physicians who were first trained in identifying common characteristics of the images from the learning sample as

either normal or abnormal. The results showed that the sensitivity and specificity of blind differentiation between normal and abnormal images when the physician interpreter did not know the patient's medical background was 82.5%. However, when the interpreter did know the patient's history, the sensitivity and specificity of blind detection of normal and abnormal images was 90% and 88%, respectively [47].

2.7 Active acoustic methodology (sound transmission into the respiratory system)

Sound transmission into the lungs, one of the oldest techniques, has been performed by several researchers [48-52]. In general, an alternation in the generation and transmission of the sounds of the respiratory system occurs in many pulmonary diseases, due to changes in the physical properties of respiratory system. Consequently, to assess the properties of the respiratory system alone, a number of researchers [48-53] injected sounds into the mouth of human subjects in an attempt to accurately measure the transmitted sound on the chest of the subject by multiple-digital stethoscopes as shown in Figure 7.

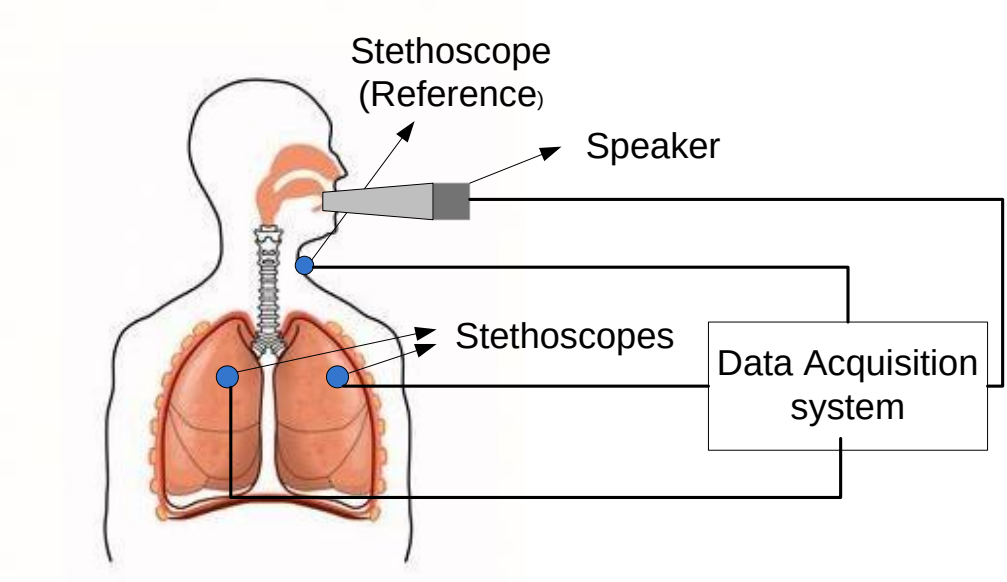

Figure 7. Schematic of typical equipment for performing the active acoustic methodology

The advantage of this method is that the static and even dynamic response of the respiratory system can be measured and compared with a model or hypothesis. In most studies, transient time (time delay between transmission of the sound and sound being

received by conditions the chest wall) and frequency response of the lung were computed. To determine the time delay of transmitted sound, the chest surface response relative to the reference signal was calculated by using a cross correlation method [50, 51, 54-56]. Time delay can be used to measure the velocity of sound in lung parenchyma as well as the respiratory system. In addition, the frequency responses of the human lungs were also calculated using Fourier analysis [57, 58].

In the following section, a brief overview of the previous studies on sound transmission into the lungs is presented. The frequency responses of healthy lungs, as well as the effect of lung volume and gas density in the lung on the transmission of the sound in healthy lungs in the previous studies, are discussed. Furthermore, the effect of pulmonary pathology on the sound transmission in the lungs is presented.

2.7.1 Sound transmission into healthy lungs

One of the earlier studies in this field was conducted by Kraman in 1983 [59]. He measured the propagation time of transmitted sounds in the respiratory system of healthy subjects. He also calculated the spectral characteristics of transmission sound. However, he only used variable input power levels above the 150-500 Hz range, an uncharacterized source sound and microphones which were calibrated in free field and not in the measurement configuration. Consequently, these parameters affected the propagation time and spectral characteristic.

The evaluation of transmission of wide band frequencies into the respiratory system was performed by Goncharof et al. [48]. They assumed that the respiratory system is linear, time invariant and stable. They measured the impulse response of human lungs in 21 male subjects over a frequency range of 0 to 20 kHz. 21 subjects were divided into four categories, as shown in Table 3. They calculated the time delay using spectrographic analysis. Their results show that the transmission of sound with frequencies above 5 kHz is not repeatable. In addition, they found that the peak level energy in categories 2 and 4 are approximately similar, in a frequency range of 0 to 5 kHz. For category 2, the peak amplitude is slightly larger than those in categories 3-4[48].

Table 3. Summary of Goncharof's clinical study [53]

Category number	Clinical status	Smokers Yes/No	Age range	Number of participations	Age in years mean (SD)
1	Normal	No	<55	3	37(15)
2	Normal	No	>55	7	69(9)
3	Normal	Yes	>55	7	73(5)
4	COPD[2]	Yes	>47	4	63(4)

To measure the time delay of transmitted sound from the trachea to the chest wall, George et al. [49] performed an evaluation of a phase delay estimation technique on eight healthy subjects. In this technique, electrical noise sounds from 100-600 Hz are transmitted to the respiratory system. A diagram of the experimental apparatus used to perform sound transmission measurement is displayed in Figure 8. Since the phase delay can be greater than one period of the signal, they employed Schafer's unwrapping algorithm [49] to detect point to point discontinuity. The advantage of this technique is that phase delay can be calculated in each frequency individually. The results showed that the estimated phase delay decreases with increasing frequency [50]. These results are also confirmed in another study performed by Lu et al. [51]. They transmitted sound between 300 and 1600 Hz in 11 adult male subjects, and calculated the phase delay using a linear parametric ARX- type statistical model.

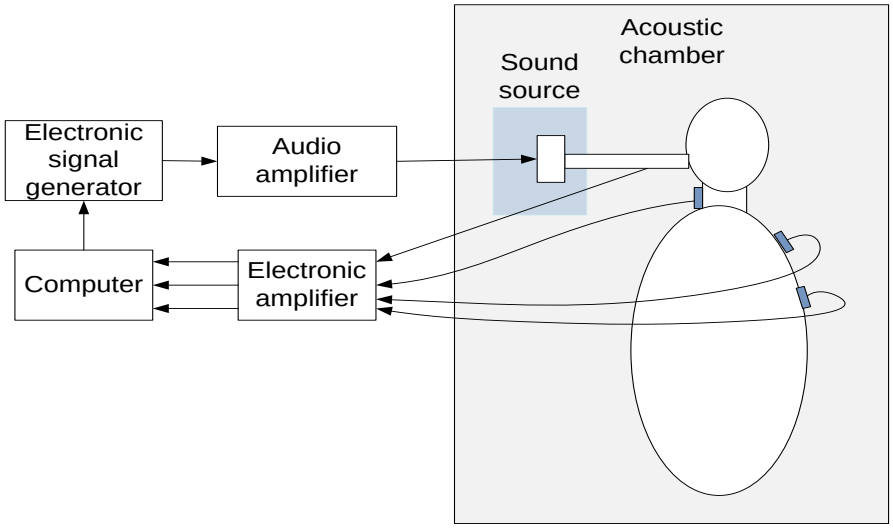

Figure 8. Diagram of the experimental apparatus used to perform sound transmission measurement in the study of George et al. [49]

[2] chronic obstructive pulmonary diseases

Patel et al. [52] studied the the effect of the composition of inhaled gas on sound propagation time through an intact human lung at frequencies of 150-1200 Hz in 11 healthy adult subjects, at the resting lung volume, after equilibration with an 80% helium 20 % oxygen mixture and an 80% sulphurhexafluoride 20 % oxygen mixture. Their experimental results showed that the gas composition strongly affected sound propagation time in the respiratory tract [52].

The spectral characteristics of sound transmission in the human respiratory system were investigated by Wodicka et al. [53]. In their study, electrical noise with equal energy at 4 Hz interval, over a frequency of 100- 600 Hz, was transmitted into the mouth of subjects as shown in Figure 9. They measured the amplitude of sound at the extrathoracic trachea and two sites on the right posterior chest wall. They found that the amplitude of acceleration decreases with increasing frequency. Their experimental results agree with a theoretical model.

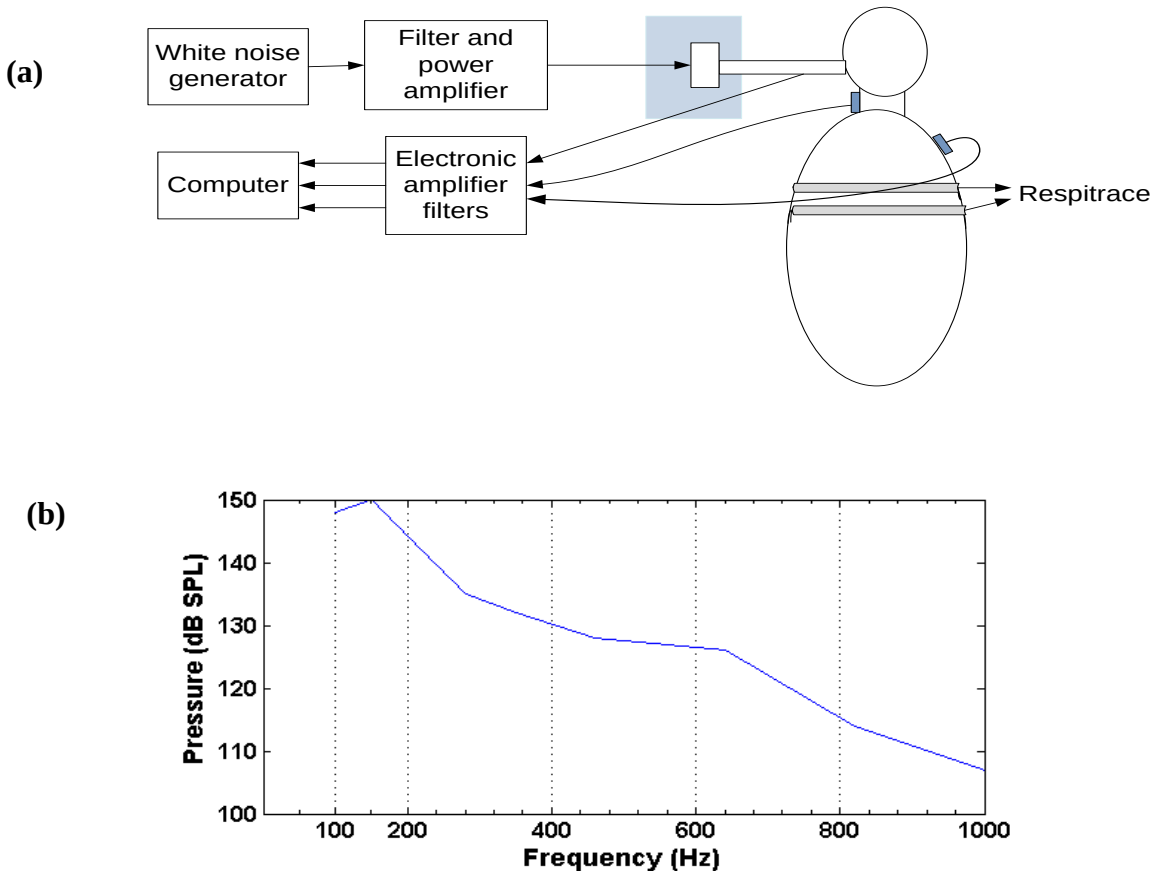

Figure 9. (a) Diagram of the experimental apparatus used in the study of Wodicka et al. [53] (b) a representative power spectrum of the sound pressure measured by a microphone in the tube through which sound is introduced into the patient mouth based on data from [53].

Another study to investigate the transfer function of the human lung was performed by Wodicka and Shannon [58]. They calculated the ratios of the estimated magnitude spectra of transmission of two transducers attached to the chest wall to the transducer attached to the trachea. They also found that transfer function decreases with increasing frequency, as was shown for the frequency response in the previous study [53]. Moreover, they found that the transfer function contains a single peak, which occurs at 143±13 Hz for the upper chest wall and 129 ±6 Hz for the lower site, over a frequency range of 100 to 600 Hz. According to their results, they suggested that the best frequency range for the transmission of sound into the respiratory system is below 250 Hz, because of the high attenuation factor in lung parenchyma at frequencies higher than 250 Hz [58].

For the first time, the bilateral asymmetry characteristics of transmitted sounds at low frequencies were observed by Karman and Austrheim [60]. They found that amplitude at low frequencies to sites overlying the right lung are significantly greater than corresponding locations from the left lung, because of the massive mediastinum lying to the left side of the major airway. This effect was also confirmed by Wodicka et al. [61]. Wodicka continued research in this field and he found that sound on the chest surface relative to that on the trachea is lower in amplitude and, with increasing frequency, the amplitude of the frequency response of the chest wall decreases rapidly [57]. They further observed that there is no asymmetry at frequencies above 600 Hz. These findings are confirmed by Pasterkamp et al. [62]. Furthermore, they discovered that the amplitude of transmitted sounds is greater at the posterior lung base.

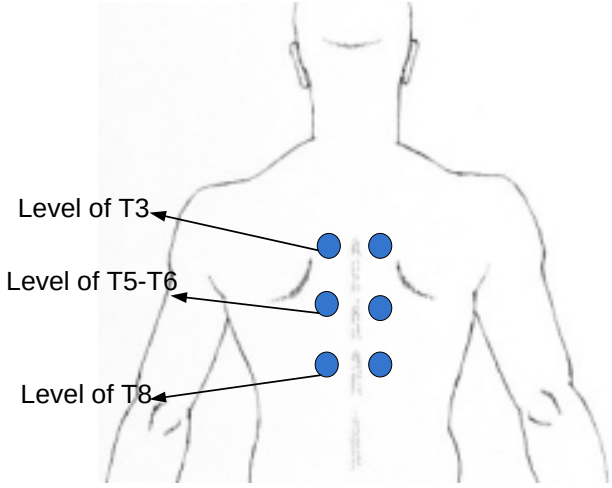

Figure 10. Locations of microphones in the study of Wodicka et al. [61]

In 2006, a study in the field of transmission of acoustic sound into the lung was performed by Bondar et al [63]. They measured the frequency response of the transmitted vocal sound 'tree-tree' in children and adolescents. They found that the slope of the descent of the voice-transmitted sound spectrum from the first spectral peak to the high- frequency region steadily increases on moving from the upper to the lower lung. Moreover, the change in amplitude of the first and second peaks of transmitted sound over the symmetric region of the lungs did not depend on sex or age [63]. Another recent work in sound transmission through the respiratory system was carried out by Korenbaum et al. [64]. They used acoustic convolution of a complex signal to find propagation time lags of an exited signal. They used this information to clarify the mechanism of sound transmission into the lungs [64].

Gas density in the lung affects the amplitude of the transmitted sound at the chest surface. This effect was first observed by Kraman and Bohadana [65]. It was later confirmed by Mahagnah and Gavriely [54]. Pohlmann et al. [55] investigated the effect of gas density on acoustic attenuation, determined in experimental studies on seven healthy volunteers. Their results show that the acoustic attenuation at frequencies of 364-436 Hz is significantly greater than the acoustic attenuation at frequencies of 177-243 Hz, with a similar change in lung volume [55]. In 2002, Bergstresser et al. [56] performed another study in this field. They found that transient time at all locations of the chest surface decreases with increasing lung volume. Moreover, they suggested a simple model for the sound transmission into the lung, which is treated as a combination of free space propagation through the trachea and a two phase system in the parenchyma.

2.7.2 Effect of pulmonary pathology on sound transmission into the lung

Since pulmonary pathologies affect the behaviour and physical properties of the lungs, sound transmission is one of the non-invasive techniques that may be useful to diagnose and monitor lung health. The effect of pulmonary pathologies on sound transmission into the lung has been investigated in a limited number of studies. Leung and Sehati [66] measured the speed of sound through the lungs to detect the area of collapsed alveoli. They transmitted sound with a frequency range of 50 Hz to 500 Hz with steps of 50 Hz to measure the time delay in the lungs. They found that it is possible to detect collapsed

lung, because the speed of sound in the collapsed lung is much faster than it is in the normal lung [66].

The evaluation of the use of a transfer function for the detection of the accumulation of lung liquid in canine lungs was carried out by Donnerberg et al. [67]. In their study, different degrees of pulmonary congestion were evaluated by post mortem wet to dry lung weight ratios. Sine swept sound from 50 Hz to 2 kHz was transmitted to the respiratory system to determine the transfer function. The increasing accumulation of intervascular and extravascular lung liquids can be detected using transfer function [67].

In 2009, Mulligan et al. [68] developed the technique using a transfer function in the detection of fluid in the lungs. The technique consists of the transmission of white Gaussian noise into the mouth and recording the sound, using four microphones on the chest, to determine the transfer function of the lung. They calculated the transfer function, using the principal of adaptive filtering, for three healthy human chests as well as a phantom model of human lungs. They found a similar trend in the transfer function in the human lungs and phantom model. However, they could not determine the effect of fluid on the transfer function or the time delay [68].

2.8 Chapter summary

Electronic respiratory sound analysis is a technique to aid in monitoring and diagnosing respiratory diseases. It can be divided into two main categories: a passive acoustic methodology and an active acoustic methodology. In the passive acoustic methodology, lung sounds are recoded using multiple digital stethoscopes. These sounds can be analysed on a computer, using signal processing techniques. However, in active acoustic methodology, sound is transmitted into the respiratory system. The applied sound is recorded using multiple digital stethoscopes on the chest of patients.

Although several researchers have employed an active acoustic methodology in an attempt to calculate the time delay in the respiratory system as well as the frequency responses of the human lungs, the measurement of these two values is still unclear. Different values for the time delay of transmitted sound in the lungs were reported in the different studies, such as the time delay in the study of [69] was reported between 1-6 ms while in the

experiment of [70] it was reported in a range of 4-13 ms. Furthermore, the stethoscopes were either placed on the anterior or the posterior of the chest of the subjects. No study has been carried out which measure both the anterior and posterior time delay or the frequency response.

Using active acoustic methodology to monitor or diagnose pulmonary diseases has been performed in a few studies. However, most of the previous studies were performed a long time ago. There is no study that has used AAM as a tool for monitoring or diagnosis of pleural effusion.

3. Evaluation of active acoustic methodology on a phantom model of the human lungs

3.1 Introduction

Since active acoustic methodology (transmission of sound) in diagnosis of pleural effusion has not yet been performed, this technique was implemented initially on a phantom model of the lung with similar acoustic properties to the lung parenchyma. Following this, testing could begin on human subjects. Pleural effusion was modelled using two plastic bags filled with water. The effect of fluid on the frequency response of the model was evaluated using a sine sweep signal over a frequency range of 100 to 700 Hz with steps of 100 Hz. Moreover, since the speed of sound in fluid is much faster than the speed of sound in the lung parenchyma (approximately 50 times faster), the use of time delay estimation on fluid detection was also evaluated.

3.2 Objective of this chapter

The objectives of this chapter are to:

- design and develop of a mechanical model of the lung ; the model should have similar acoustic properties to the respiratory system;
- investigate different techniques to transmit sound into the model and select the best technique to transmit sound;
- investigate of the use of frequency response as a tool for the detection of fluid in the lung ;
- investigate of the use of time delay estimation as a technique for the identification of fluid in the lung.

3.3 Development of a phantom model

This section includes information about the specifications of previous mechanical models of the lung as well as the selection of appropriate materials for modelling the respiratory system. Detailed information about the design of the model is also presented.

3.3.1 Previous mechanical models of the lungs

Three types of mechanical models of the respiratory system have been developed. Ozer et al. [71] designed and fabricated the phantom model of the lung to validate the simulation of the propagation of sounds in the lung parenchyma using an acoustic boundary element model. The geometry of the model is a tapered cylinder which has a 12 cm diameter at the bottom of the model and 15 cm diameter at the top, across a cylindrical height of 11 cm, as shown in Figure 11. In addition, they only modelled lung parenchyma [71].

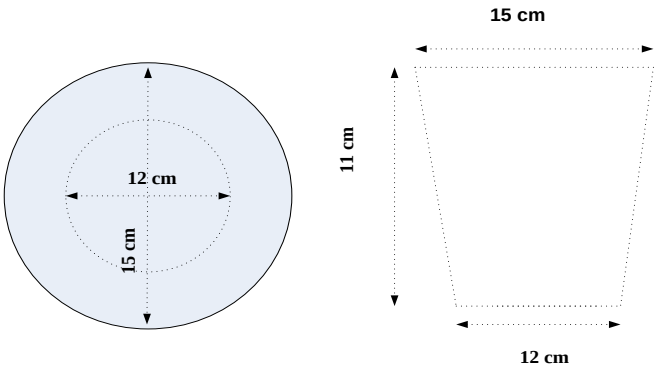

Figure 11. Schematic of the phantom model in Ozer's et al. study [65]

Acikgoz et al. [72] developed a phantom model of the lung to compare numerical and theoretical simulation of sound propagation in the lung parenchyma surrounded by the chest wall, with their experimental studies. The phantom model was used to model the lung pathology of pneumothorax (collection of air in the space around the lungs). They used flex foam IT-X to model the lung parenchyma. CF-11, which has Young's modulus 72 kPa, a poisson ratio 0.496 and a density of 1049 kg/m^3 was used in their phantom model to the model soft tissue wall. Moreover, they modelled ribcages by using Garolite, which has a density of 1900 kg/m^3. The Garolite with a size of 6×12×250 mm was embedded in the CF-11, as shown in Figure 12 .The geometry of the model is cylindrical in shape, with a 275 mm diameter across a cylindrical height of 225 mm. To model the pneumothorax, two bladders behind the ribs were used. The first one started at 160° and ended at 210°, whereas the second bladder started at 60° and ended at 110° as shown in Figure 12 [72] .

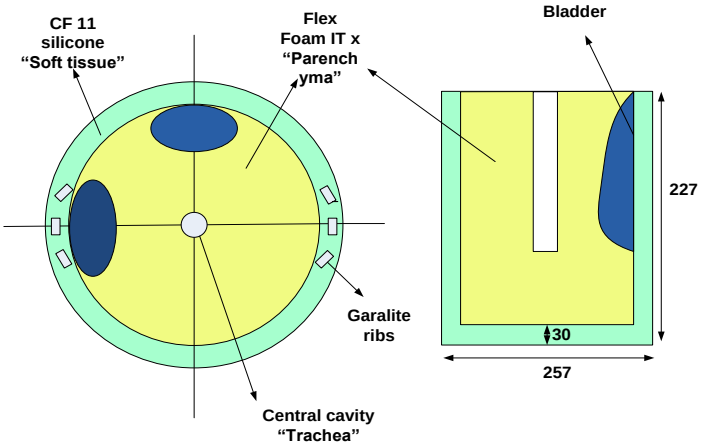

Figure 12. Schematic of the phantom model in Acikgoz et al. study [66]

Recently, Mulligan et al. [68] constructed a phantom model of the chest to evaluate the use of audio transfer functions in the detection of fluid in the lung. The phantom model comprises of foam (ρ= 0.01875 g/cm^3), pipe insulation, a tyre inner tube, clear tubing, and a syringe. The camping foam was rolled to form a cylinder with a diameter of 0.12 m and a length of 0.52 m and held in a cylindrical position using hot glue as shown in Figure 13. They used the pipe and syringe to put water in to the model [68].

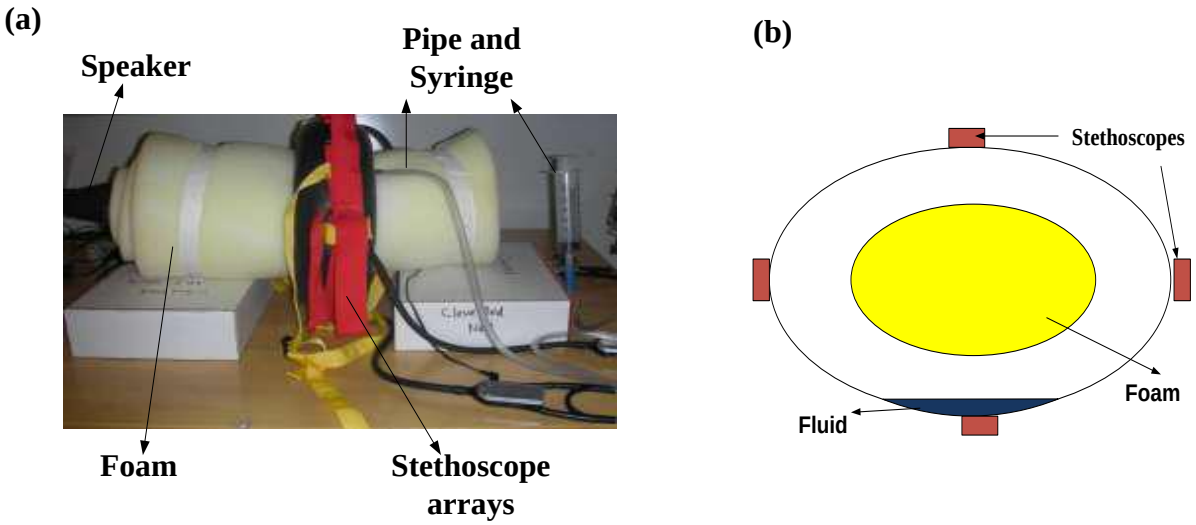

Figure 13. (a) The model in Mulligan's study [68], (b) the cross section of the model

Three different types of the phantom models have been developed in previous studies, but the previous models were designed based on very simple geometries which cannot model the respiratory system accurately. Moreover, the geometry of the human lung is asymmetric, but most of the previous models had symmetrical shapes. Furthermore, the effect of bronchial

trees has not been considered in previous studies. Therefore, an asymmetric model based on previous studies has been developed to test the hypothesis on the model.

3.3.2 Materials selection

Parenchyma tissue is one of the more complicated tissues of the human body and it can be represented as a homogenous mixture of gas and tissue [73]. The parenchyma tissue can be defined by its density ρ_K and complex wave number K_P, whose real part is linked to the phase speed and imaginary part linked to attenuation [71, 72]. The complex wave number is a function of frequencies, as presented in Appendix D. To model the parenchyma tissue, Flex foam IT-X (Smooth-On Inc., Easton, PA) was used, which has been used in previous studies. This material has a similar density (160 kg/m^3) and phase speed (27.5 m/s) to lung parenchyma [71, 72].

The soft tissue regions are composed of fat, muscles and connective vascular or materials which can be defined by a density of $\rho_t \approx 1000$ kg/m^3 and complex wave number of K_t . To model the soft tissue, silicon rubber has been used in several studies [74, 75]. In this study, Body Double® Skin-Safe Silicone rubber with a density of 1170 kg/m^3 was used. This material is a durable platinum-curve silicone rubber with specific volume of 23.7 m^3/kg and curve time 5 min with a tensile stress of 450 psi and tear strength of 40 psi. More information about this material is presented in Appendices B, C and D.

The human ribcage (thoracic cage) is a bony and cartilaginous structure which typically consists of 24 ribs. The density of ribs varies highly and it depends on several factors such as age and gender [22]. The PVC with a density of 1550 kg/m^3 was used to model the rib cage. The speed of sound in this material is 2380 m/s with an acoustic impedance of 3.27 N.s.m^{-3}.

3.3.3 Model design

The asymmetric phantom model was designed and fabricated based on the average dimensions of a healthy adult male human [76]. The geometry of the model is cylindrical with a 278 mm diameter and a height of 230 mm. Two phantom models were fabricated: a healthy model and a pleural effusion model (model with fluid inside). The healthy model

consists of the rib-like cage integrated with soft tissue, and the lung parenchyma with the trachea and the bronchial tress.

The shape of the lung parenchyma is cylindrical, with a 218 mm diameter and 225 mm. The lung parenchyma was created using Flex foam IT-X by a moulding process. A rib which has a cylindrical band shape with internal diameter of 218 mm, external diameter 258 mm and the thickness of 15 mm, was made from PVC. The distance between adjacent ribs is 12 mm, as shown in Figure 14. The thickness of soft tissue is 3 cm between two rib bands.

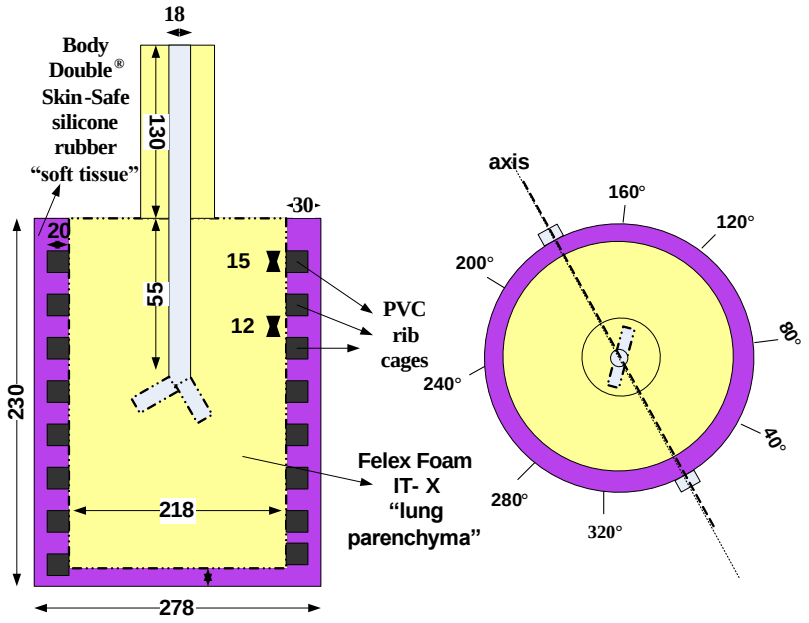

Figure 14. The schematic of the healthy phantom model (all dimensions in mm)

The trachea was modelled using a moulded cylindrical hole with a 28 mm diameter and a length of 185 mm long. Two main bronchial trees were also modelled at the end of the trachea, with an 18 mm diameter and 55 mm deep hole, as shown in Figure 14. The position of two the bronchial trees in the model is also displayed in Figure 14. The angle of the two bronchial trees with the axis of the model is approximately 50°. The trachea and bronchial trees in the model have a similar shape to the normal anatomical shape of the trachea and bronchial trees of the body. The right bronchial tree is at an angle of 73° and left bronchial tree 35° to the axis of the trachea, as presented in Figure 15.

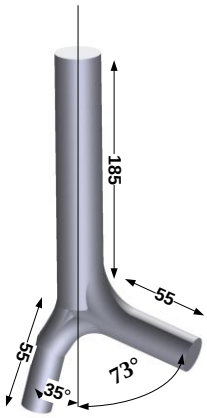

Figure 15. Model of the trachea and two main bronchus

To fabricate the model, Body Double® Skin-Safe Silicone rubber was moulded around the rib-like components. The two section of soft tissue integrated with rib-like components were attached together using four screws. After this process, the plastic tubes, which were deformed to have a similar shape to normal anatomical trachea and bronchial trees (Figure 15) were placed into the model. Flex foam IT-X was moulded inside of the model. After the deformation time, the plastic tubes were removed from the model.

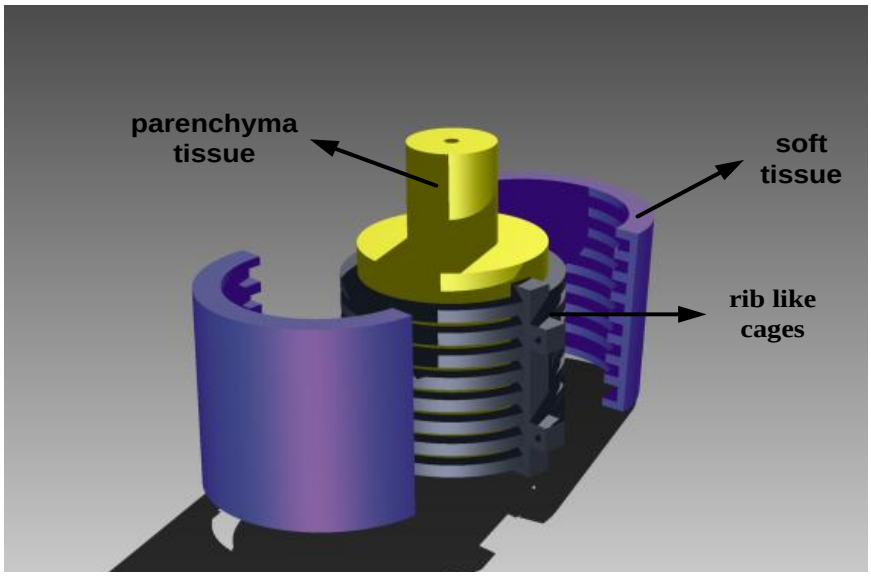

Figure 16. The assembly process of phantom model

The pleural effusion model, which has the same geometry as the healthy model, was designed to model effusion (bulk fluid in the lung). Two latex plastic bags were used to model the fluid in the lung, one of which was filled with 600 ml of water using a syringe,

while the other contained 250 ml water as shown in Figure 17. The 250 ml plastic bag was located at 80° and attached to the inside skin of the model while the other one was located at 240° and was also attached to the skin of the model. The flex foam IT-X was moulded in the model such that it covered the two plastic bags. A schematic view of the model is shown in the Figure 17.

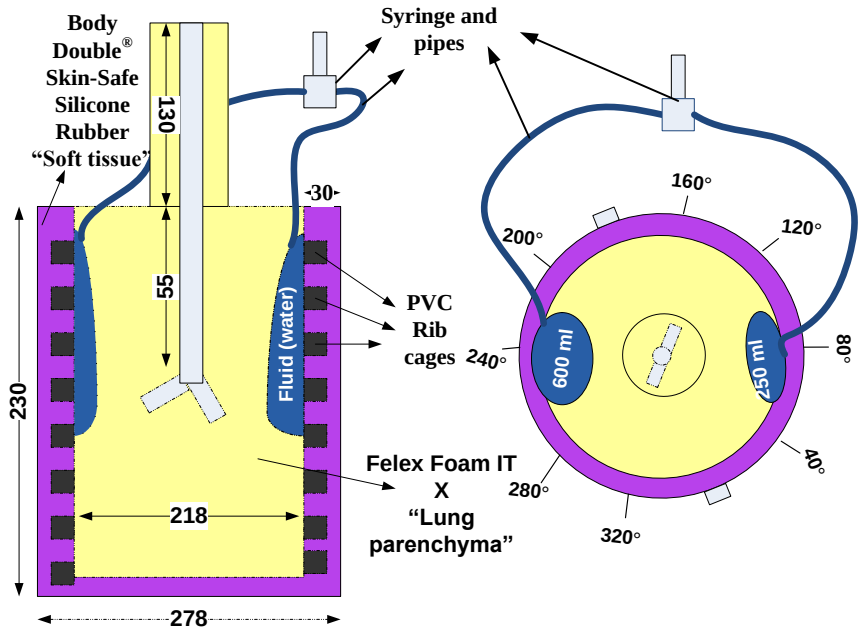

Figure 17. The schematic of pleural effusion model

3.4 Transmission of sound into the model

Generally, there are two methods to transmit sound into the model. In the first, sound can be transmitted from the chest of the model to be received at the trachea. This technique needs only one transducer for recoding the sound. The advantages of this technique include simplicity and low cost. However, the sound should be transmitted into the model from different locations on the model chest. Therefore, capturing data from the model should be performed as several different measurements. In the second method, sound can be transmitted into the model from the trachea of the model to be picked up by multiple transducers attached to the chest of the model. The main advantage of this technique is that the capturing of data from the model can be performed in a single measurement. Two hypotheses were evaluated on the model, including the evaluation of using frequency responses in detection and evaluation of using time delay for fluid identification in the model.

3.5 Investigation of using the frequency response of the model in the detection of pleural effusion

Since pleural effusion affects the behaviour and physical properties of the lungs, the assessment of using the frequency responses of the model was performed in order to aid in the diagnosis and monitoring of lung health. This section is followed by the data acquisition system, sensors calibration, signal generation, environmental conditions and noise, data analysis, results and discussion.

3.5.1 Data acquisition system

The data acquisition system for this measurement includes: a SigLab 4246, a Spider, a load cell, a Visaton 4692 FX 10 speaker, two PCB piezotronics 387 B02 microphones, a custom designed funnel and a custom made clamp. A full range Visaton 4692 FX 10 speaker with an approximately flat frequency response over a frequency range of 70 – 22000 Hz and maximum power of 70 W, was connected to a 50 mm long custom made PVC funnel in such a way that it covered the entire surface of the speaker. The other side of the funnel has a 7 cm diameter, which was cut with a special curve, so that it can fit completely into the chest of the model.

A pre-recorded sound was generated by a speaker and transmitted through the chest of the model. A PCB piezotronics 387 B02 microphone, which has a flat frequency response over a frequency range of 3Hz to 20 KHz, was put in the trachea of the model 3 cm below the top of the trachea, as shown in Figure 19. Another microphone was placed outside of the model, close to the first microphone, to record the ambient noise. The recorded signal was amplified 100 times using Kemo ® BM 8 amplification system. The amplified signal was digitized at 2560 Hz using a SigLab 4246 and recorded by a computer for the post processing. Measurements were made at 24 points that form a grid around the cylindrical surface of the model. The measurement points include eight angular positions of 40°, 80°, 120°, 160°, 200°, 240°, 280°and 320° degrees and the three axial positions of 35, 105 and 175 mm. To investigate the repeatability of the measurement, each point was measured 30 times.

It was found experimentally that the amplitude of the recorded sound from the chest of the model depends on the applied force behind the speaker. The applied force was monitored before each measurement using a loadcell S2 –HBM and fixed at approximately at 20 kN. However, the force changed less than 1% over the time of measurement because of the non-linear behaviour of the Body Double® Skin-Safe Silicone rubber. The force exerted by the custom made clamp was measured using a loadcell S2 –HBM, which was placed behind the microphone. The loadcell was connected to the Spider for digitization and monitoring by the computer during the measurement. In order to reduce the effect of gravity on the measurement, four pieces of wood with same the length as the axial positions on the model support the clamp, as shown in Figure 18. The experiment of setup is summarized in Table 4. Summary of experimental setup

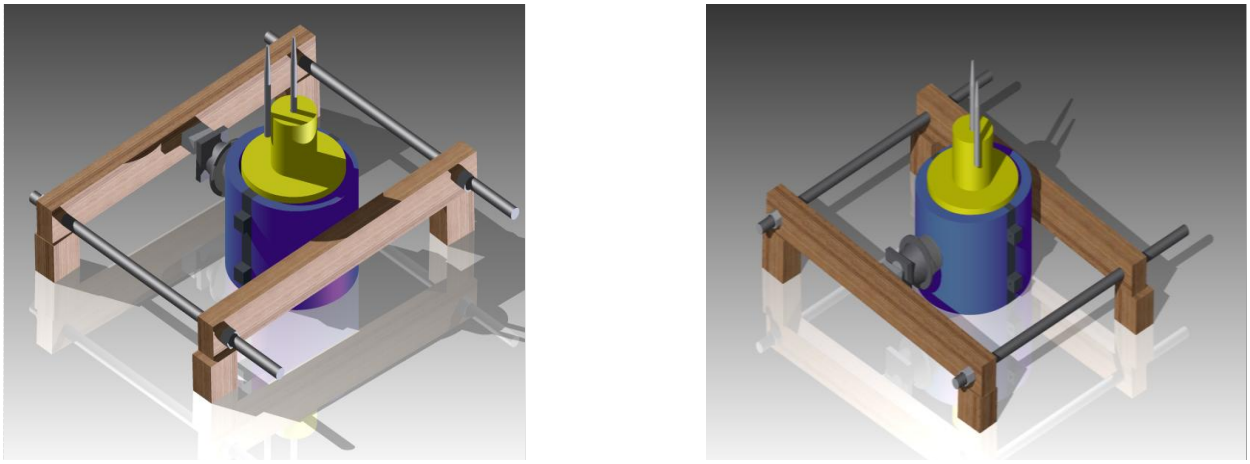

Figure 18. Two views of experimental setup

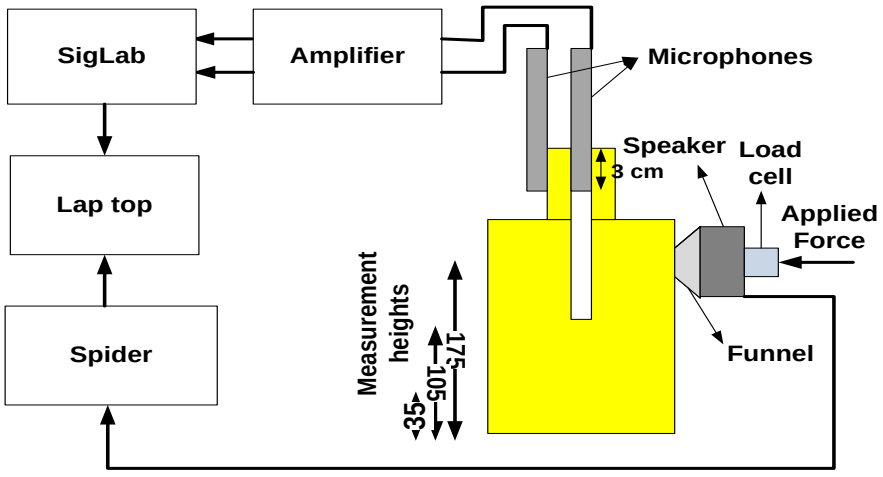

Figure 19. Schematic of experimental setup

Table 4. Summary of experimental setup

Description	Type
Speaker	Visaton 4692 FX 10
Load cell	S2 –HBM
Microphones	A PCB piezotronics 387 B02
Funnel	Custom-design
Amplifier	Kemo ® BM 8
Audio to digital convertor	SigLab 4246, Spider 8

The pre-recorded sine sweep signal with a frequency range of between 100 Hz and 1000 Hz, with step of 100 Hz and with flat frequency response, was programmed using the mathematical software MATLAB and it was generated using the SigLab. The pre-recorded sound contains 10240 sample points with a total duration of 4 seconds. The frequency content of input signal is shown in Figure 20. The pre-recorded sound was played by the speaker continuously. The recorded signal contains 81920 sample points with a total duration of 32 seconds which was eight complete cycles of recorded sound.

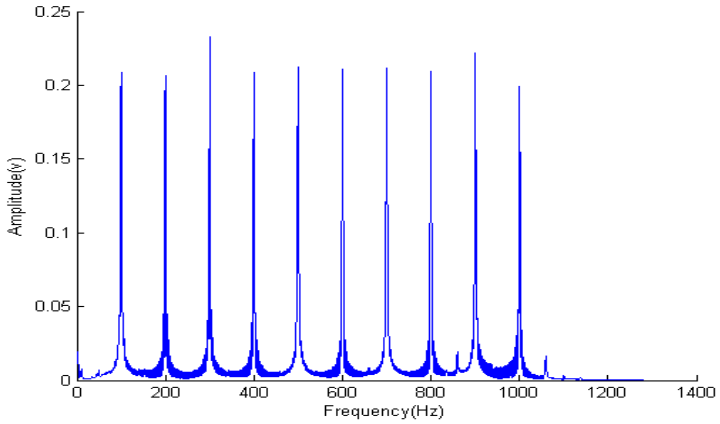

Figure 20. The frequency domain of the input signal

3.5.2 Sensors calibration

Before each recording session, the microphones, the loadcell and the speaker were calibrated to record accurately. The microphone was calibrated using a Larson Davis CA 200 which calibrates the microphone at 1000 Hz and 94 dB. According to the characteristics of

each microphone, pressure is converted to voltage by an appropriate factor, which was obtained from the Larson Davis CA 200.

Since the speaker could not generate a flat frequency response over the frequency range of 100 to 1000 Hz, the speaker was calibrated using a feedback loop to obtain a flat frequency response. The sine sweep signal with a frequency range of 100 to 1000 Hz with a step of 100 Hz was generated and recorded using the SigLab software. This sound was played by the speaker and recorded using the microphone which was placed 3 cm above the speaker and was connected to the Siglab. The amplitudes of the signal at each step frequency were calculated using a Fast Fourier Transform (FFT). After that, the calculated amplitudes at each step frequency were divided by the minimum amplitude to obtain the ratio factor. These ratios were multiplied by the amplitudes of the sine sweep function generated by SigLab to create another pre-recorded signal. This process was continued until the recorded signal had a approximately flat frequency response over a frequency range of 100 to 1000 Hz in three iterations. This process was shown in Figure 21(a). The frequency response of speaker in each step was plotted as shown in Figure 21(b).

(a)

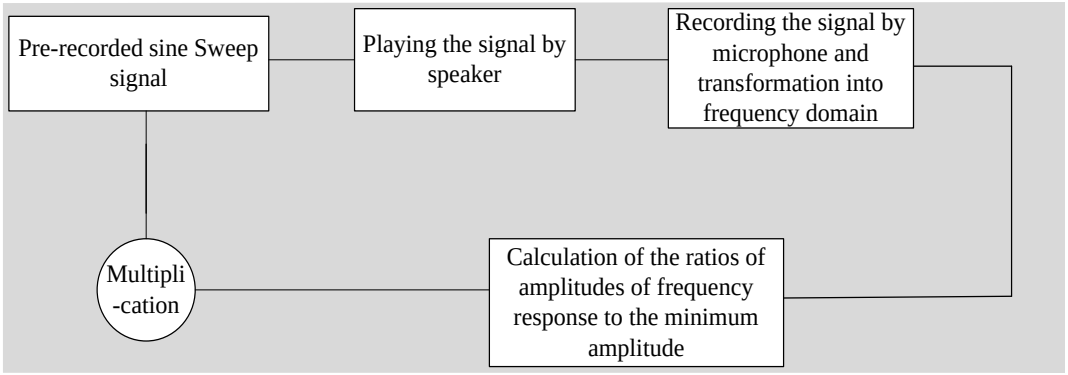

(b)

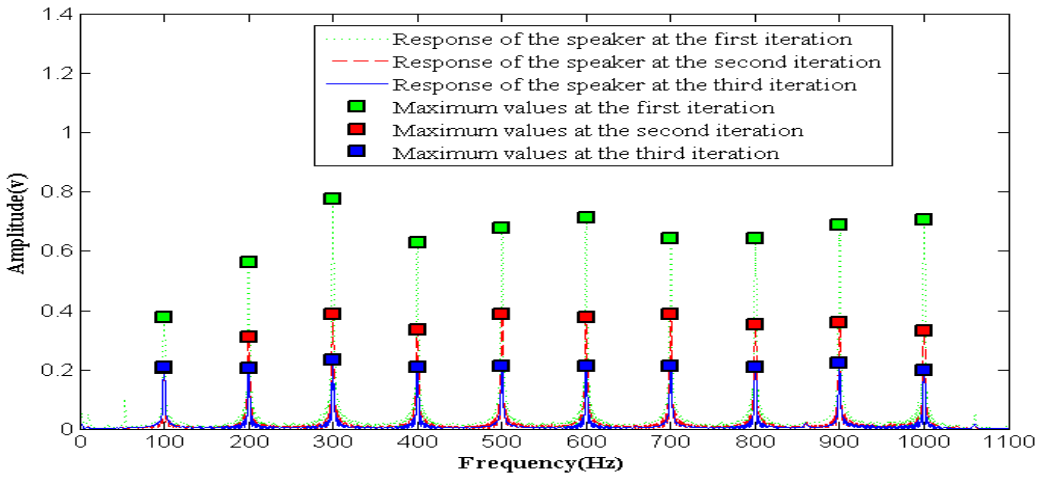

Figure 21. (a) Diagram of speaker calibration, (b) responses of speaker at each iteration

3.5.3 Environmental conditions and noise cancelling

The measurement was performed in a room that was quiet, but not sound proofed. The ambient noise was recorded during each measurement using a microphone placed on the outside of the model close to the main microphone.

In each measurement, the signal to noise ratio (SNR) was significantly small. However, the recursive least square (RLS) adaptive filter was applied to the signal to remove the noise from the main signal. The RLS adaptive filter consists of a transversal filter with finite impulse response (FIR) and an RLS algorithm which recursively finds the filter coefficients that minimize a weighted linear least squares cost function relating to the input signals. A schematic view of the adaptive filter is presented in Figure 22, which shows the input or reference signal $r(n)$, the adaptive filter output $y(n)$, the primary input $d(n)$ and the de-noised signal $e(n)$.

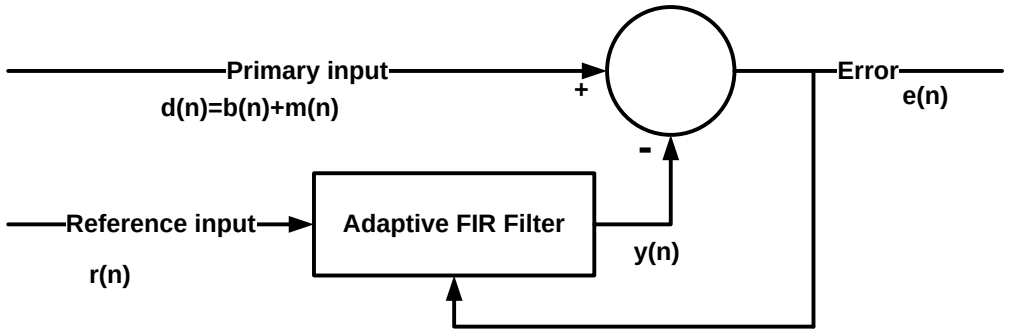

Figure 22. Schematic view of adaptive filter

According to Figure 22, a signal $d(n)$, recorded by using a microphone located at the trachea of the model, consists of a transmitted signal $b(n)$and ambient noise $m(n)$. A reference input which was captured using a second microphone placed outside of the model was provided into an adaptive FIR filter to minimize the error between primary and reference signal by updating the filter weights. The reference signal was arranged in an $M \times N$ rectangular matrix $u(n)$ using the covariance method of data windowing, where M is filter order (32 in this study) and N is the length of input vector. The signal output was calculated using the following equations:

$$K(n) = \frac{\lambda^{-1}P(n-1)u(n)}{1+\lambda^{-1}u^{H}\,(n)\,p(n-1)u(n)} \quad (1)$$

$$y(n) = \dot{w}^{H}(n-1)u(n) \quad (2)$$

$$e(n) = d(n) - y(n) \quad (3)$$

$$\dot{w}(n) = \dot{w}(n-1) + K(n)e(n) \quad (4)$$

$$P(n) = \lambda^{-1}P(n-1) - \lambda^{-1}K(n)u^{H}(n)P(n-1) \quad (5)$$

where $P(n)$is the inverse correction matrix at step n. The matrix P is initialized as $P(0) = I\delta$, where I is the identity matrix and δ is a regularization parameter which was chosen as less than 0.01 times the variance of the primary input [77]. The λ is a forgetting factor which represents the memory of the algorithm, and for this study λ=1, which implied infinite memory. The $K(n)$ and $\dot{w}(n)$ are the gain vector at step n and the vector of the filter of step estimation at step n respectively. The signals recorded by applied sound at a position of 40° on the circumference and axial position 175 mm, using a first and second microphone, are presented in Figure 23 (a) and (b) respectively. The de-noised signal after applying an RLS adaptive filter is also displayed in Figure 23 (c).

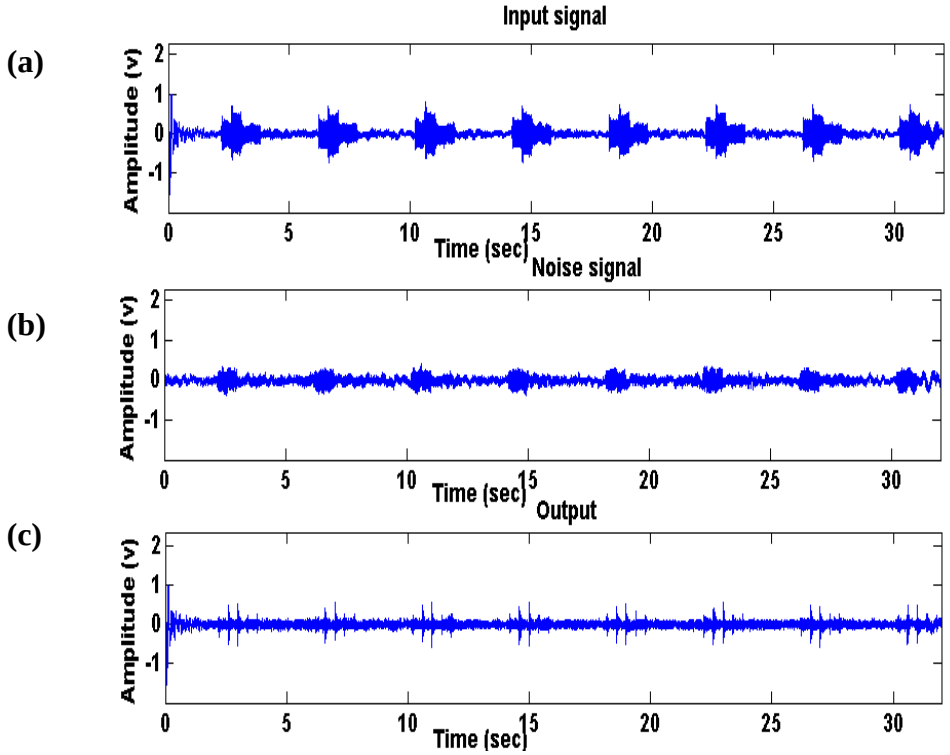

Figure 23. (a) Input signal recorded at angular position 40° and axial position 175 mm; (b) noise signal ; (c) the output signal after noise cancellation

3.5.4 Data analysis

The data analysis was performed using the mathematical software (MATLAB®, Natick, MA, USA) and was processed offline. After the ambient noise was removed from the recorded signal using the RLS adaptive filter, the signal was transformed into the frequency domain using a FFT. Since the applied signal comprises sine waves at frequencies of 100 to 1000 Hz with a step of 100 Hz, the amplitudes of the signal at those frequencies were obtained. These processes were performed for thirty measurements at each grid position around the model. The average amplitude of the signal for each position around the model was computed, as shown by the blue bar at Figure 24 for the signal recorded for the healthy model an axial position of 135 mm and angular position of 40°. The standard deviation for each frequency was computed as plotted by the red line in Figure 24. To obtain the frequency response of the system at the other frequencies, a curve was fitted to the average amplitude using a 1-D cubic interpolation method, which is shown with a green line in Figure 24.

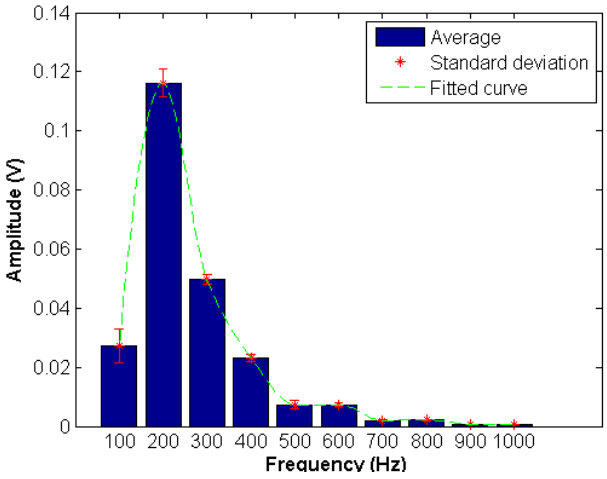

Figure 24. Calculated data of healthy model at the axial position of 135 mm and angular position of 80°

After the computation of the frequency response of the model for all frequencies between 100 Hz and 1 kHz, the data was plotted as a function of frequencies, angular positions of measurement around the model with the same axial position, and amplitude in 3D format, as shown in Figure 25- 30.

3.5.5 Results and discussion

To investigate the effect of the bulk of fluid on the frequency responses of the system, the measurements were performed in both healthy and pleural effusion phantom models. The results of frequency responses for the healthy model with the axial position of 175 mm are presented in Figure 25. The results show that the frequency responses at the angular positions between 80 and 120° have an amplitude of approximately 220 Hz. Moreover, semi-symmetric behaviour can be observed. The model acted like a low pass filter, which means that the signal attenuated at high frequency, as discussed in the study of Reichert et al. [37].

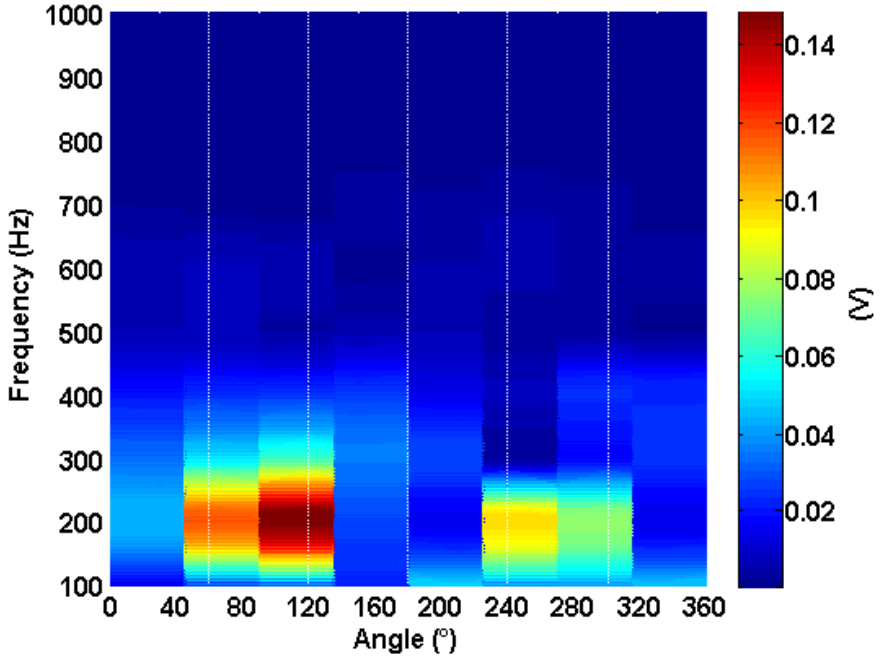

Figure 25. The frequency responses of the healthy model with axial position of 175 mm

The frequency responses of the healthy model recorded at an axial position of 105 mm are displayed in Figure 26. The highest amplitudes of the signals occur at the angular positions between 320 and 360°. This is most likely due to the locations of the bronchial tree, such that the applied sound can pass a shorter distance through the foam, or because of a resonance effect. The results also show that the level of attenuation at frequencies above 500 Hz is significantly high.

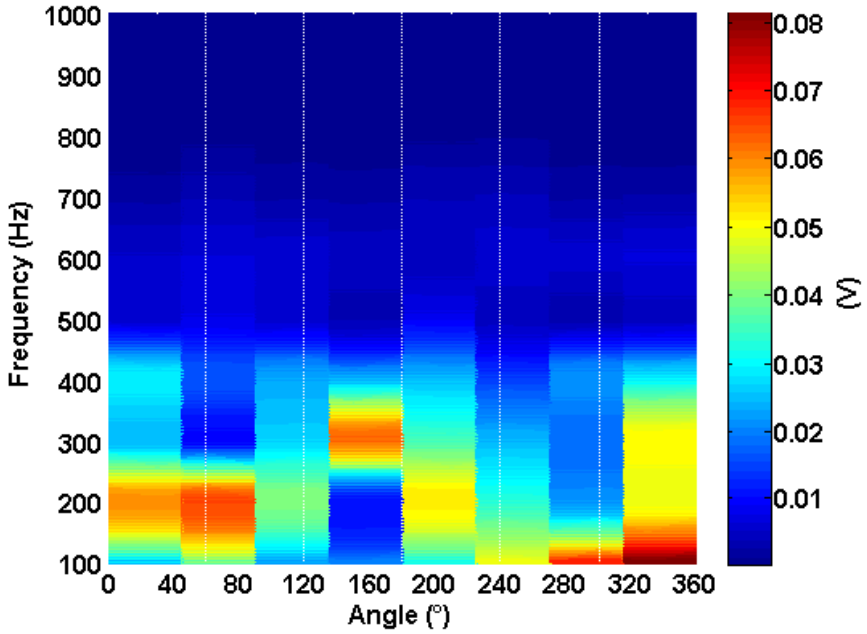

Figure 26. The frequency responses of the healthy model with axial position of 105 mm

Figure 27 shows the frequency responses of the healthy model with an axial position of 35 mm. The highest amplitudes occur at the locations on the model with angular positions of 80 - 160°, and at frequencies between 180 and 220 Hz. Furthermore, no symmetric behaviour can be observed.

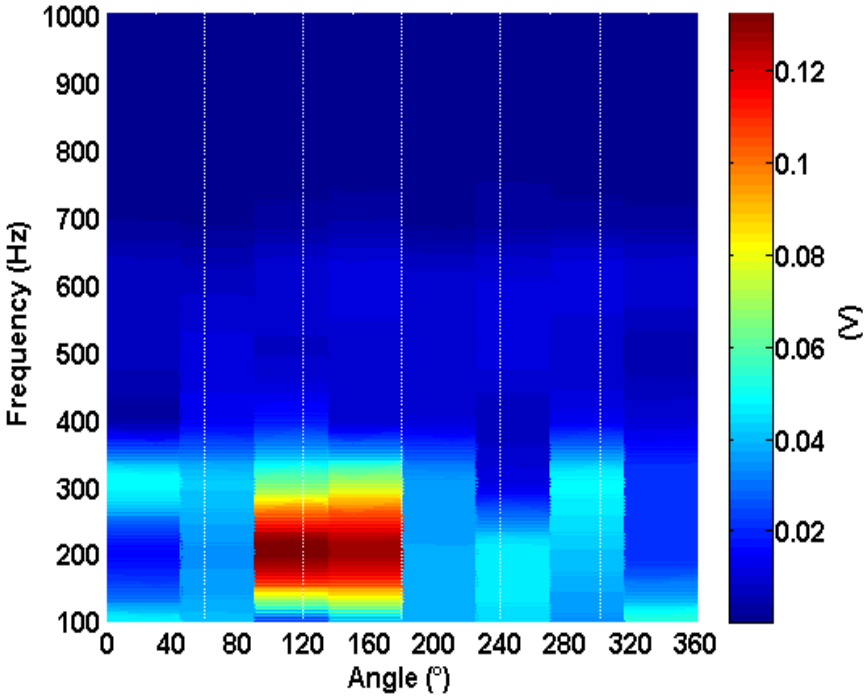

Figure 27. The frequency responses of the healthy model with axial position of 35 mm

The results from the model with two plastic bags in place for modelling the pleural effusion were plotted in Figure 28-30. The two plastic bags were located at angular positions of 80 - 120° and 220 - 260° approximately, as shown in Figure 17. Figure 28 shows that the highest amplitudes occur at the locations with angular positions of 80 - 120° and 220 - 260°, at a frequency of 200 Hz. These positions correspond to the angular locations in the model where the water bags were placed. By comparing the results of the healthy model and the pleural effusion model with same axial position (Figure 25 and Figure 28 respectively), the locations of the plastic bags are clearly detectable.

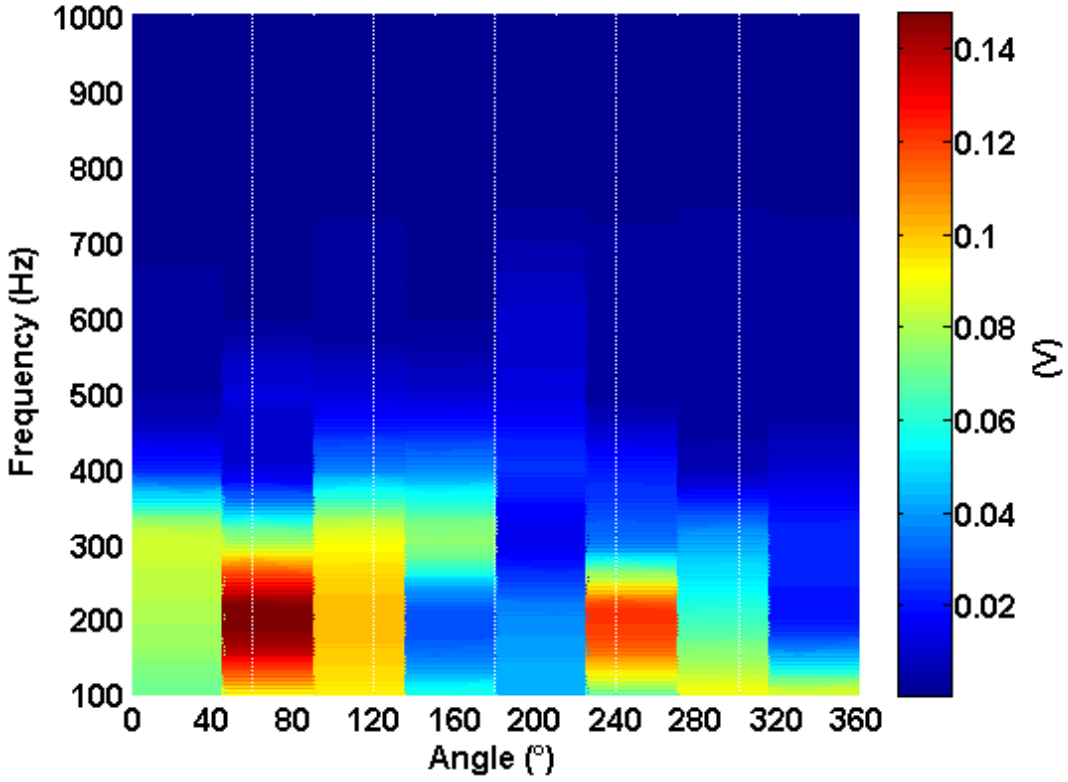

Figure 28. The frequency responses of the pleural effusion model with axial position of 175 mm

The frequency responses of the model at the axial position of 135 mm are shown in Figure 29. The calculated results show that the highest amplitudes occur at the locations with angular positions of 280 - 360°. By comparing Figure 26 to Figure 29 (i.e., corresponding to the results of healthy model and plural effusion model respectively), the bulk of fluid is easily detectable.

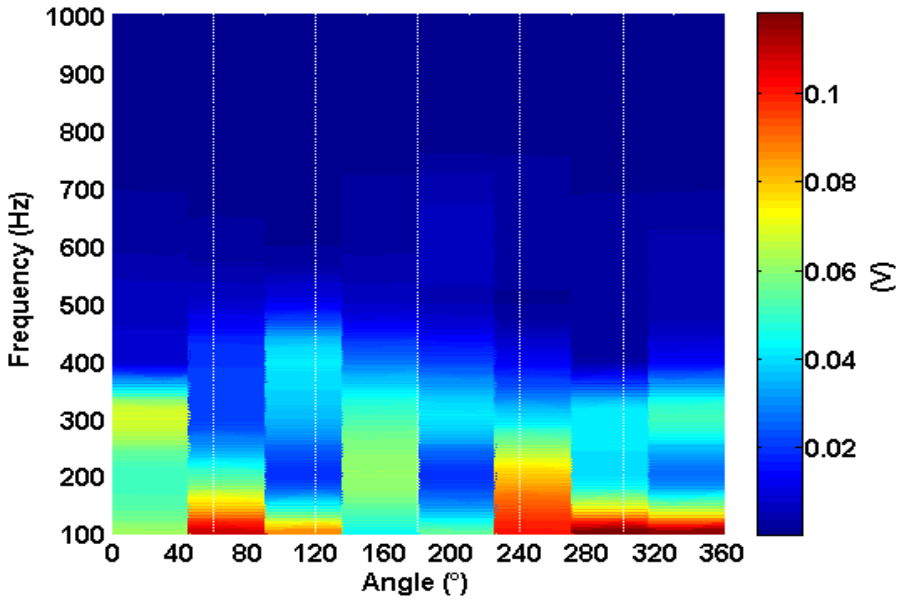

Figure 29. The frequency responses of the pleural effusion model with axial position of 135 mm

The results of the pleural effusion model with axial position of 35 mm are plotted in Figure 30. As the results show, the maximum amplitudes occur at the locations with angular positions of 80 - 120° and 220 - 260° (i.e., corresponding to the angular locations in the model where the water bags were placed). Although there is no bulk of fluid at the axial position of 35 mm, the location of the fluid is still detectable because the sound was propagated in all directions as it passed through the bulk of fluid to reach the microphone located at the trachea of the model.

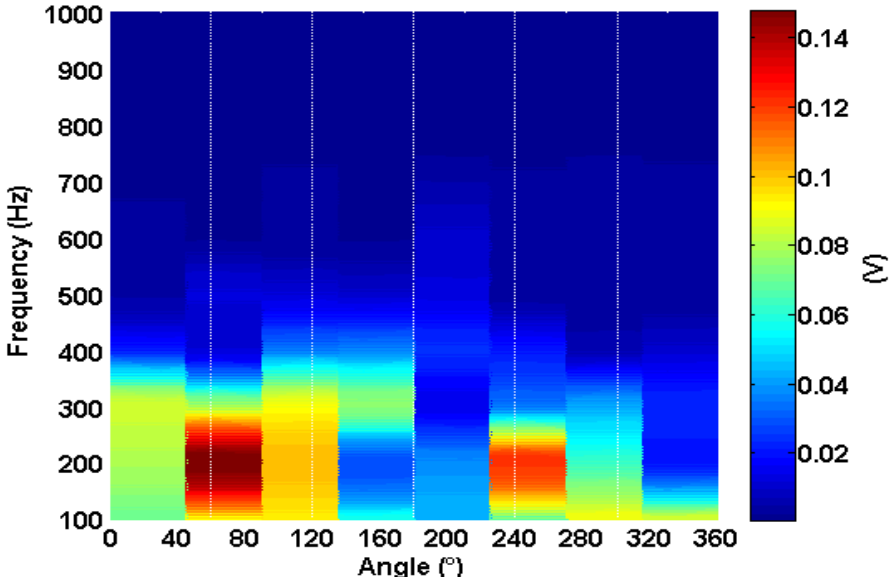

Figure 30. The frequency responses of the pleural effusion model with axial position of 35 mm

The evaluation of the use of the frequency responses for detection of pleural effusion in the phantom model by applying the signal from the chest of model showed that this technique could be used in human subjects for detecting fluid. However, it was found experimentally that the amplitude of the received signal was strongly depends on the force applied to the chest of the model. Therefore, using this technique for human subjects requires a lot of equipment, and it would therefore be impractical to use this technique in a clinical environment.

3.6 Investigation of time delay estimation in the detecting of pleural effusion

Since the speed of sound in the fluid is much greater (approximately 60 times faster) than it is in the lung parenchyma, the evaluation by using the transient time of the transmitted sound through a phantom model of the lung was performed as a novel technique for detecting pleural effusion. This section will be followed by a description of the data acquisition system, data analysis, results and discussion and conclusion.

3.6.1 Data acquisition

A full range Viston 4692 FX 10 speaker was connected to a 250 mm long funnel in such a way that the entire surface of the speaker was covered. The funnel was placed at the trachea of the phantom model as presented in Figure 31. The speaker was driven with a linear frequency modulation (chirp) signal over a frequency range of 100 to 250 Hz. The chirp signal was transmitted because it has a sharp autocorrelation function which allow clearly peak detection. A frequency range of 100 to 250 Hz was selected, as it was found experimentally that signals with frequencies above 250 Hz were severely attenuated by the model and the speaker limited the lower frequency to 100 Hz.

The signal was amplified using a Technics SU-V300 amplifier. The amplification factor was adjusted and fixed for all measurements. A PCB Piezotronics Inc. 333B32 piezoelectric accelerometer was placed inside the funnel, close to the speaker. The sound was introduced into the model from the trachea and then passed through the model to the chest wall. Measurements were made at 24 points that form a grid around the cylindrical surface of the model. Eight piezoelectric accelerometers were connected to the chest wall of the model

using cyanoacrylate glue at equal angular positions from the centre of the model, as shown in Figure 31 and 32. The test was performed at three equally axial positions as indicated in Figure 19.

The data were digitized using an analogue to digital convertor (LMS Instrument Co, SC305) and were saved to a laptop computer simultaneously at a sampling frequency of 51200 Hz. Each data acquisition segment consisted of 16384 samples per channel which is equivalent to 0.32 seconds. After the data were recorded, the latex plastic bag filled with 600 ml of water was removed from the phantom model. The experiment was repeated on the model to evaluate the effect of the bulk of water on the measurements. The experimental equipment is summarized in Table 5.

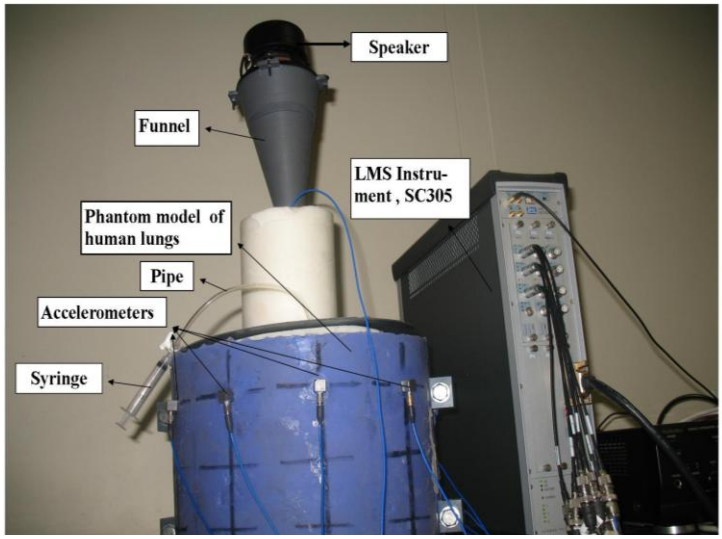

Figure 31. Experimental setup

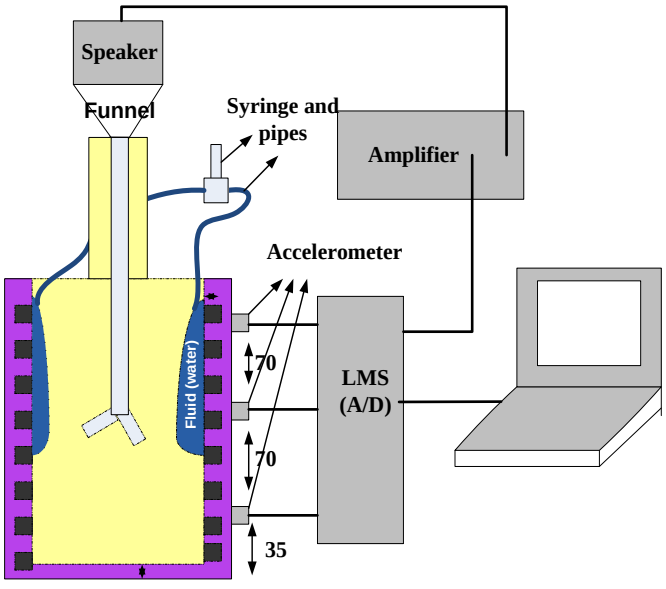

Figure 32. Schematic of experimental setup

Table 5. Summary of experimental equipment

Description	Type
Speaker	Visaton 4692 FX 10
Accelerometers	A PCB Piezotronics Inc. 333B32
Funnel	PVC custom-design
Amplifier	Technics SU-V300 LMS
Audio to digital convertor	Instrument Co, SC305

3.6.2 Data analysis

After digitization, the data were saved on a laptop computer. The signals recorded by the accelerometers were imported to the mathematical software (MATLAB®, Natick, MA, USA) and processed offline. The signal from an accelerometer mounted in the funnel was used as an input *x(n)* while the other eight accelerometers represented the output signal $y(n)$, where (n) is the sample number in the time domain. To estimate the time delay, the cross correlation function (CCF) of the input and output signals was calculated using:

$$R_{xy}(\tau) = \sum_{n=1}^{N-\tau} \frac{x(n)y(n+\tau)}{N} \quad (6)$$

$$D = arg\max\,(R_{xy}) \quad (7)$$

Here N is the number of samples in the records. R_{xy} has a maximum value when τ is the actual time shift between the input and output signals. The time delay was calculated by identifying the peak of highest magnitude on the CCF.

3.6.3 Results and discussion

The reference signal is shown in Figure 33(a). Since the speaker could not generate a flat signal over a frequency range of 100 to 250 Hz, the signal has a maximum value at 175 Hz and decreases over time, as shown in Figure 33(a). The recorded signal at the angular position of 80° and axial position of 105 mm (i.e., corresponding to the angular location in

the model where the 240 mm water bag was placed) is displayed in Figure 33(b). Figure 34 shows the corresponding cross correlation curve for the signal.

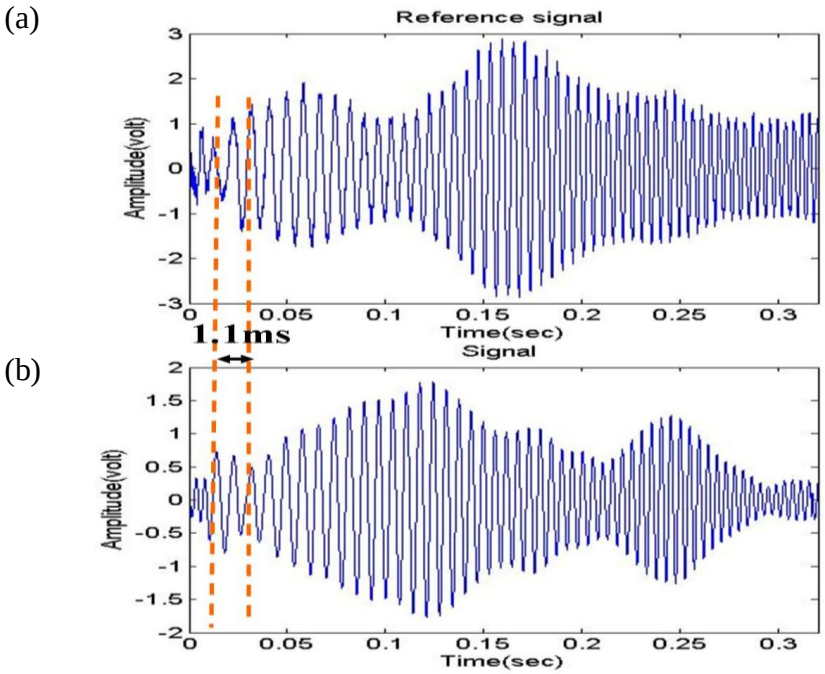

Figure 33. (a) Reference signal, (b) recorded signal at the angular position of 80° and axial position of 105 mm

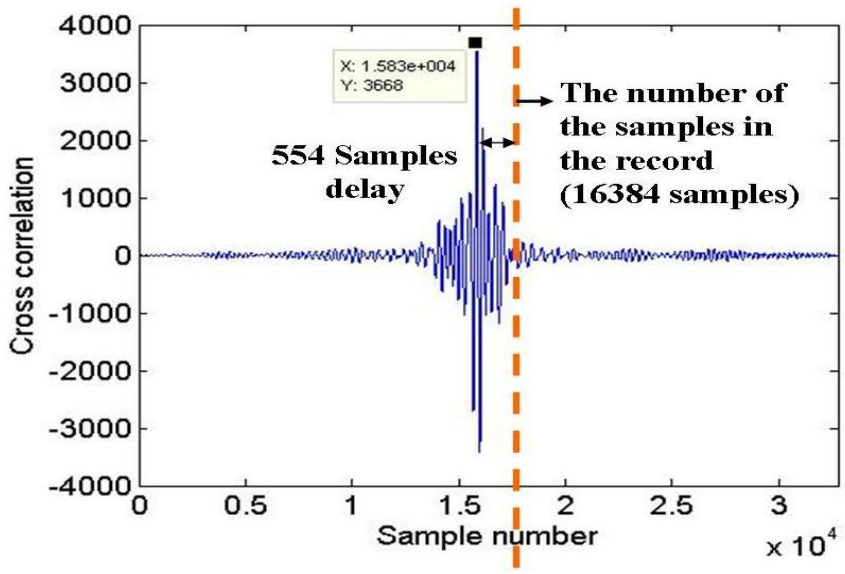

Figure 34. Cross correlation function corresponding to the reference signal and signal in signal in Figure 33

The calculated time delay for the pleural effusion model is plotted in Figure 35. The results show that the estimated time delays at the angular positions of 80 and 240° with axial positions of 105 and 175 mm (i.e., corresponding to the angular locations in the model where the water bags were placed), were significantly less than observed at other measurement locations. At 80° the estimated time delay was as much as 54% less than at other adjacent points, while at 240 degrees it was as much as 62 %. This occurs because the speed of sound in the water is significantly greater (approximately 54 times faster) than the speed of sound in the Felex foam.

The average time delay at the axial position of 35 degrees was 15% and 23% larger than the average time delay at axial positions of 105 and 175 mm respectively. This occurred because the speed of sound in Flex foam is 27.5 m/s and because the sound has to travel a longer distance to reach the surface of model.

The estimated time delays at 80° with axial position of 105 mm and 175 mm (i.e., corresponding to the angular location in the model where the fluid was placed) were 27% and 52% respectively less than at other adjacent points with same axial position, as shown in Figure 36.

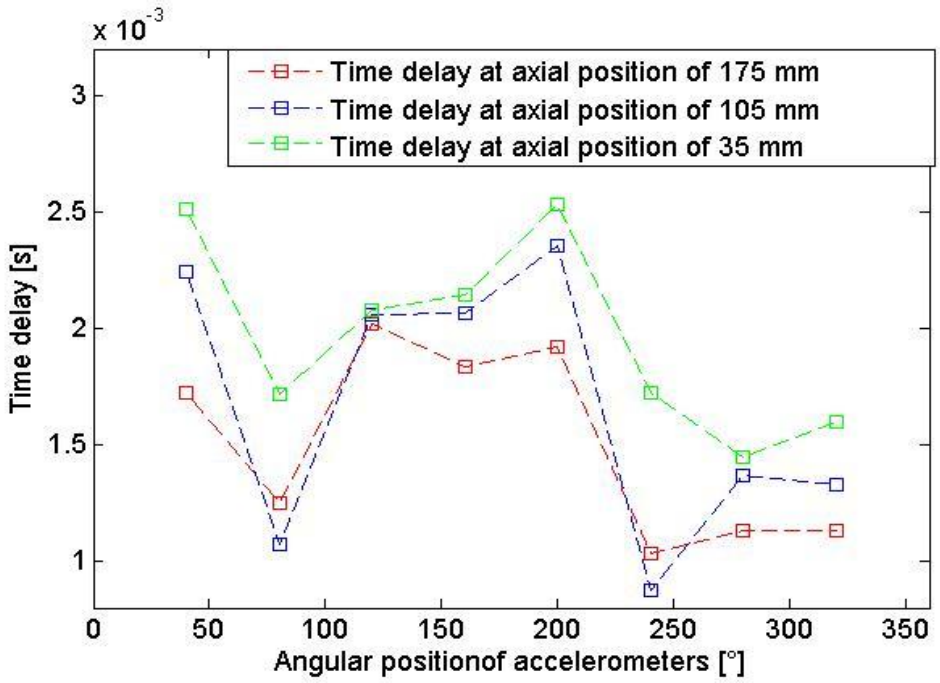

Figure 35. Time delay calculated in the phantom model of the lungs with two water bags on either side.

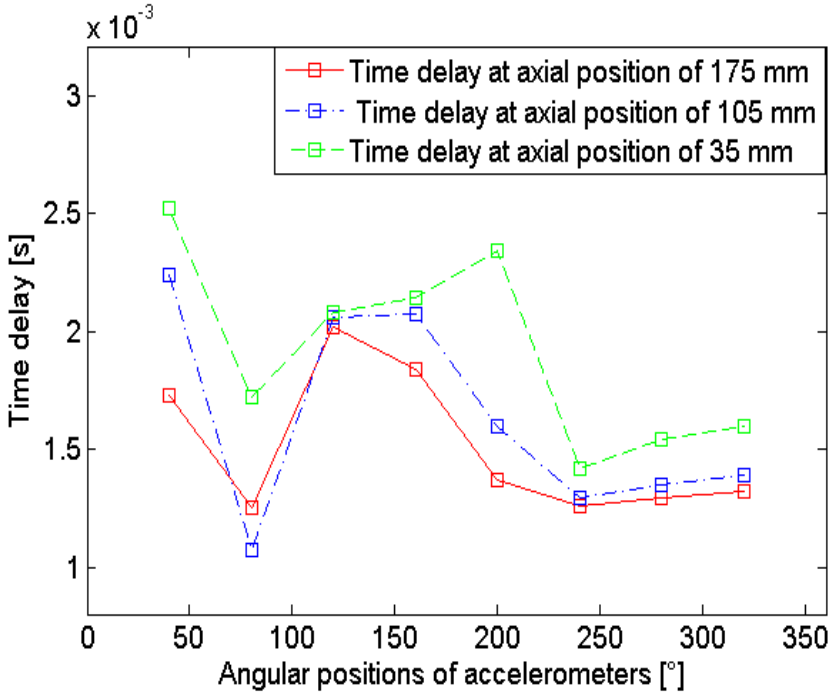

Figure 36. Time delay calculated in the healthy phantom model of the lungs (without water inside)

The estimated time delays at 240° with axial positions of 175 mm and 105 mm (i.e., corresponding to the angular location in the model after removing the 600 ml plastic bag) are 2.4 % and 4% less respectively than those of adjacent points with a similar axial position. The results also show that fluid in the model has a significant effect on the estimated time delay.

Since the results show that the fluid has a significant effect on the time delay, this technique may be used as a diagnosis technique in a clinical setup. However, the effect of different sizes of lungs and of gender should be investigated in future research.

3.7 Chapter summary

In this chapter, the phantom model, which has similar acoustic properties to the respiratory system, was developed in order to test hypotheses on the model. Two models of the lung were fabricated: a healthy model and a pleural effusion model. Pleural effusion was modelled using two plastic bags filled with 600 ml and 250ml of water respectively. The evaluation of frequency responses in fluid detection was performed on the model by applying the sound into the model from the chest wall of the model. The experiments were carried out for both the healthy model (without any fluid inside) and the pleural effusion model (two plastic bags filled with water were placed inside of the model). The sound was recorded

using a microphone located at the trachea of the model. The noise signal was recorded instantaneously and it was subtracted from the main signal using an adaptive noise cancelling algorithm. The frequency responses were computed using the a FFT. The results show that the positions of fluid are indeed detectable by comparison of the healthy model with the pleural effusion model. However, since the amplitude of the received signal depends on the applied force behind the speaker, performing this technique for clinical studies requires a lot of equipment. Therefore, it would be impractical to use this technique in a clinical environment.

Since the speed of sound in the fluid is much greater than the speed of sound in the lungs (approximately 60 times faster), the evaluation of using time delay estimation in fluid detection in the model was also performed. A chirp signal with a frequency range of 100 to 250 Hz was transmitted into the model of the lung. The time delay between transmitted sound and sound received from the chest of the model was calculated using cross correlation. The results show that the calculated time delays at points on the model corresponding to the locations where two plastic bags are located (simulating pleural effusion) are significantly less than at other points. This technique may lead to the developmental of an inexpensive, non-invasive and accurate diagnostic tool which can be used in clinical settings. The next stage of this research is to evaluate this technique in human subjects, and is the subject of the following chapter.

4. Clinical study

4.1 Introduction

In the evaluating active acoustic methodology for the detection of fluid in the model, the results have indicated that this technique can be used for a clinical study. In this chapter, the results of using the methodology for the detection of pleural effusion are presented. Furthermore, current technique in computation and measurement of transient time of transmitted sound in the respiratory system is developed.

This chapter also details the development of the data acquisition system to perform the AAM in human subjects, including discussions of the data acquisition procedure and data analysis performed. The effects of inhalation and lung size on transient time of the acoustic signal for healthy patients, are elaborated on. Finally, the case study using AAM in the detection of fluid is also discussed.

4.2 System development

Currently, two commercial devices are available to measure lung sounds: Multi Channel Stethograph® and Deep Breeze VRIxp™®. The Multi Channel Stethograph consists of 16 electronic stethoscopes embedded in foam padding, as shown Figure 37(a), a signal conditioning box, and a standard PC. The device can record and display the lung sounds. The acoustic energy of the recorded sounds can be computed to detect wheezes, crackles and rhonchi. The main advantages of the device are low cost, a fast setup and simplicity. However, the Multi Channel Stethograph has some limitations, such as that it cannot be used for patients with different body sizes, as the microphones are fixed in the foam. Moreover, this device can record and analyse the lung sounds only from the posterior chest.

Deep breeze VRIxp™© has forty active piezoelectric contact sensors and two inactive contact sensors, as presented in Figure 37 (b). These sensors are assembled in two planar arrays and attached to the posterior chest of the subject by using a computer controlled low vacuum. The device can record and visualize the vibration response of the lungs. Furthermore, it can automatically detect adventitious lung sounds such as wheezes and crackles. The main advantage of the device is that it can analyse the lung sounds and create a

grey image of the lungs. However, it cannot record the lung sounds from the anterior and lateral sides of the lungs and it cannot be used for patients with different body sizes.

Because of the limitations of the commercial devices at Tygerberg Hospital, South Africa, a data acquisition system was developed to perform AAM in human subjects. The data acquisition system consists of hardware equipment to transmit sound into the respiratory system and to record the transmitted signal on the chest.

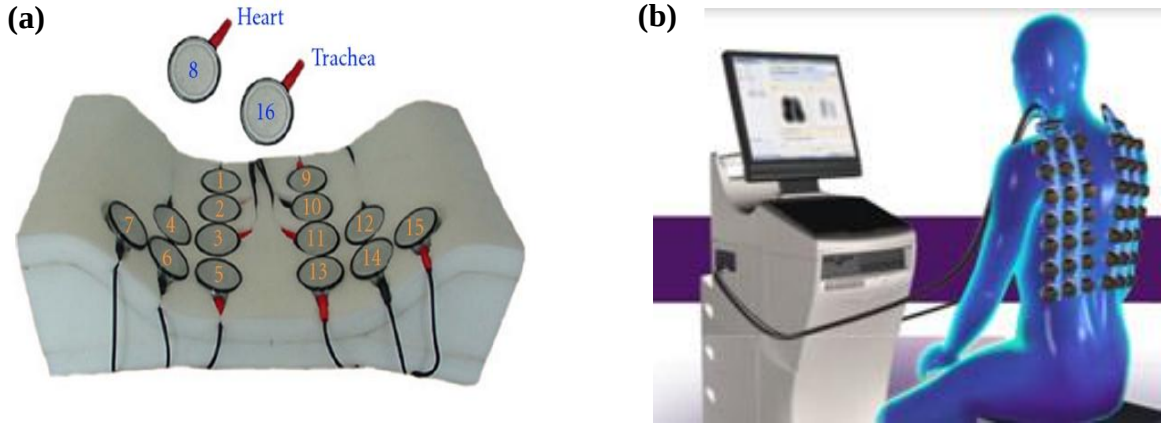

Figure 37. (a) Multi Channel Stethograph [78], (b) deep breeze VRIxp™ [79]

4.2.1 Stethoscope designs

Commonly, there are two kinds of transducers to measure the lung sounds: electret microphones with a coupling chamber, and accelerometers. Small electret microphones are widely used to record speech and music. These microphones can be used to record lung sounds when they are coupled to the skin by a sealed chamber [80]. Karman et al. [81] found that the diameter and shape of the air coupler chamber have no significant effects on the detected sound. However, Wodicka et al. [82] suggested that stethoscopes with smaller cavity depths are more appropriate to measure the lung sounds over a wider bandwidth. The accelerometer is another type of transducer which has been used in several studies [45-47]. Generally, accelerometers are more expensive than microphones. Therefore, microphones were used as transducers in this study.

The custom-designed stethoscope, based on the standardization of respiratory sound measurement [83], consists of Panasonic® Omni-directional Back Electret Condenser Microphone WM 61A Cartridges placed in a conical plastic housing. The microphone has a

signal–to–noise ratio of 62 dB and flat frequency response of 20–20000 Hz, as recommended by Vannuccini et al [83] . The chamber of the stethoscope housing is vented by a 1 mm hole to equalize internal pressure to ambient. The couplers have a depth of 5 mm and the conical shape tapers to a 15 mm diameter at the skin as suggested by [81-83][2-4]. The stethoscope housing is shown in Figure 38(a) and (b). Development and machining was carried out at Stellenbosch University, South Africa.

(a) **(b)**

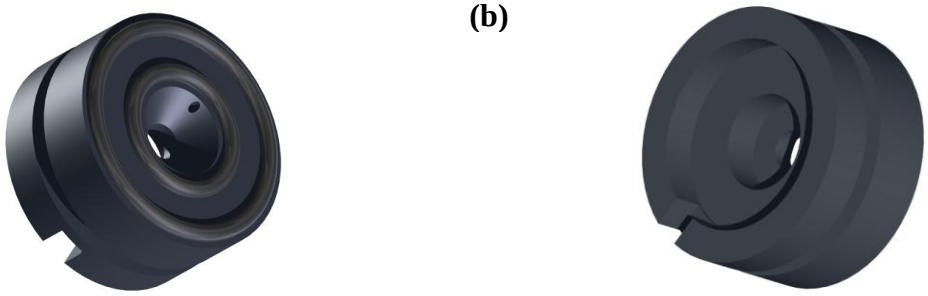

Figure 38. (a) Front view of stethoscope housing, (b) rear view of stethoscope housing

The signals of all microphones were offset by 2.5 Volt. Additionally, the signal was amplified in two stages; at first, the signal was amplified with gain 30 by a Burr Brown OPA343 single-supply, rail-to-rail operational amplifier. After first stage amplification, the signal was amplified by a maximum gain of 10, using a second Burr Brown OPA343 amplifier. The gain of the second amplifier can be decreased by changing the value of a variable resistor. After amplification, the signal was transmitted to the SigLab using BNC cables. The specifications of the stethoscope design and amplifier are summarized in Table 6. The design of the amplifier for the microphones was based on Becker's studies [35].

Table 6. Stethoscope design and amplifier specification

Stethoscope specifications	
Shape	Conical vented
Diameter	15 mm
Depth	5 mm
Microphone	Panasonic® WM 61A

Amplification specifications	
Chip	Burr Brown OPA343
Offset	2.5 v
Max voltage	5 V
Gain	Max(10×30=300)

4.2.2 Data acquisition system

The final hardware setup consists of a laptop, three SigLab 4246 systems, a speaker, ten custom designed electronic stethoscopes, a funnel, disposable cardboard mouthpieces and BNC cables. A full range Viston FX 10 speaker was connected to a 250 mm long funnel so that the funnel covered the entire surface of the speaker. A disposable cardboard mouthpiece, which has one-way air flow valves for infection protection, was attached to the funnel as shown in Figure 39. The funnel was designed so that the mouthpiece can easily be removed and replaced.

The mouthpiece connected to the funnel and speaker was placed in front of the mouth of the subjects, using a RexRoth aluminium arm as shown in Figure 39. The aluminium arm was attached to the table as is shown in the Figure 39.

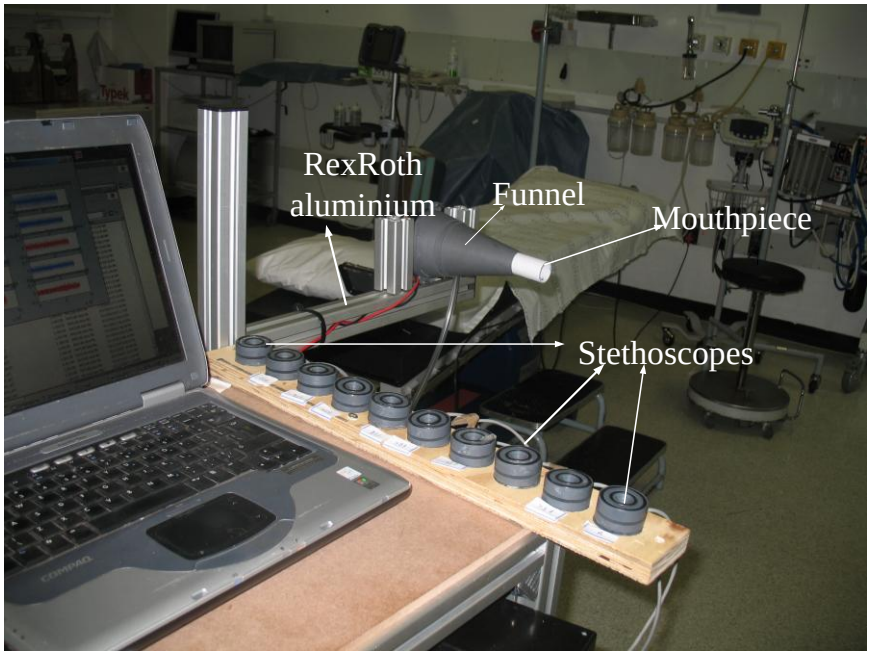

Figure 39. The view of acquisition system

The speaker was connected to the Technics SU-V300 amplifier for amplification of the applied sound. The SigLab was used to generate the pre-recorded sound which was created using (MATLAB® Natick, MA, USA). The sound was passed through the respiratory system from the introduction at the mouth to reach the chest wall. After that, the sound was recorded by nine electronic microphones attached to the chest of the subject using elastic straps and double sided tape. The elastic straps were used for the stethoscopes connected to the lower side of the chest wall, below the fourth rib. Double sided tape with a 15 mm hole through the tape was used for the stethoscope attached to the upper side of the chest wall, above the fourth rib. One more stethoscope was used to measure ambient noise during the measurement. The ten electric stethoscopes were connected to the amplification box to amplify the received signal. The amplified signals were transmitted to the Siglab systems using BNC cables for digitization.

To measure the lung volume during inhalation, a sturdy piezoelectric respiration transducer, 1132 Pneumotrace, was used. The Pneumotrace II was connected to the Kemo ® BM 8 amplifier and the data was recorded by laptop using the SigLab. A schematic of the data acquisition system is shown in Figure 40.

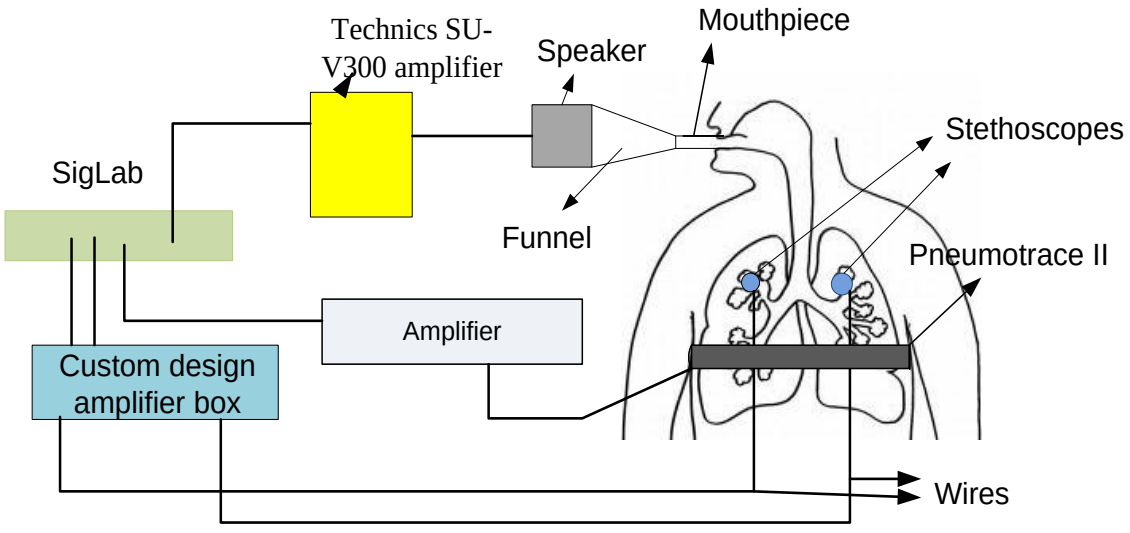

Figure 40. Schematic view of the data acquisition system

4.2.3 Transmitted signals

To measure the transient time in the lungs, different types of signals have been transmitted in several studies over the past few decades. However, different values were reported in various studies, for example the time delay of applied sound in the lungs measured in a range of 1-6 ms according to Bergstresser et al. [69] while in the other studies measured between 4 and 13 ms [70]. The precise transient time of transmitted sound in the lungs is still unclear due to the complex structure of the human lungs. In order to calculate the time delay accurately, the applied signals should have a sharp auto correlation function to allow easier detection. Moreover, the applied sound should have minimal attenuation in the lung. Since the human lung acts as a low pass filter, filtering the signal with frequencies above 250 Hz, the applied signal should have frequencies of less than 250 Hz. It was found experimentally in this study that the speaker used could not generate sound with frequencies less than 100 Hz. To overcome the above limitations, two types of signal were transmitted into the lungs to accurately measure the time delay in the respiratory system.

Polyphonic sound, which was used in study [69], was transmitted into the respiratory system. The signal contains 11 cycles in which the cycle frequencies varied in the following pattern (130, 130, 140, 140, 150, 150, 150, 140, 140, 130 and 130 Hz). The amplitude of the signal increases linearly until the middle of the signal and then it decreases linearly, as shown Figure 41.

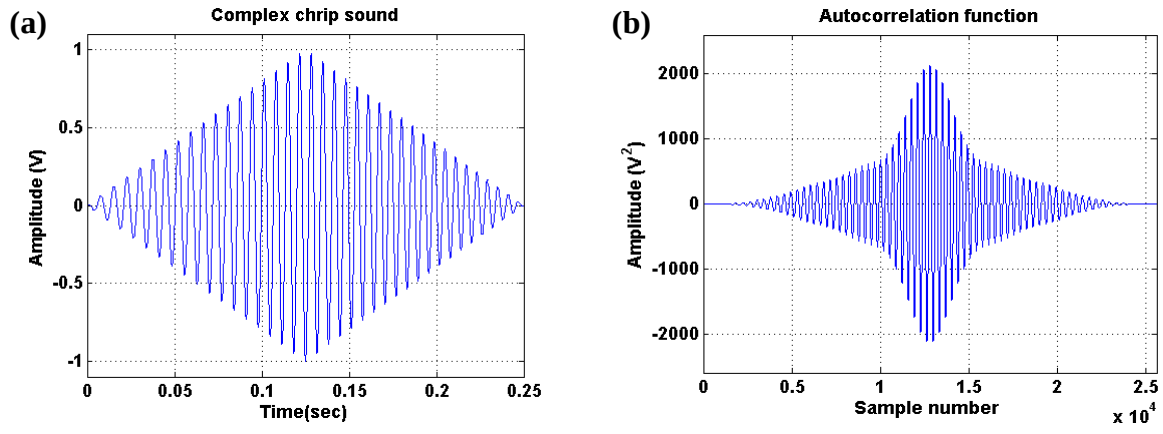

Figure 41. (a) Polyphonic sound, (b) autocorrelation function of polyphonic sound

The linear frequency modulation signal (chirp signal), with frequencies between 130 Hz and 150 Hz, was also transmitted into the respiratory system. The signal contains all

frequencies between 130Hz and 150 Hz with the frequency linearly increasing over the time period of the signal. This signal has a sharper autocorrelation function. The amplitude of the signal is a complex triangular shape with dominant peak at the middle of the signal. It was found experimentally that if the signal has a dominant peak at the middle of signal, the time delay could be easily calculated. The signal and the autocorrelation function associated with the signal are plotted in Figure 42(a) and (b) respectively.

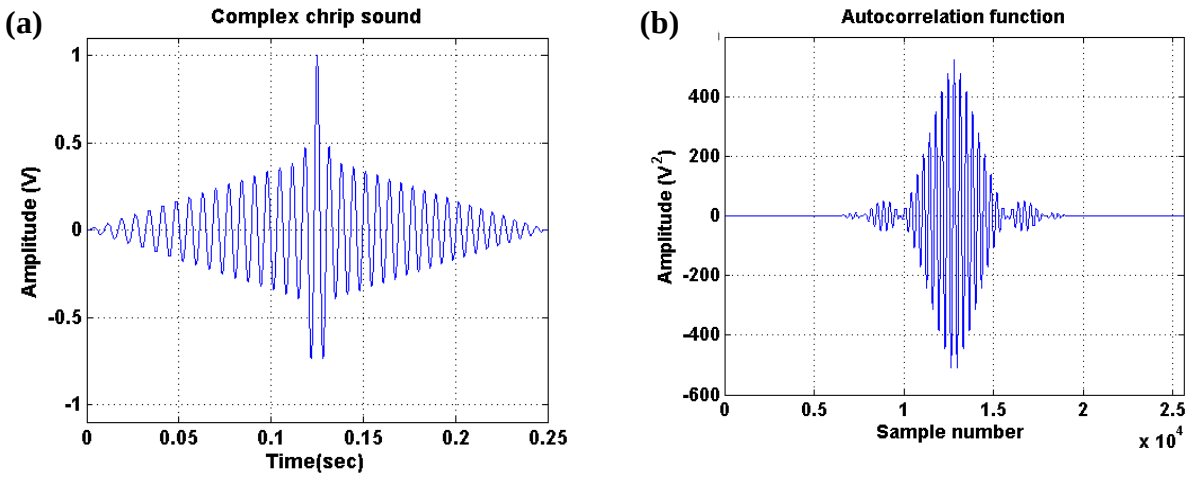

Figure 42. (a) Complex chirp sound, (b) autocorrelation function of complex chirp sound

Experimental measurement of the transient time of sound in the lungs, in previous studies, showed that the resolution needed for the measurement should not be less than 1 millisecond. To satisfy this resolution, the complex chirp signal and polyphonic signal were digitized at 12800 Hz which provided a resolution of 8×10^{-5} second. Each measurement which was recorded in 6.40 seconds thus contains 81920 samples. Table 7 is represented summary of transmitted sounds into the respiratory system.

Table 7. Summary of transmitted sounds into the respiratory system

Transmitted Signals for the measurement of transient time	Digitalization	Number of samples
Complex Chirp signal	12800	81920
Polyphonic signal	12800	81920

4.3 Research protocol of clinical trials

The application for clinical trials, which includes the protocol, consent form and budgets, was submitted to the Human Research Committee (HRC) at the Faculty of Health Sciences of Stellenbosch University. The protocol was reviewed and approved by the HRC. According to the protocol, the maximum study population consists of 52 participants, who have been diagnosed without any respiratory diseases and classified as the "healthy group", and 52 patients who have been diagnosed with pleural effusion and confirmed by X-ray, or ultrasound and who are classified as the "pleural effusion group". No additional tests are required for this thesis. The inclusion criteria and exclusion criteria include the following:

- All participants of this study are over the age of eighteen.
- Pleural effusion subjects were selected from a cohort of patients for clinical treatment at Tygerberg hospital. Pleural effusion should have been diagnosed using X-ray or ultrasonic imaging before performing the test.
- Healthy participants, who have not been diagnosed with any respiratory disease, were selected from students and medical personnel on the hospital and campus grounds.

According to the protocol, all data was stored anonymously in a password protected computer. Only the principal investigator and co-investigator had access to the data. The participants' names will not appear in any publications (thesis report, articles, etc.). Moreover, there is no benefit to the participants of this study. The research will prove beneficial to future designers and researchers in the field of biomedical engineering. After the protocol had been approved by HRC, recording commenced at the following places:

- The biomedical lab, which is located on the second floor of the Mechanical Engineering building at Stellenbosch University, for recording the healthy people.
- Theatre five at the pulmonary unit at Tygerberg hospital, for recording healthy subjects as well as those who were diagnosed with pleural effusion.

4.4 Signal acquisition processes

This section contains the recording procedure used to perform active acoustic methodology for the healthy subjects as well as patients with pleural effusion.

4.4.1 Stethoscopes calibration

To record sound accurately, all stethoscopes were calibrated before the recording session. To calibrate the microphones, sine waves with frequencies of 140 Hz, 250 Hz and 500 Hz were transmitted into each microphone, set to the same recording condition. The sounds were recorded on a computer and the amplitude of the transmitted sounds was calculated using an FFT. Based on the calculated amplitude, the gain of each microphone was adjusted to obtain the same amplitude for all microphones. This process was repeated five times to check the repeatability of measurement with the same signal.

4.4.2 Stethoscopes placement

To determine the transient time in the lungs nine stethoscopes were attached to the posterior and anterior chest of the participants. Although multiple stethoscopes have been used for performing the AAM, there is no study that used stethoscopes on both posterior and anterior of the chest at the same time. The positions of the microphones were determined during a meeting with Prof. Diacon in June 2012.

The positions of the nine microphones on the chest are displayed in Figure 43. One microphone was placed at the trachea as a reference microphone to record the applied signal, as shown in Figure 43. To assess the symmetrical behaviour of the human lungs, eight electronic stethoscopes were placed symmetrically on the chest of the participant as follows:

- Microphones were placed on the left and right anterior chest between the 2nd and 3rd intercostal spaces.
- Microphones were placed on the left and right lateral side of the chest between the 4^{th} and 6^{th} intercostal spaces.
- Microphones were placed on the left and right posterior of the chest between the scapula.

- Microphones were placed on the left and right posterior of the chest, below the scapula.

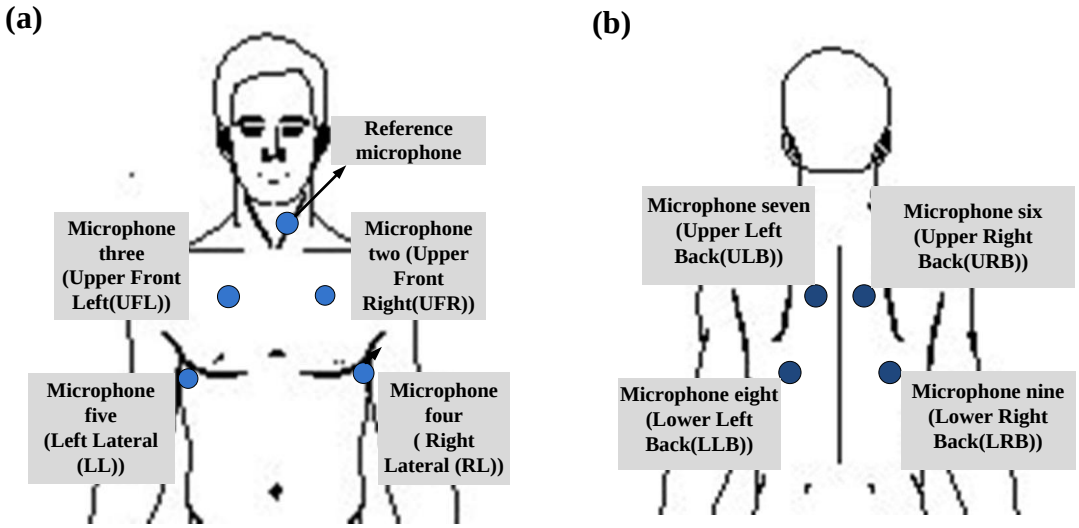

Figure 43. (a) Location of stethoscopes on the anterior chest, (b) location of stethoscopes on the posterior chest

4.4.3 Sound transmission recording procedure

Before beginning each recording, the objective of the project was explained to each participant. After that, an informed consent form was signed by the participant. Information such as age, gender and chest circumference were recorded.

In order to put digital stethoscopes on the chest of the participants, they were asked to remove their clothing as far as to expose the upper chest area. The participants were asked to sit on an adjustable chair. The stethoscopes were attached to the chest of the participant by using the double sided tape, with a 15 mm hole in it and elastic straps. The double sided tape was used to connect microphones two, three, six and seven according to Figure 43. Microphone four, five, eight and nine were connected to the body using elastic straps.

Before, the recording process is started, all equipment was checked and a pre-screening of the microphones was conducted. Moreover, all equipment was sterilized with the appropriate antibacterial cleaners. For each participant, a special mouthpiece was used which was disposed of after the recording session. For pleural effusion recordings, surgical masks and latex gloves were also used.

Two types of sound were transmitted into the respiratory system. Firstly, the complex chirp signal was transmitted the whilst participants were asked to put their mouth on the mouthpiece. After that, the participants were asked to exhale the air in their lungs through the nose. After this exhalation process, the data was recorded for 6.40 seconds during the inhalation. The inhalation and exhalation were monitored and recorded using the piezoelectric strap (Pneumotrace II). After each recording measurement, the data was monitored to check the quality of measurement. If no significant noise was recorded, the data was saved as a MATLAB file. To assess the repeatability of measurement, the above process was repeated three times. The polyphonic sound was also transmitted into the respiratory system by the same procedure in two recording sessions. A picture of a participant during the recording is shown in Figure 44.

(a) **(b)**

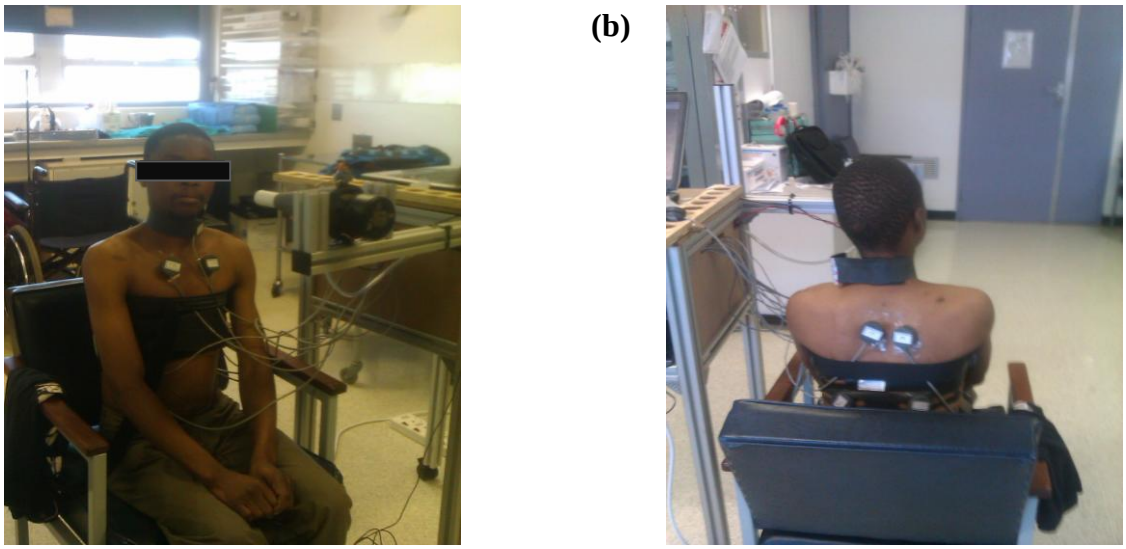

Figure 44. The pleural effusion recording from front view (a) and back view (b)

4.4.4 Environmental condition and noise

Since the measurements were performed in different locations, the environmental noise might have affected the measurements. Generally, there are two types of noise as a threat to recording in this study. Environmental noise, which includes all noise related to the environmental conditions, such as traffic sound, people talking, door slamming, nearby construction and electronic disturbances such as tube lights, fans and air conditioning. The

second main noise that could affect recording includes respiratory sounds, chest movement, heart beats, stomach and other abdominal sounds [84].

According to the guidelines for respiratory sound measurements, the level of noise should be less than 45 dB during the measurement [84]. However, the measurements were not performed in a soundproof room. During the measurement, adequate light, ventilation and temperature conditions provided comfort for participants. Moreover, one microphone recorded the ambient sounds to check the level of noise. In order to overcome the high attenuation level in the lungs, the signal was amplified before transmission into the respiratory system. The amplification factor was adjusted to a suitable range such that the signal could be passed through the lungs with minimum distortion.

4.4.5 Study population

The tests were performed on 22 healthy participants without any respiratory diseases and with an average weight of (73.21 ±10.45 kg) and an average height of (176.43±9.43 cm). The average chest circumference was (93.9±8.01 cm). The participants included 20 male subjects and two female subjects. Detailed information about the participants is presented in Table 8. The tests were also performed on four participants diagnosed with pleural effusion in either right or left lungs.

Table 8. Detailed healthy subjects

Subject number	Gender	Weight(kg)	Height (cm)	Circumference of chest (cm)	Smoking	Age (year)
1	Male	75	176	96	No	23
2	Male	78.5	175	100	No	22
3	Male	71.1	182	90	No	26
4	Male	79.3	176.5	98	Yes	23
5	Male	85.5	195	94	No	23
6	Male	88.1	168	110	No	24
7	Male	72.6	181	93	No	22
8	Male	64.7	171	92	No	24
9	Male	71	192	71.5	No	24
10	Male	82	184	94	No	21
11	Male	87.3	187	99	Yes	21
12	Female	45.1	161	87	No	27
13	Male	66.6	177	90	No	27
14	Male	83	188	93	No	21
15	Male	61.8	158	87	No	25

16	**Female**	**60.5**	**160**	**87.5**	**Yes**	**24**
17	**Male**	**79**	**178**	**95.5**	**No**	**21**
18	**Male**	**65.8**	**171**	**92.5**	**No**	**26**
19	**Male**	**75.6**	**179**	**92**	**No**	**25**
20	**Male**	**64**	**172**	**86**	**No**	**29**
21	**Male**	**82.8**	**173**	**110**	**No**	**25**
22	**Male**	**71.4**	**177**	**90**	**No**	**29**

4.5 Data analysis

This section provides information regarding processing the data and it includes filtering, and the technique used for the time delay estimation.

4.5.1 Filtering

Since the recorded signals contained the transmitted signal and ambient noise, the noise signals were filtered from the main signal. Two types of filters were used in this study for filtering the signal namely:

- High Pass Filter (HPF): with a cut off frequency in the lower frequency range to remove low frequency noise such as muscle sound and electronic disturbances noise.
- Low Pass Filter (LPF): with a cut off frequency in the upper frequency range to avoid aliasing, as well as for elimination of noise from the signal

The transmitted sounds have frequencies between 130 to 150 Hz. Consequently, all signals with frequencies higher than 150 Hz and lower than 130 Hz were included as part of the noise signal. The noise signals were removed using a Butterworth band pass filter, which is a combination of an eighth order Butterworth high and low pass filter. The cut off frequency of the high pass filter was set to 130 Hz and, the cut off frequency of the low pass filter was set to 150 Hz. Furthermore, the LPF for the anti-aliasing of the frequencies was performed by the SigLab itself. This device already had anti-aliasing functionality designed into its hardware that can be set via its software. The filtered signals of subject number seven are presented in Figure 45.

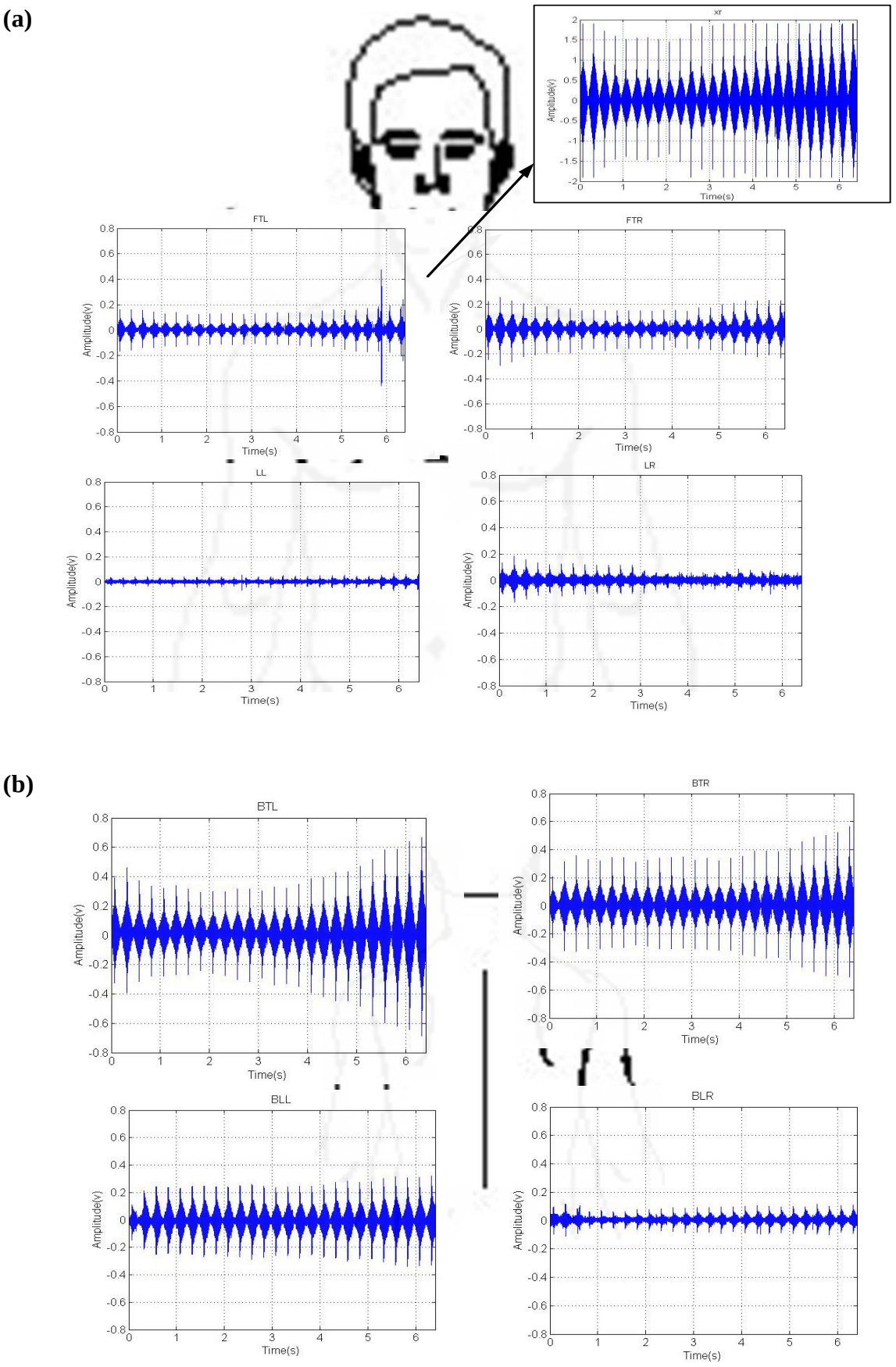

Figure 45. The filtered signal of subject number seven from the anterior(a) and posterior (b) chest (refer to Figure 42)

4.5.2 Time delay estimations

After filtering the signal, to find and select part of the recorded data during the inspiration, the signal was synchronized using the piezoelectric elastic strap (Pneumotrace II) data. After this process, the time delays between the reference signal recorded at the trachea and eight signals recorded on the chest of the body were calculated using the algorithm based on the cross correlation method for both the complex chirp sound and polyphonic sound.

Since the signals were recorded in 6.40 seconds during the inhalation process and the pre–recorded sound every 250 milliseconds, the signal contains 25.6 cycles of the pre-recorded sound. The recorded signals were divided into 25 segments with equal sample length (3723 samples). The cross correlation function for each segment with the corresponding segment of the reference signal was calculated, as was shown in Figure 47. This was done for the first segment of signal, recorded from microphone one on the chest of subject number seven. According to the previous publications and to the maximum possible theoretical time delay, the computed time delay should be in a range of 0 to 25 milliseconds. If the computed time delay satisfied the above condition, the time delay was saved in vector form for each measurement location. The median value for each vector (i.e. corresponding to the time delay during the inhalation for each location measurement) was selected as the median computed time delay for each location measurement during the inhalation. The estimated time delay algorithm is shown in Figure 46.

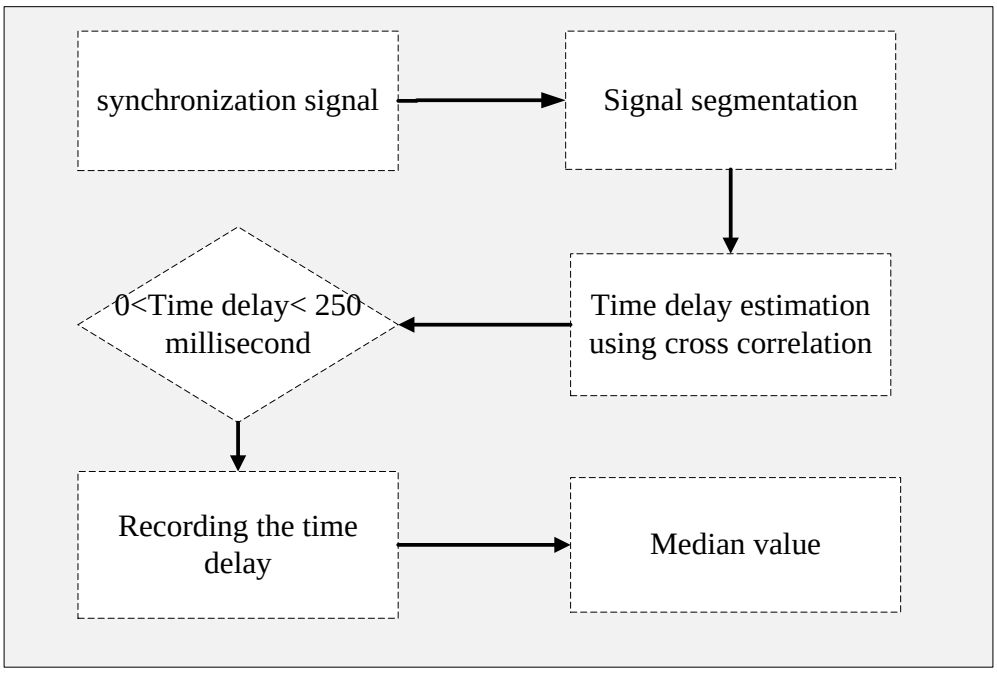

Figure 46. The algorithm used for the computation of the time delay during the inhalation

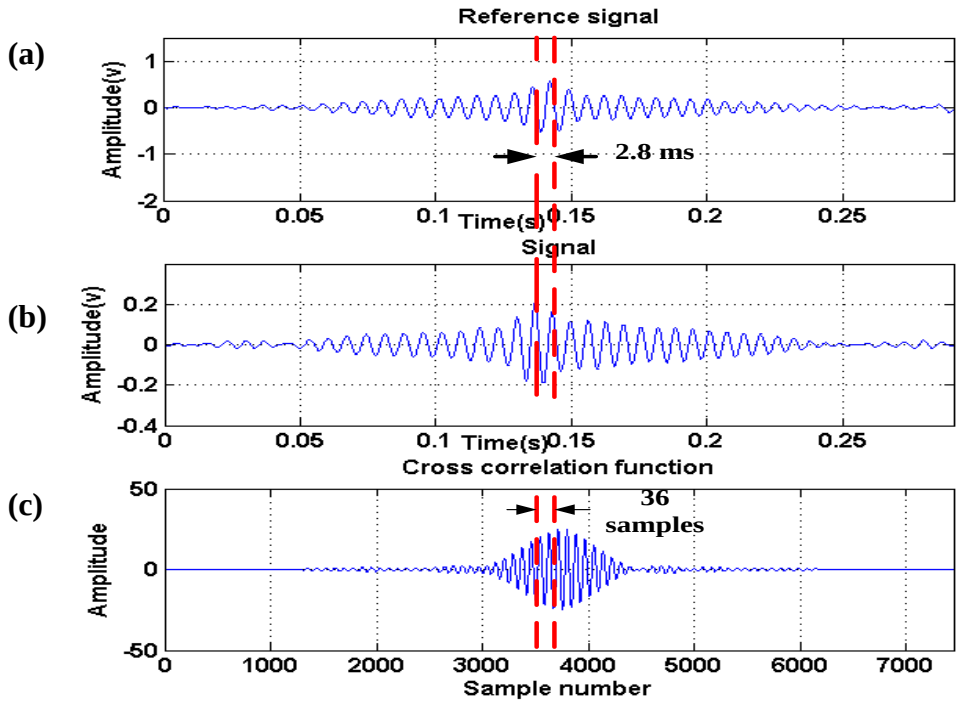

Figure 47. (a) The first segment of the reference signal of subject number seven, (b) the first segment of microphone two of subject number seven (c) cross correlation function between the reference signal and the signal from microphone two

The computed time delay by transmission of complex chirp and polyphonic sound for each subject and for each location measurement, was tabulated as shown in Table 18 and Table 19 respectively in Appendix J. To evaluate the effect of inhalation on the calculated time delay, the signal was divided into ten equal segments. The time delay was computed for each segment using the cross correlation methods and it was plotted as a function of approximate percentage of vital capacity. These results were plotted for subject number seven in Figure 48 and Figure 49.

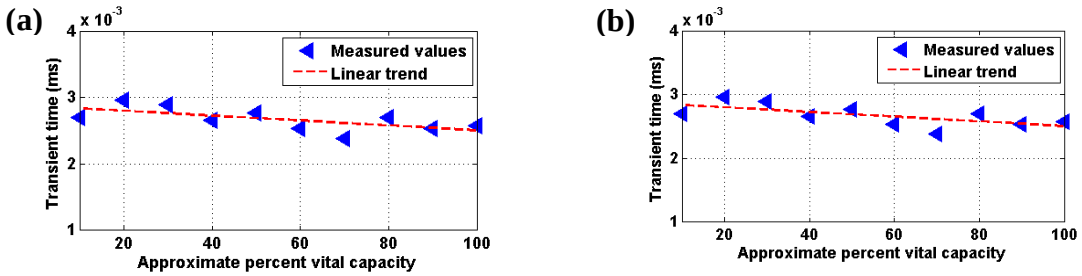

Figure 48. The changing of the transient time over the approximate percent vital capacity for microphone two (a) and three (b) for subject number seven

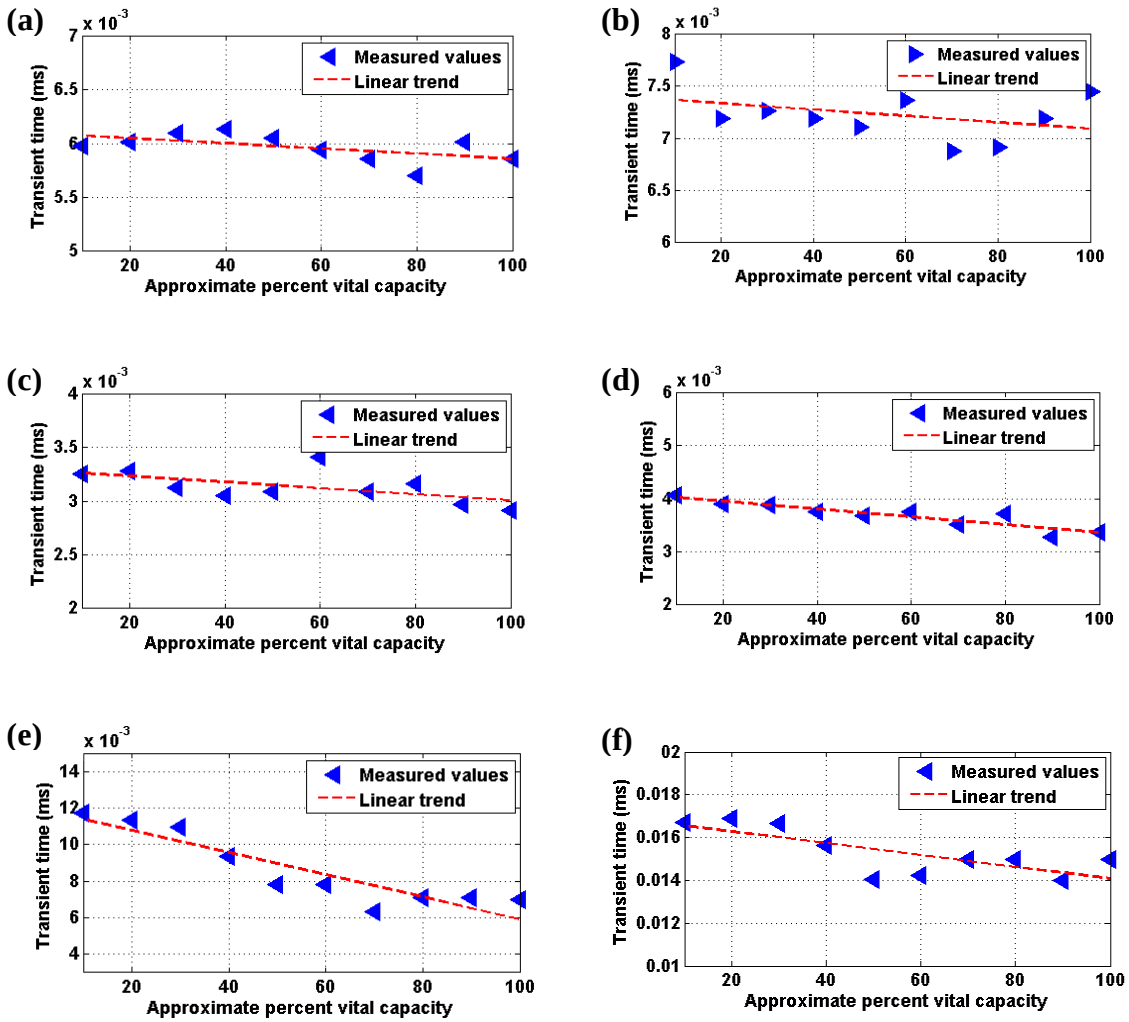

Figure 49. The changing of the transient time over the approximate percent vital capacity for microphone four (a), five (b), six (c), seven(d), eight(e) and nine (f) for subject number seven

4.5.3 Correlation analysis

To investigate the correlation between the calculated time delay for each subject and the weight, height, chest circumference and body mass index (BMI), the correlation coefficient was calculated using the following equation:

$$r_{xy} = \frac{\sum_{i=1}^{n}(x-\bar{x})(y-\bar{y})}{\sqrt{\sum_{i=1}^{n}(x-\bar{x})^2 \sum_{i=1}^{n}(y-\bar{y})^2}} \quad (8)$$

where r_{xy} is the correlation coefficient between variables x and y, and $\bar{x}$ and $\bar{y}$ are the mean of x and y respectively. The results show that the correlation coefficients of the time delay and chest circumference is larger than that of the other parameters. The calculated correlation coefficients are summarized in Table 9.

Table 9. Correlation coefficient between transient time in each stethoscope for chest circumference, weight, height and BMI

	UFR	UFL	RL	LL	URB	ULB	LRB	LLB
Chest circumference	**0.48**	**0.40**	**0.28**	**0.11**	**0.14**	**0.11**	**0.53**	**0.55**
Weight	**0.03**	**0.04**	**0.55**	**0.22**	**-0.28**	**-0.40**	**0.58**	**0.57**
Height	**-0.24**	**-0.25**	**0.42**	**0.11**	**-0.24**	**-0.40**	**0.31**	**0.20**
BMI	**0.23**	**0.27**	**0.31**	**0.20**	**-0.15**	**-0.15**	**0.44**	**0.54**

4.6 Results and discussion

In this section, the results of the calculated time delay in the respiratory system of healthy subjects are presented. The effects of inhalation and the size of the lung on the calculated time delay are discussed. The case study using the time delay of sound passing through the respiratory system in detection of fluid in the lung is presented.

4.6.1 Time delay in healthy human lungs

The results of the transmission of the complex chirp sound and polyphonic sound to calculate the transient time of sound in the respiratory system in healthy subjects are presented and compared. According to calculated results the average time delay in the right lung is larger than that in the left lung. This finding was confirmed in previous studies [56, 85].

The results of the transmission of the complex chirp signal shows that the time delay of microphone two, located on the right anterior chest between the 2nd and 3rd intercostal spaces, varied between 0.6 and 3 milliseconds. The time delay of microphone three, located on the left anterior chest varied between 0.6 and 3.9 milliseconds. The average time delay calculated for 22 subjects, for microphone two is 1.9 milliseconds with standard deviation of

0.6 milliseconds. However, the average time delay, calculated for microphone three is 1.8 milliseconds with standard deviation of 0.66 milliseconds.

The calculated time delays for microphone four, placed on the right lateral side of the chest between the 4^{th} and 6^{th} intercostal spaces, varied in a range of 3 to 12 milliseconds. The calculated time delays for microphone five, placed on the left lateral side of the chest, varied in a range of 3 to 8.20 milliseconds. The average time delay calculated for 22 healthy subjects for microphone four is 6.2 milliseconds with a standard deviation of 2.5 milliseconds, while the average time delay for microphone five is 5.5 milliseconds with a standard deviation of 1.7 milliseconds. According to these calculated results, asymmetrical behaviour is observed. The time delay at the lateral right lung (i.e., microphone three) is approximately 12 % bigger than therefore the lateral left lung (i.e., microphone four). This may be a result of the heart's location near the left lung and the bigger size of the right lung.

The average calculated time delay for 22 healthy subjects for microphone six, located at the right posterior of the chest between the scapulae, is 1.84 milliseconds with standard deviation of 0.6 milliseconds. The average time delay for microphone seven, placed on the left posterior of the chest between the scapulae, is 1.83 milliseconds with standard deviation of 0.9 milliseconds. The time delays for microphone six, varied in a range of 0.7 to 3.1 milliseconds, whilst the time delays between the reference microphone and microphone seven varied in a range of 0.6 to 3.3 milliseconds. Symmetrical behaviour can be observed for the calculated time delay for the locations of microphone three and four, because the distance between the two microphones was relatively small.

The average calculated time delay in 22 subjects, between the reference microphone and microphone eight, placed on the right posterior of the chest and below than the scapula, is 10.1 milliseconds with standard deviation of 2.81 milliseconds. However, the average calculated time delay between the reference signal and microphone nine, located at left posterior of the chest and below the scapula, is 9.8 milliseconds with standard deviation of 3.2 milliseconds. The time delay at the location of microphone eight, varied between 5.5 and 14.1 milliseconds, whereas the time delay at the location of microphone nine varied in a range of 3.4 to 15.1 milliseconds. Asymmetrical behaviour can also be observed between microphones eight and nine because of the size of the right lung, which is slightly bigger than the left lung.

By transmission of the polyphonic sound into the respiratory system, similar results were obtained. The calculated time delay for polyphonic sound is also tabulated in Table 19 in Appendix J. There are two kinds of error in the calculation, which include the high attenuation factor of transmitted sound in the lung and the environmental noise. These factors distort the signal. Therefore, the time delay cannot be calculated accurately.

By the transmission of the polyphonic sound, the algorithm could not calculate the time delay in 23% (77/334) of measurements, while by the transmission of the complex chirp signal the algorithm could not calculate the time delay in 8% (43/512) of measurements. These results for each location of microphone vary, as summarized in Table 10 for transmission of the complex chirp signal and in Table 11 for transmission of the polyphonic sound. The results show that the miscalculation percentage in the lower part of the lung is significantly higher than the upper part of the lung, because the sound travels a longer distance and therefore the sound attenuates highly. Furthermore, the results show that the miscalculation percentage of transient time in the transmission of the complex chirp signal, is significantly less than the miscalculation percentage of transient time in the transmission of the polyphonic signal.

Table 10. Miscalculation percentage in transmission of complex chirp sound in the lung

Location of microphones							
UFR	**UFL**	**RL**	**LL**	**URB**	**ULB**	**LRB**	**LLB**
2%	**2%**	**12%**	**22%**	**3%**	**6 %**	**12%**	**7%**

Table 11. Miscalculation percentage in transmission of polyphonic sound in the lung

Location of microphones							
UFR	**UFL**	**RL**	**LL**	**URB**	**ULB**	**LRB**	**LLB**
6 %	**6%**	**14%**	**25%**	**2%**	**8%**	**39%**	**24%**

4.6.2 The effect of inhalation on the time delay

The lung parenchyma is a complex mixture of air and tissue. The density of the lung changes during inhalation and exhalation. Therefore, the transient time of transmitted sound in the lung should also change during the inhalation process. Transient time of sound in the

lung as a function of vital lung capacity for subject number seven is shown in Figure 48 and Figure 49.

According to the calculated results for subject number seven, the time delay decreased linearly during the inhalation process. Furthermore, the average time delays for the 22 healthy subjects showed a similar trend, as presented in Figure 50 and Figure 51. The decrease in the time delay with increasing percentage of vital capacity can be observed in all microphones. This is because the lungs, at vital capacity, have more air and the speed of sound in air is faster than the speed of sound in the lung tissue. This effect was also observed in the study of Bergstresser et al. [56], but they only measured the time delay at the anterior chest.

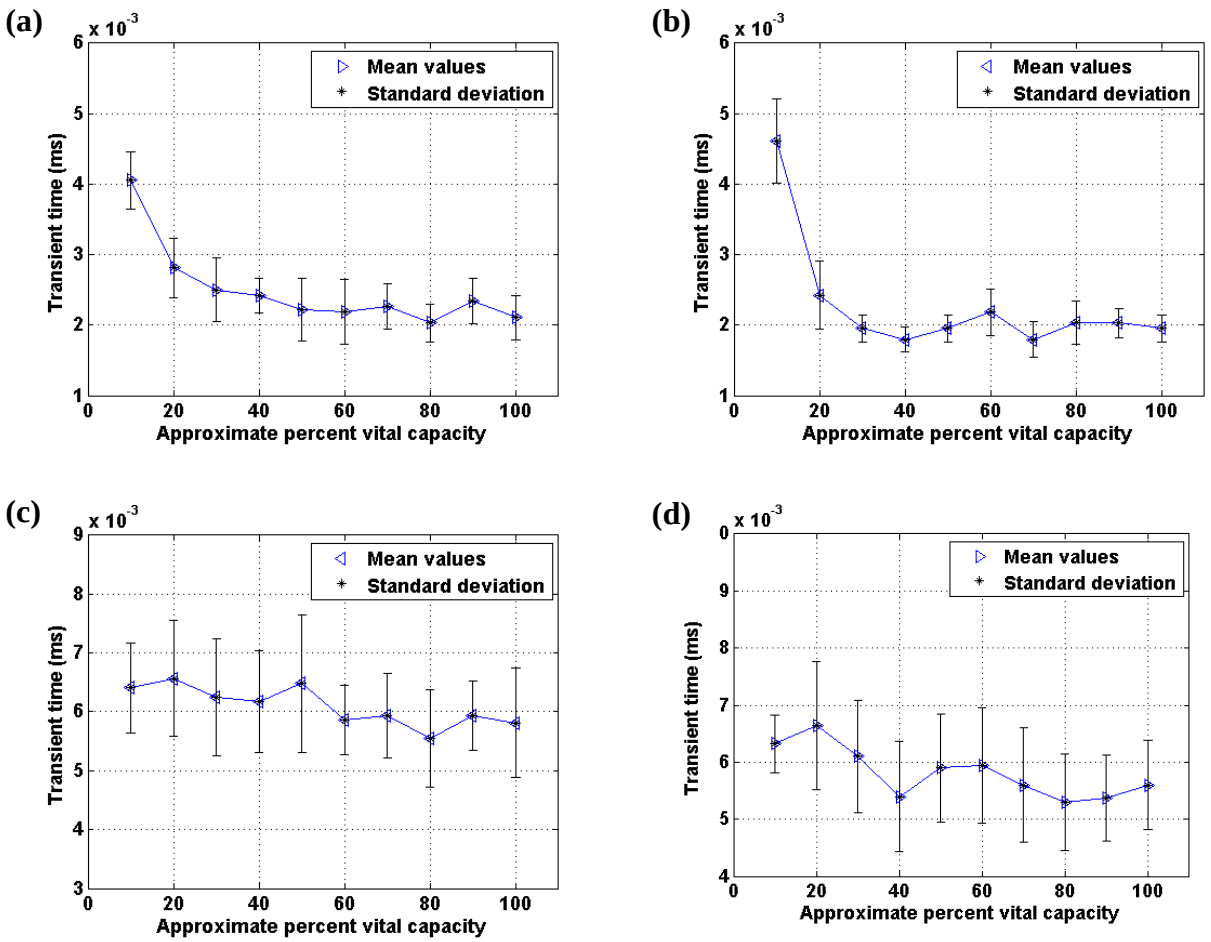

Figure 50. The effect of inhalation on the time delay for microphones two (a), three (b), four (c) and five (d)

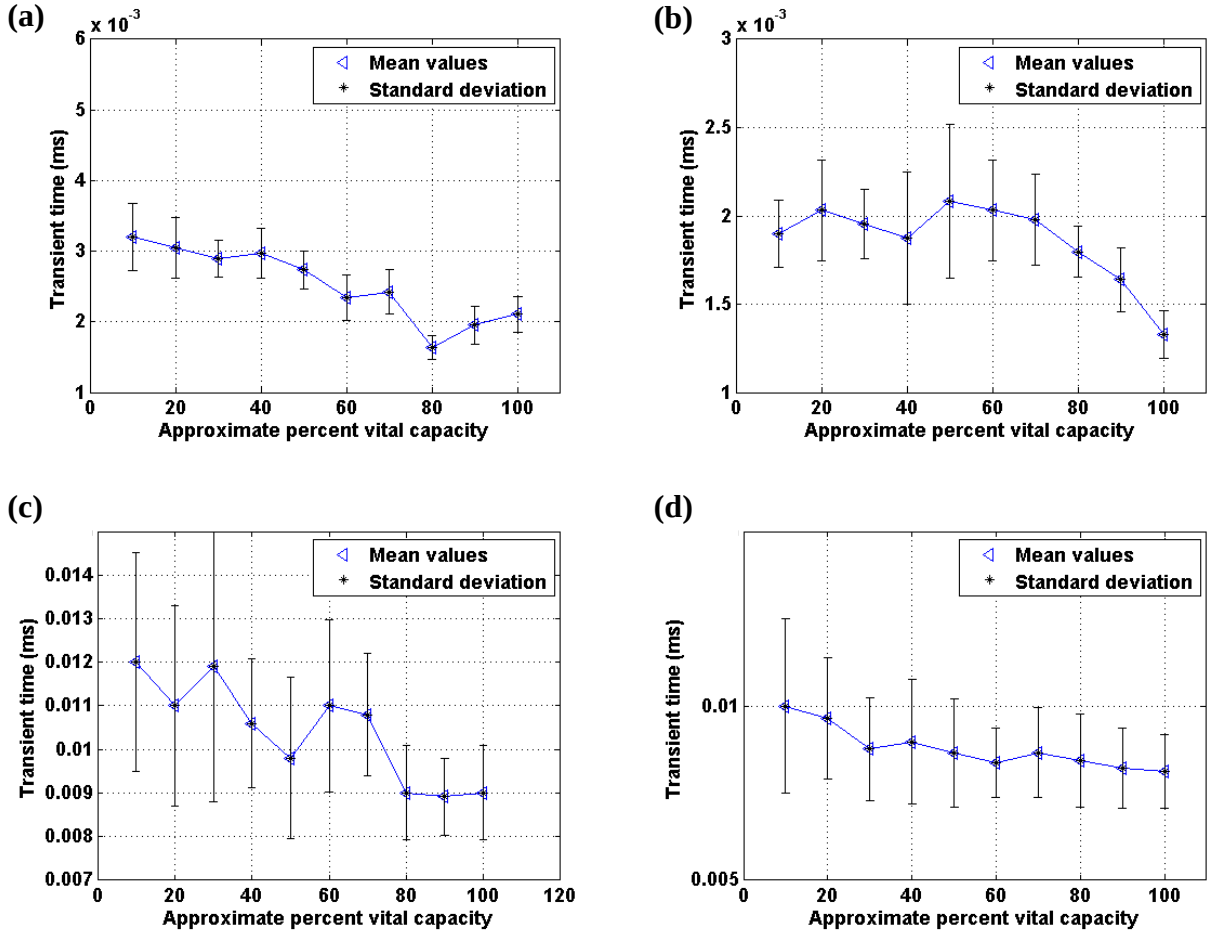

Figure 51. The effect of inhalation on the time delay for microphones six (a), seven (b), eight(c) and nine (d)

4.6.3 The effect of lung volume on the time delay

Since the size of the lungs of the participants in this study varied greatly and as the transient time of propagated sound in the respiratory system may be a function of the lung size, the investigation of the effect of lung size on transient time was performed using the correlation coefficient method. The correlation coefficient shows that the lung size has a larger effect than the other factors such as height, weight and BMI.

The calculated transient time for each subject at each location of measurement was plotted as a function of chest circumference. The results show that with increasing chest circumference, the transient time of propagated sound in the lung increases. These results were plotted for each location on the lung as shown in Figure 52 and Figure 53. Furthermore,

the results show that the transient times for the participants with chest circumferences in a range of 85 to 100 cm vary highly. The one reason for the high variation of transient times for the subjects with this chest circumference range, is that each subject has a different anatomy. To elaborate, the size of muscles could effect the transient time of propagated sound in the lung.

Table 12. Correlation coefficient between transient time for each stethoscope and chest circumference

Location of microphones							
UFR	**UFL**	**RL**	**LL**	**URB**	**ULB**	**LRB**	**LLB**
0.48	**0.40**	**0.28**	**0.11**	**0.14**	**0.11**	**0.53**	**0.55**

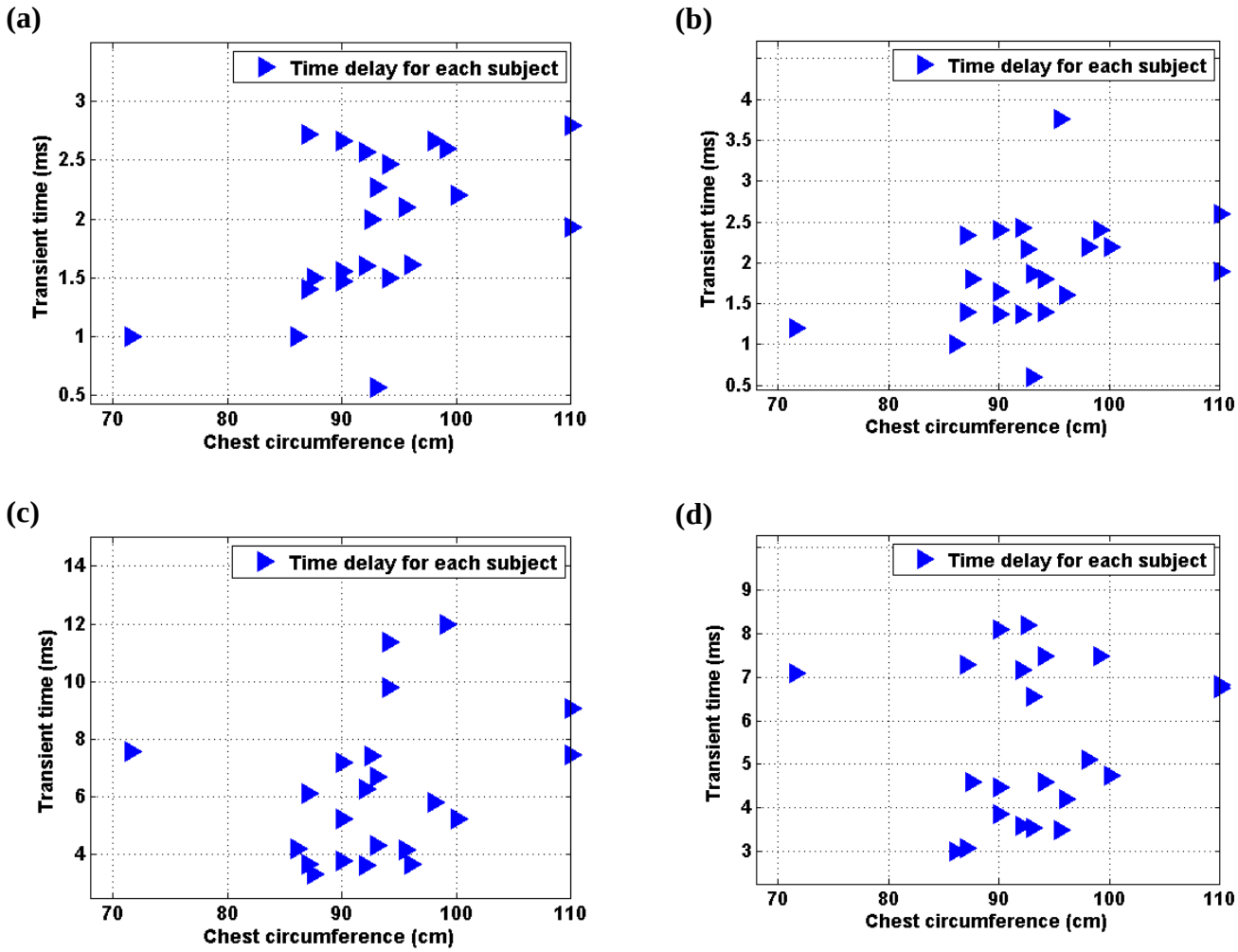

Figure 52. The effect of chest circumference on time delay for microphone two (a), three (b), four (c) and five (d)

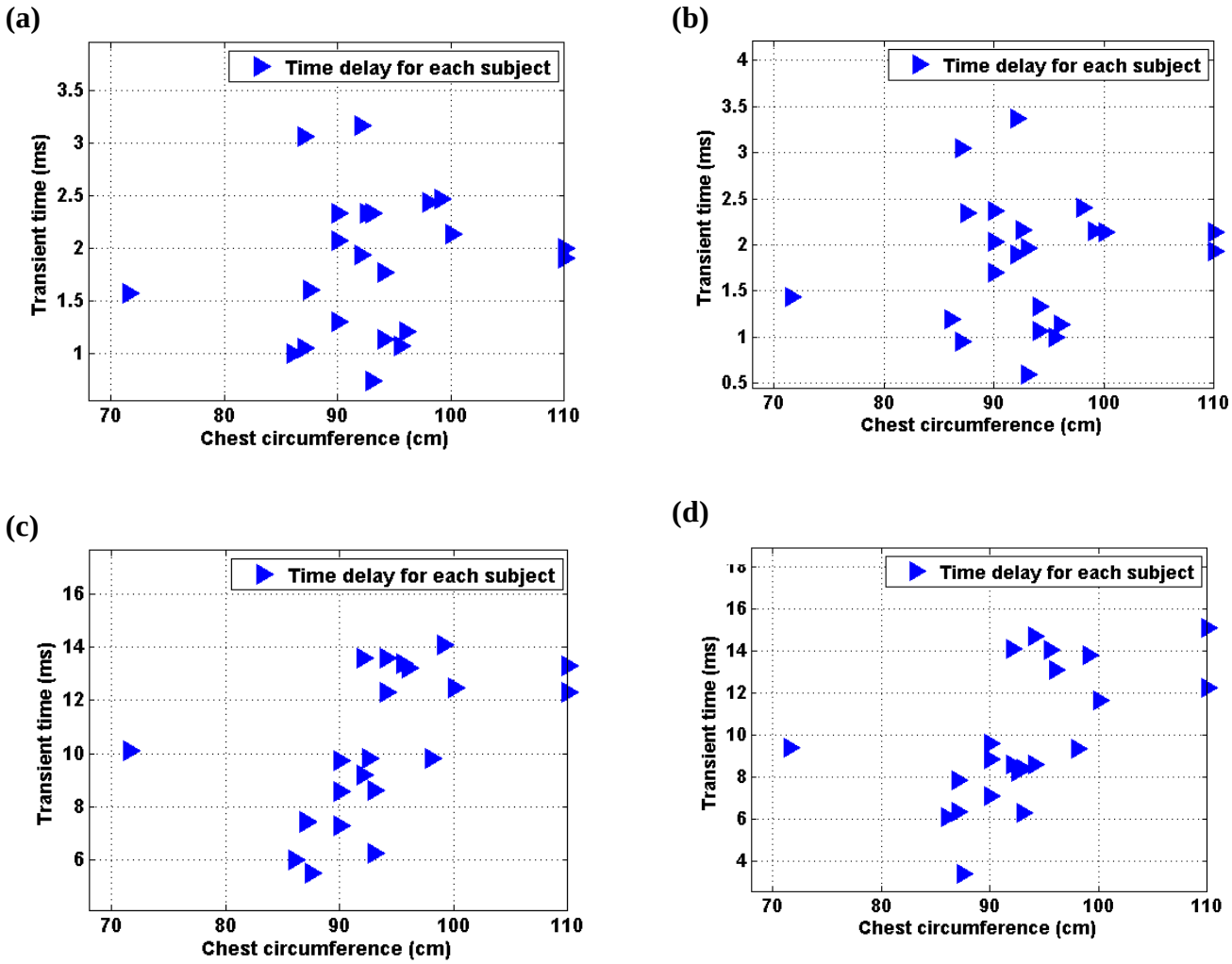

Figure 53. The effect of chest circumference on time delay for microphone six (a), seven (b), eight (c) and nine (d)

4.6.4 The effect of pleural effusion on the time delay

A case study was performed using active acoustic methodology. The method was tested on four pleural effusion diagnosed patients with pleural effusion in either the right lung or the left lung. The tests were performed in Theatre five at the pulmonary unit at Tygerberg hospital. Detailed information about the participation is summarized in Table 13. Furthermore, calculated time delays for patients diagnosed with pleural effusion by transmission of complex chirp sound and poly phonic sound are tabulated in Table 14 and 15 respectively.

Table 13. Details of the pleural effusion subjects

Subject number	Gender	Weight(Kg)	Height (cm)	Circumference of chest (cm)	Location of effusion	Age
1	Female			74	Right	70
2	Female	50	154	80	Right	62
3	Male	84	171	111	Right	76
4	Male	55	176	81	Right	34

Table 14. Calculated time delay for patients diagnosed with pleural effusion by transmission of complex chirp sound

Subject number	Trial number	Location of microphones							
		UFR	UFL	RL	LL	URB	ULB	LRB	LLB
1	1	0.6	0.8	2.3	2.4	0.6	0.6	3.1	2.9
1	2	0.8	0.8	2.4	2.2	0.8	0.7	3	2.8
1	3	0.9	0.8	2.5	2	0.7	0.6	3.1	2
2	1	0.6	1	3.1	3.1	0.6	0.6	3.6	4.5
2	2	1	1	2.9	3	0.8	0.8	3.5	4
2	3	1.1	1.2	3	2	0.7	0.7	3.4	Nan
3	1	1.09	1	3.4	3	1.4	1.8	Nan	14.8
3	2	1.01	1	Nan	3	1.5	1.9	6.4	15
3	3	1	Nan	Nan	3.2	1.4	1.8	Nan	14
4	1	1.4	1	3.5	3.5	1.8	1.8	4.4	4.4
4	2	1.2	1.1	Nan	Nan	1.5	1.5	Nan	4
4	3	1.1	1	3.4	3.2	1.2	1.3	4.6	4.4

Table 15. Calculated time delay for patients diagnosed with pleural effusion by transmission of polyphonic sound

Subject number	Trial number	Location of microphones							
		UFR	UFL	RL	LL	URB	ULB	LRB	LLB
1	1	0.7	0.6	2.4	2.2	0.6	0.5	3.1	Nan
1	2	0.6	0.5	Nan	Nan	0.5	0.5	3	2.6
2	1	1	1	3.1	3	0.6	0.5	3.4	Nan
2	2	1.1	1	2.9	2.8	0.8	0.6	3.3	3
3	1	1	1.1	3.4	3.2	1.4	1.8	Nan	Nan
3	2	1	1	Nan	Nan	1.5	1.7	6.4	9
4	1	1.2	1.1	3.5	3.4	1.4	1.2	Nan	Nan
4	2	1.2	1.1	3.4	3.2	1.1	1	Nan	Nan

By comparison of the calculated time delay for microphones eight and nine, which are located on the right and the left lower posterior chest, it was found that the computed time delay at the location in which the effusion is located, is less than the computed time delay for the other lung with a similar axial position. This effect was observed for subject number one, two and three, while in subject number four, the time delays for the microphones eight and nine were approximately the same. This may have resulted due to the volume of the effusion in the subject 4 being relatively small.

To investigate the effect of effusion on the time delay, each subject diagnosed with pleural effusion was compared with a healthy subject which has an approximately similar body size to the subject diagnosed with pleural effusion. By comparison of the calculated time delays for subject number one and two with subject number 12 in the healthy group, it was found that the time delay for microphone eight (e.g. corresponding to the location in which effusion is located) for subject number one and two is 3 and 3.5 ms respectively, while the time delay for subject number 12 in a same location is 7.5 ms. Furthermore, for subject number 12, the time delay at right lower posterior chest is 15 % bigger than at left lower posterior chest, while for subject number one the time delays at right and left lower posterior chest are approximately similar and for subject number two, the time delay at right lower posterior chest is 15 % less than for left lower posterior chest.

By comparison the time delays for subject number three with the time delays for subject number six in the healthy group; it was found that the time delay for subject number three at right lower posterior (e.g. corresponding to the location where the effusion is located) is 6.4 ms. However, the time delay for subject number six is 16 ms. Moreover, the calculated time delay for subject number six at right lower posterior chest is 15% bigger than at left posterior chest, whereas the calculated time delay for subject number three at right lower posterior chest is significantly less (60%) than at the left lung. The time delay for subject number four can also be approximately compared with subject number 20 in the healthy group. The computer time delay for subject number four at the location where the effusion is located is 4 ms, while for subject number 20 at a similar location it is 6 ms.

The effect of fluid on the transient time of applied sound in the lung shows that the time delay technique is a promising technique to detect fluid on the lung. Furthermore, the results confirm the results obtained in the model. However, future investigation using a large sample size is essential.

4.7 Conclusion

In this chapter, a data acquisition system to compute the transient time of transmitted sound in the respiratory system, was developed. Two types of signals including a complex chirp sound and a polyphonic sound, were transmitted into the respiratory system of 22 healthy participants and four patients diagnosed with pleural effusion.

A pre-recorded sound was played by a speaker located in front of the participant's mouth. The sound was introduced into the participant's mouth using a disposable mouthpiece. A custom-designed stethoscope placed on the participant's neck close to the subject's trachea recorded the transmitted sound which was saved on a laptop as reference signal. The sound passed through the respiratory system to reach the chest wall and it was recorded by eight microphones attached to the chest during inhalation. The time delay between the reference signal and eight microphones was calculated using the cross correlation method.

The results show that the time delay in the lungs varied in a range of 0.6 to 15 milliseconds. By the transmission of the complex chirp sound, the time delay was calculated in 91.7% (469/512) of the measurements, while the time delay was computed in 77.4% (257/334) of measurements using the polyphonic sound. The results also indicated that the time delay decreases linearly with increasing lung volume (during inhalation) because there is more air in the lung and the speed of sound in air is faster than it is the lung parenchyma. Furthermore, the correlation between the lung size (chest circumference) and computed time delay was found. A case study using time delay estimation was carried out, and the results show that using time delay estimation technique is a promising technique in detection of fluid. However, future investigation with a bigger sample size is essential.

5. Conclusions and recommendations

5.1 Conclusions

Transmission of sound into the respiratory system is one of the more recent methods in respiratory sound analysis. Based on this method, sound with low frequencies (less than 1 KHz) was transmitted into the respiratory system in order to compute the static and dynamic properties of respiratory system. In this study, this method was evaluated as a novel technique to detect pleural effusion in the lung. First, the method was evaluated on a phantom model of the human lung. According to the results obtained from the model, the technique was suitable to be used in a clinical study. This method has several advantages, such as non-invasiveness, low cost, ease of clinical review and simplicity.

Two phantom models of the lung, including a healthy model (without any fluid inside the model) and a pleural effusion model (with a bulk of fluid inside the model) were developed. The model contains materials with similar acoustic properties to the lung parenchyma, soft tissue and rib-like components. Pleural effusion was modelled by using two plastic bags filled with 600 ml and 250 ml water respectively, which were placed inside the model.

Since the fluid in the lung changes the characteristics of sound in the lung, the evaluation of the use of frequency responses as a technique to detect fluid was performed on both the healthy model and the pleural effusion model. In this technique, a sine sweep signal with a frequency range of 100 to 1000 Hz and a step of 100 Hz was applied to the model from 24 grid points around the chest of the model. After filtering the noise, using an adaptive noise cancelling algorithm, the frequency responses were computed using a FFT. The results show that the position of the fluid can be detected by comparison of the healthy model with the pleural effusion model. However, since the amplitude of the received signal depends on the applied force behind the speaker, performing this technique for clinical studies requires a great deal of equipment. Therefore, it would be impractical to use this technique in areas with low resources (rural) area. Moreover, since the sound should be applied to various locations on the chest of the model, the technique is time consuming.

Since the speed of sound is faster in fluid than in the lung (approximately 60 times faster), the evaluation using time delay estimation for fluid detection in the model is also performed. A chirp signal with a frequency range of 100 to 250 Hz was transmitted into the model of the lung. The time delay between the transmission of the sound and sound received from the chest of the model was calculated using cross correlation. The results show that the calculated time delays at the points on the model corresponding to the locations where the two plastic bags are located indicating (pleural effusion), are significantly less than at other points. This technique may lead to the development of an inexpensive, non-invasive and accurate diagnostic tool which can be used in low resource (rural) settings. The next stage of this research was to evaluate this technique in human subjects.

To implement the technique for human subjects, the data acquisition system was developed. Ethically approved trials were performed in the biomedical lab at Stellenbosch University and the pulmonary unit at Tygerberg hospital. Two types of signal, including a polyphonic sound and complex chirp signal, were transmitted into the respiratory system of 22 healthy participants and four patients diagnosed with pleural effusion. The time delay between the transmission of the reference signal located at the trachea of the subject and its reception by eight microphones placed on the chest of the participant was calculated using the cross correlation during the inhalation.

The results obtained from the healthy group indicate that that the time delay in the lungs varied in a range of 0.6 to 15 milliseconds. By transmission of the complex chirp sound, the time delay was calculated in 91.7% (469/512) of the measurements, while by transmission of the polyphonic sound, the time delay was computed in only 77.4% (257/334) of the measurements. The results also indicated that the time delay decreases linearly with increasing the lung volume during inhalation. This is because there is more air in the lung and the speed of sound in air is faster than it is in the lung parenchyma. Furthermore, the correlation between the size of the lung and the computed time delay was found.

A case study using time delay in the detection of fluid in the lung was performed on four subjects. The results show that the time delay at the location were the effusion is located less than the time delay at the other microphone with the same axial location. This is a promising technique in the diagnosis of pleural effusion. However, the test was only

conducted on subjects diagnosed with effusion on the right lung. Further investigation is necessary.

5.2 Recommendations

The results obtained show that the transient time technique is a promising technique in the diagnosis of pleural effusion. However, the following recommendations are made for future research in this area:

- In this study, a microphone with a coupling chamber was used as a transducer. It was found experimentally that this type of transducer is not appropriate for respiratory sound measurement, because the stethoscope cannot attach to the skin properly. Furthermore, the attachment of the microphone to the skin is time consuming. Therefore, for future research, development of the transducer should be concentrated on. The transducer should be small enough to connect to the skin easily. Moreover, the appropriate transducer should be also sensitive at low frequencies.
- The piezoelectric strap, Pneumotrace II, was used to measure the lung volume during the inhalation. However, the lung volume cannot be measured accurately by using the piezoelectric strap. A spirometer was not used in this study, because the applied signal was disturbed. Furthermore, the clinical trials were performed on patients with Tuberculosis (TB). Therefore, to prevent infection, the spirometer was not used. For future research, the development of a method to accurately measure the lung volume is necessary.
- In this study, the effect of inhalation on the transient time was investigated. For future research, the effect of inhalation as well as exhalation can be investigated.
- For future research, the evaluation should be performed with a bigger study population.

References

[1] T. Bergstresser, D. Ofengeim, A. Vyshedskiy, J. Shane and R. Murphy, "Sound transmission in the lung as a function of lung volume," *J. Appl. Physiol.*, vol. 93, 2002, pp. 667-674.

[2] "Auscultation (medicine) -- Britannica Online Encyclopedia," [Online]. Availabe: http://www.britannica.com/eb/article-9011297/auscultation.[2012, September 23].

[3] J. Martínez-Alajarín, J. López-Candel and R. Ruiz-Merino, "Classification and diagnosis of heart sounds and murmurs using artificial neural networks," *Bio-Inspired Modeling of Cognitive Tasks*, pp. 303-312, 2007.

[4] J. D. Leuppi, T. Dieterle, I. Wildeisen, B. Martina, M. Tamm, G. Koch, A. P. Perruchoud and B. M. Leimenstoll, "Can airway obstruction be estimated by lung auscultation in an emergency room setting?" *Respir. Med.*, vol. 100, 2006, pp. 279-285.

[5] D. Bray, R. Reilly, L. Haskin and B. McCormack, "Assessing motility through abdominal sound monitoring," in *Engineering in Medicine and Biology Society, 1997. Proceedings of the 19th Annual International Conference of the IEEE*, 1997, pp. 2398-2400.

[6] N. R. Carlson, W. Buskist, M. E. Enzle, C. D. Heth and G. Alder, "Psychology: The science of behaviour," *Canadian Psychology*, vol. 43, 2002, pp. 278-280.

[7] J. Webster, *Medical Instrumentation: Application and Design*. John Wiley & Sons, 2009.

[8] R. Mor, I. Kushnir, J. J. Meyer, J. Ekstein and I. Ben-Dov, "Breath sound distribution images of patients with pneumonia and pleural effusion," *Respir. Care*, vol. 52, 2007, pp. 1753-1760.

[9] M. Kompis, H. Pasterkamp and G. R. Wodicka, "Acoustic imaging of the human chest," *Chest Journal*, vol. 120, 2001, pp. 1309-1321.

[10] G. Benedetto, F. Dalmasso and R. Spagnolo, "Surface distribution of crackling sounds," *Biomedical Engineering, IEEE Transactions on*, vol. 35, 1988, pp. 406-412.

[11] S. Reichert, R. Gass, C. Brandt and E. Andrès, "Analysis of respiratory sounds: state of the art," *Clinical Medicine.Circulatory, Respiratory and Pulmonary Medicine*, vol. 2, 2008, p. 45.

[12] V. Korenbaum, A. Nuzhdenko, A. Tagiltsev and A. Kostiv, "Investigation into transmission of complex sound signals in the human respiratory system," *Acoustical Physics*, vol. 56, 2010, pp. 568-575.

[13] D. A. Rice, "Sound speed in pulmonary parenchyma," *J. Appl. Physiol.*, vol. 54, 1983, pp. 304-308.

[14] D. Anantham, F. J. F. Herth, A. Majid, G. Michaud and A. Ernst, "Vibration response imaging in the detection of pleural effusions: a feasibility study," *Respiration*, vol. 77, 2009, pp. 166-172.

[15] S. A. Sahn, "Malignant pleural effusions," *Clin. Chest Med.*, vol. 6, 1985, pp. 113-125.

[16] J. M. Porcel and R. W. Light, "Diagnostic approach to pleural effusion in adults," *Am. Fam. Physician*, vol. 73, 2006, pp. 1211-1220.

[17] L. Valdés, D. Alvarez, J. M. Valle, A. Pose and E. San José, "The etiology of pleural effusions in an area with high incidence of tuberculosis," *Chest*, vol. 109, 1996, pp. 158-162.

[18] "SA TB Guidelines 2004," [Online]. Available: http://www.kznhealth.gov.za/chrp/documents/Guidelines.[2012, September 23].

[19] D. Barr, A. Padarath and L. Sait, "The stop TB partnership in south Africa," *a review Durban, South Africa*: Health system Trust.

[20] J. Joseph, C. Strange and S. A. Sahn, "Pleural effusions in hospitalized patients with AIDS " *Ann. Intern. Med.*, vol. 118, Jun 11993, pp. 856-859.

[21] C. Mostert and N. Pannell, "The pleural effusion in HIV-an approach to diagnosis," *SA fam pract*, vol. 54, 2009, pp. 280-284.

[22] M. Roberts, M. Reiss and G. Monger, *Advanced Biology*. Nelson Thornes, 2000.

[23] L. Sherwood, *Fundamentals of Human Physiology*. Brooks/Cole Publishing Company, 2011.

[24] "Internal Art - Medical Illustration, Medical Legal Illustration & Medical Art by Mike Austin - Portfolio," [Online]. Available: http://www.internalart.com/mike_austin_portfolio.htm. [2012, September 23].

[25] M. Noppen, M. DE Waele, R. Li, K. Vader Gucht, J. D'haese, E. Gerlo and W. Vincken, "Volume and cellular content of normal pleural fluid in humans examined by pleural lavage," *American Journal of Respiratory and Critical Care Medicine*, vol. 162, 2000, pp. 1023-1026.

[26] R. W. Light, *Pleural Diseases*. Lippincott Williams & Wilkins, 2007.

[27] "Diseases of the Pleura » Health Informations, " [Online]. Available: http://www.practicalhospital.com/diseases-of-the-pleura/diseases-of-the-pleura. [2012, September 25].

[28] S. A. Sahn, "The differential diagnosis of pleural effusions," *West. J. Med.*, vol. 137, 1982, p. 99.

[29] D. Rolston, E. Diaz-Guzman and M. M. Budev, "Accuracy of the physical examination in evaluating pleural effusion," *Cleve. Clin. J. Med.*, vol. 75, 2008, pp. 297-303.

[30] J. M. Porcel and R. W. Light, "Diagnostic approach to pleural effusion in adults," *Am. Fam. Physician*, vol. 73, 2006, pp. 1211-1220.

[31] "Christy Krames - Portfolio, " [Online]. Available: http://www.kramestudios.com/port.asp. [2012, September 25].

[32] A. Sovijärvi, J. Vanderschoot and J. Earis, "Standardization of computerized respiratory sound analysis," *Crit. Care Med.*, vol. 156, 1997, pp. 974-987.

[33] J. Earis and B. Cheetham, "Current methods used for computerized respiratory sound analysis," *European Respiratory Review*, vol. 10, 2000, pp. 586-590.

[34] A. Sovijarvi, L. Malmberg, G. Charbonneau, J. Vanderschoot, F. Dalmasso, C. Sacco, M. Rossi and J. Earis, "Characteristics of breath sounds and adventitious respiratory sounds," *European Respiratory Review*, vol. 10, 2000, pp. 591-596.

[35] K. W. Becker, "Research into Adventitious Lung Sound Signals Originating from Pulmonary Tuberculosis using Electronic Auscultation," 2009.

[36] A. S. Lyons, R. J. Petrucelli, J. Bosch, J. Duffy, W. Rawls, J. P. Cottereau and D. Authier, *Histoire Illustrée De La Médecine*. Presses de la Renaissance, 1979.

[37] S. Reichert, R. Gass, C. Brandt and E. Andrès, "Analysis of respiratory sounds: state of the art," *Clinical Medicine.Circulatory, Respiratory and Pulmonary Medicine*, vol. 2, 2008, p. 45.

[38] B. E. Shykoff, Y. Ploysongsang and H. Chang, "Airflow and normal lung sounds," *American Journal of Respiratory and Critical Care Medicine*, vol. 137, 1988, pp. 872-876.

[39] Y. Ploy-Song-Sang, P. Macklem and W. Ross, "Distribution of regional ventilation measured by breath sounds." *Am. Rev. Respir. Dis.*, vol. 117, 1978, p. 657.

[40] "The R.A.L.E. Repository " [Online]. Available: http://www.rale.ca/Wheezingc.htm. [2012, September 23].

[41] Z. Hantos, T. Asztalos, J. Tolnai, F. Petak and B. Suki, "Volume increments and crackle sounds during lung reinflation," in *[Engineering in Medicine and Biology, 1999. 21st Annual Conf. and the 1999 Annual Fall Meeting of the Biomedical Engineering Soc.] BMES/EMBS Conference, 1999. Proceedings of the First Joint*, 1999, p. 354.

[42] P. Piirila and A. Sovijarvi, "Crackles: recording, analysis and clinical significance," *European Respiratory Journal*, vol. 8, 1995, pp. 2139-2148.

[43] P. Forgacs, *Lung Sounds*. Baillière Tindall, 1978.

[44] S. Chowdhury and A. Majumder, "Frequency analysis of adventitious lung sounds," *J. Biomed. Eng.*, vol. 4, 1982, pp. 305-312.

[45] R. P. Dellinger, J. E. Parrillo, A. Kushnir, M. Rossi and I. Kushnir, "Dynamic visualization of lung sounds with a vibration response device: a case series," *Respiration*, vol. 75, 2008, pp. 60-72.

[46] D. Anantham, F. J. F. Herth, A. Majid, G. Michaud and A. Ernst, "Vibration response imaging in the detection of pleural effusions: a feasibility study," *Respiration*, vol. 77, 2009, pp. 166-172.

[47] R. Mor, I. Kushnir, J. J. Meyer, J. Ekstein and I. Ben-Dov, "Breath sound distribution images of patients with pneumonia and pleural effusion," *Respir. Care*, vol. 52, 2007, pp. 1753-1760.

[48] V. Goncharoff, J. Jacobs and D. Cugell, "Wideband acoustic transmission of human lungs," *Medical and Biological Engineering and Computing*, vol. 27, 1989, pp. 513-519.

[49] A. V. Oppenheim, R. W. Schafer and J. R. Buck, *Discrete-Time Signal Processing*. Prentice hall Englewood Cliffs, NJ, 1989.

[50] G. Wodicka, A. Aguirre, P. DeFrain and D. Shannon, "Phase delay of pulmonary acoustic transmission from trachea to chest wall," *Biomedical Engineering, IEEE Transactions on*, vol. 39, 1992, pp. 1053-1059.

[51] S. Lu, P. Doerschuk and G. Wodicka, "Parametric phase-delay estimation of sound transmitted through intact human lung," *Medical and Biological Engineering and Computing*, vol. 33, 1995, pp. 293-298.

[52] S. Patel, S. Lu, P. Doerschuk and G. Wodicka, "Sonic phase delay from trachea to chest wall: spatial and inhaled gas dependency," *Medical and Biological Engineering and Computing*, vol. 33, 1995, pp. 571-574.

[53] G. R. Wodicka, K. N. Stevens, H. Golub and D. Shannon, "Spectral characteristics of sound transmission in the human respiratory system," *Biomedical Engineering, IEEE Transactions on*, vol. 37, 1990, pp. 1130-1135.

[54] M. Mahagnah and N. Gavriely, "Gas density does not affect pulmonary acoustic transmission in normal men," *J. Appl. Physiol.*, vol. 78, 1995, pp. 928-937.

[55] A. Pohlmann, S. Sehati and D. Young, "Effect of changes in lung volume on acoustic transmission through the human respiratory system," *Physiol. Meas.*, vol. 22, 2001, pp. 233.

[56] T. Bergstresser, D. Ofengeim, A. Vyshedskiy, J. Shane and R. Murphy, "Sound transmission in the lung as a function of lung volume," *J. Appl. Physiol.*, vol. 93, 2002, pp. 667-674.

[57] G. R. Wodicka, K. N. Stevens, H. Golub and D. Shannon, "Spectral characteristics of sound transmission in the human respiratory system," *Biomedical Engineering, IEEE Transactions on,* vol. 37, 1990, pp. 1130-1135.

[58] G. R. Wodicka and D. C. Shannon, "Transfer function of sound transmission in subglottal human respiratory system at low frequencies," *J. Appl. Physiol.,* vol. 69, 1990, pp. 2126-2130.

[59] S. Kraman, "Speed of low-frequency sound through lungs of normal men," *J. Appl. Physiol.,* vol. 55, 1983, pp. 1862-1867.

[60] S. Kraman, "Effects of lung volume and airflow on the frequency spectrum of vesicular lung sounds," *Respir. Physiol.,* vol. 66, 1986, pp. 1-9.

[61] G. Wodicka, P. DeFrain and S. Kraman, "Bilateral asymmetry of respiratory acoustic transmission," *Medical and Biological Engineering and Computing,* vol. 32, 1994, pp. 489-494.

[62] H. Pasterkamp, S. Patel and G. Wodicka, "Asymmetry of respiratory sounds and thoracic transmission," *Medical and Biological Engineering and Computing,* vol. 35, 1997, pp. 103-106.

[63] G. Bondar' and V. Korenbaum, "A new method for estimating voice sounds transmitted to the chest wall in children and adolescents," *Hum. Physiol.,* vol. 32, 2006, pp. 533-538.

[64] V. Korenbaum, A. Nuzhdenko, A. Tagiltsev and A. Kostiv, "Investigation into transmission of complex sound signals in the human respiratory system," *Acoustical Physics,* vol. 56, 2010, pp. 568-575.

[65] S. S. Kraman and A. B. Bohadana, "Transmission to the chest of sound introduced at the mouth," *J. Appl. Physiol.,* vol. 66, 1989, pp. 278-281.

[66] A. Leung and S. Sehati, "Sound transmission through normal and diseased human lungs," *Eng. Sci. Educ. J.,* vol. 5, 1996, pp. 25-31.

[67] R. L. Donnerberg, C. K. Druzgalski, R. L. Hamlin, G. L. Davis, R. M. Campbell and D. A. Rice, "Sound transfer function of the congested canine lung," *Br. J. Dis. Chest,* vol. 74, 1980, pp. 23-31.

[68] K. Mulligan, A. Adler and R. Goubran, "Detecting regional lung properties using audio transfer functions of the respiratory system," in *Engineering in Medicine and Biology Society, 2009. EMBC 2009. Annual International Conference of the IEEE,* 2009, pp. 5697-5700.

[69] T. Bergstresser, D. Ofengeim, A. Vyshedskiy, J. Shane and R. Murphy, "Sound transmission in the lung as a function of lung volume," *J. Appl. Physiol.,* vol. 93, 2002, pp. 667-674.

[70] R. Paciej, A. Vyshedskiy, J. Shane and R. Murphy, "Transpulmonary speed of sound input into the supraclavicular space," *J. Appl. Physiol.*, vol. 94, 2003, pp. 604-611.

[71] M. Ozer, S. Acikgoz, T. Royston, H. Mansy and R. Sandler, "Boundary element model for simulating sound propagation and source localization within the lungs," *J. Acoust. Soc. Am.*, vol. 122, 2007, pp. 657.

[72] S. Acikgoz, M. Ozer, T. Royston, H. Mansy and R. Sandler, "Experimental and computational models for simulating sound propagation within the lungs," *Journal of Vibration and Acoustics*, vol. 130, 2008, pp. 021010-021011.

[73] D. A. Rice, "Sound speed in pulmonary parenchyma," *J. Appl. Physiol.*, vol. 54, 1983, pp. 304-308.

[74] T. J. Hall, M. Bilgen, M. F. Insana and T. A. Krouskop, "Phantom materials for elastography," *Ultrasonics, Ferroelectrics and Frequency Control, IEEE Transactions on*, vol. 44, 1997, pp. 1355-1365.

[75] A. M. Okamura, C. Simone and M. D. O'Leary, "Force modeling for needle insertion into soft tissue," *Biomedical Engineering, IEEE Transactions on*, vol. 51, 2004, pp. 1707-1716.

[76] E. R. Weibel, "Morphometry of the human lung," *Anesthesiology*, vol. 26, 1965, p. 367.

[77] S. Haykin, "Adaptive filter theory,4th Edition,", *Prentice-Hall*, 2003.

[78] "Sound Patterns, " [Online]. Available: http://www.prenhall.com/divisions/ect/app/heartlungsounds/main/sp/sp1.htm.[2012, September 23].

[79] "Deep Breeze - Diagnostic Imaging & Disease Monitoring for Lung Cancer, COPD, Asthma, CHF, " [Online]. Available: http://www.deepbreeze.com/. [2012, September 23].

[80] H. Pasterkamp, S. S. Kraman and G. R. Wodicka, "Respiratory sounds advances beyond the stethoscope," *American Journal of Respiratory and Critical Care Medicine*, vol. 156, 1997, pp. 974-987.

[81] G. R. Wodicka, S. S. Kraman, G. M. Zenk and H. Pasterkamp, "Measurement of respiratory acoustic signals: effect of microphone air cavity depth," *CHEST Journal*, vol. 106, 1994, pp. 1140-1144.

[82] S. S. Kraman, G. R. Wodicka, Y. Oh and H. Pasterkamp, "Measurement of Respiratory Acoustic Signals," *Chest*, vol. 108, 1995, pp. 1004-1008.

[83] L. Vannuccini, J. Earis, P. Helisto, B. Cheetham, M. Rossi, A. Sovijarvi and J. Vanderschoot, "Capturing and preprocessing of respiratory sounds," *European Respiratory Review*, vol. 10, 2000, pp. 616-620.

[84] M. Rossi, A. Sovijarvi, P. Piirila, L. Vannuccini, F. Dalmasso and J. Vanderschoot, "Environmental and subject conditions and breathing manoeuvres for respiratory sound recordings," *European Respiratory Review,* vol. 10, 2000, pp. 611-615.

[85] G. Wodicka, P. DeFrain and S. Kraman, "Bilateral asymmetry of respiratory acoustic transmission," *Medical and Biological Engineering and Computing,* vol. 32, 1994, pp. 489-494.

Appendix A. Phantom model design

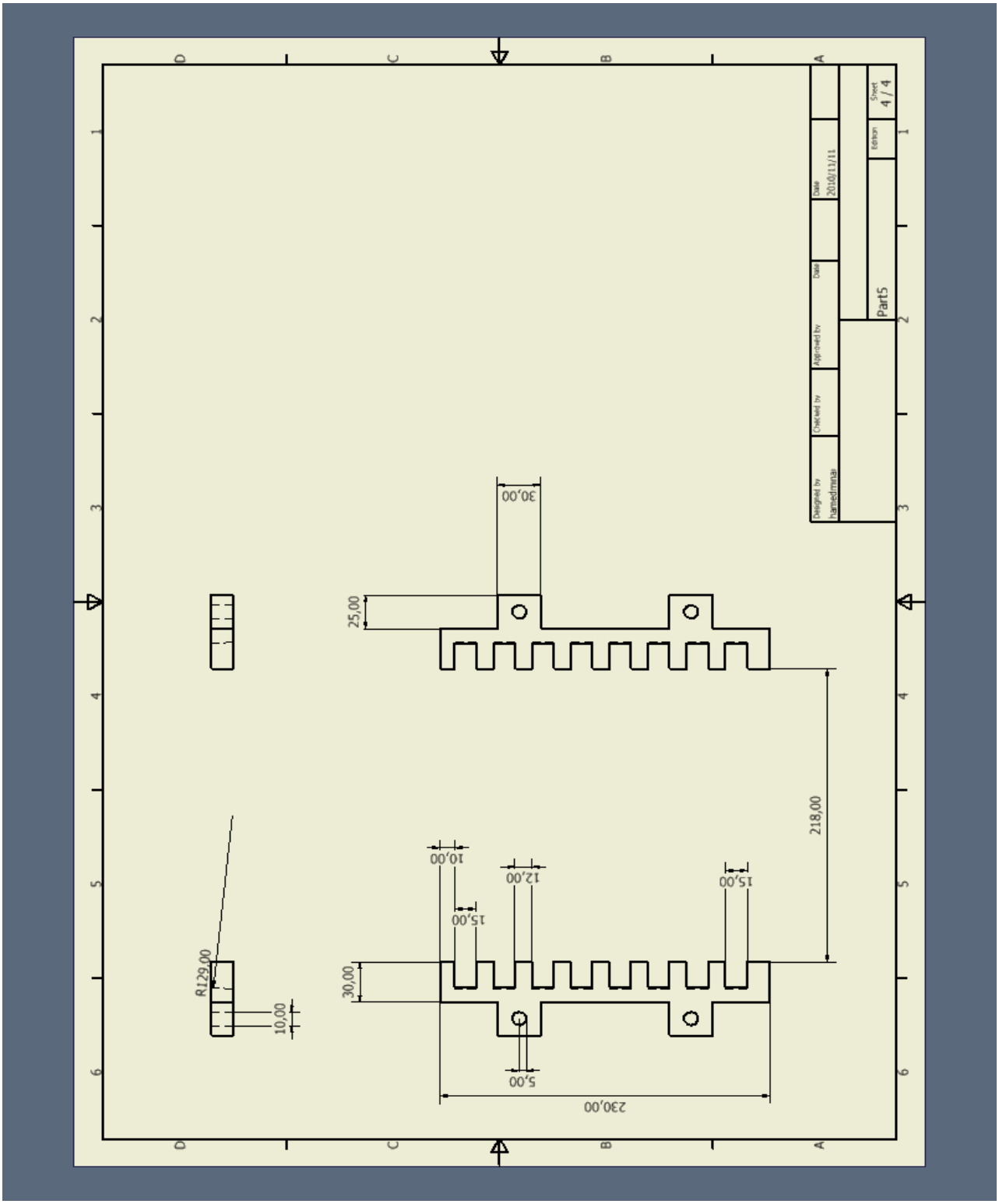

Figure 54. Model design

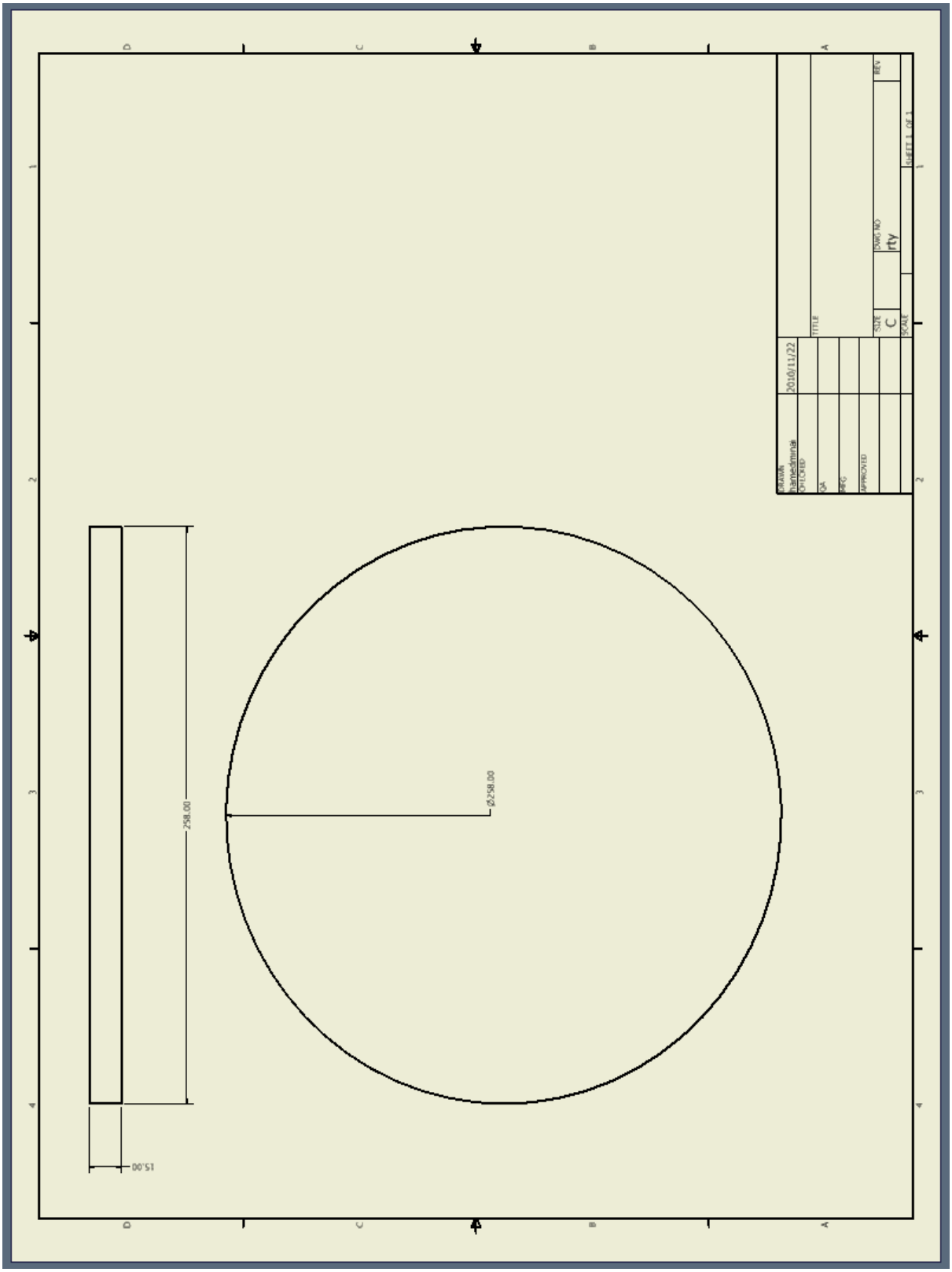

Figure 55. Phantom model design (lower part of model)

Appendix B. Data sheet of Flex Foam IT X

FlexFoam-iT!® Series

Flexible Polyurethane Foams

3lb., 4 lb., 5lb., 6 lb., 8 lb., 10 lb., 17 lb. or 25 lb.

SMOOTH-ON

www.smooth-on.com

PRODUCT OVERVIEW

FlexFoam-iT!® Series foams are premium quality flexible foams that can be used for a variety of industrial, special effects and art & crafts and projects. With several to choose from, uses include making theatrical props (swords, knives, hammers, etc.), industrial gaskets, custom padding and cushioning, and more. SO-Strong® colorants can be added for color effects.

Part A and B liquids are combined, mixed and poured into a mold or other form (apply release agent if necessary). Mixture will rise and cure quickly to a solid, flexible foam. Foams vary by density and offer good physical properties. The lower the number, the more the foam expands. **Flex-Foam-iT® III** is the lowest density foam and expands the most. **FlexFoam-iT!® 25** is the highest density foam and expands the least.

TECHNICAL OVERVIEW

	A:B Mix Ratio by Volume	A:B Mix Ratio by Weight	Specific Gravity (g/cc) (ASTM D-1475)	Specific Volume (cu. in./lb.)	Pot Life (Cream Time) (ASTM D-2471)	Tack-Free Time	Approx. Volumetric Expansion	Lbs. / Cu. Foot = Kgs. / Cu. Meter
FlexFoam-iT!® III	1:2 pbv	57.5:100 pbw	0.06	400-450	35 sec	25 min.	15 times	3 lb/ft^3 = 48 kg/m^3
FlexFoam-iT!® 4	N/A	80:100 pbw	0.08	275-300	30 sec	20 min.	10 times	5 lb/ft^3 = 80 kg/m^3
FlexFoam-iT!® V	1:1 pbv	105:100 pbw	0.10	275-300	50 sec	25 min.	10 times	5 lb/ft^3 = 80 kg/m^3
FlexFoam-iT!® 6	1:1 pbv	105:100 pbw	0.12	275-300	35 sec	2 hrs.	10 times	5 lb/ft^3 = 80 kg/m^3
FlexFoam-iT!® VIII	1:2 pbv	52.6:100 pbw	0.13	175-225	35 sec	25 min.	8 times	8 lb/ft^3 = 128 kg/m^3
FlexFoam-iT!® X	1:1 pbv	105:100 pbw	0.18	150-200	50 sec	25 min.	6 times	10 lb/ft^3 = 160 kg/m^3
FlexFoam-iT!® 17	1:2 pbv	100:185 pbw	0.27	95-103	60 sec	25 min.	3.5 times	17 lb/ft^3 = 270 kg/m^3
FlexFoam-iT!® 25	N/A	1:2 pbw	0.4	50-75	50 sec	25 min.	2 times	25 lb/ft^3 = 400 kg/m^3

***Mixed Viscosity** (ASTM D-2393):* 1000 cps
Color: White
Handling Strength: 30 Minutes
Cure Time: 2 Hours

* Values measured at room temperature (73°F/23°C)

PROCESSING RECOMMENDATIONS

PREPARATION...

Preparation - Store and use at room temperature (73°F/23°C). Environmental humidity should be as low as possible. Good ventilation (room size) is essential. This product has a limited shelf life and should be used as soon as possible. Wear safety glasses, long sleeves and rubber gloves to minimize contamination risk. **Because no two applications are quite the same, a small test application to determine suitability for your project is recommended if performance of this material is in question.**

Figure 56. Page one of data sheet Flex Foam iT X

IMPORTANT: Shelf life of product is reduced after opening. Remaining product should be used as soon as possible. Immediately replacing the lids on both containers after dispensing product will help prolong the shelf life of the unused product. **XTEND-IT® Dry Gas Blanket** (available from Smooth-On) will significantly prolong the shelf life of unused liquid urethane products.

Safety First!

The Material Safety Data Sheet (MSDS) for this or any Smooth-On product should be read prior to use and is available upon request from Smooth-On. All Smooth-On products are safe to use if directions are read and followed carefully.

Keep Out Of Reach Of Children.

Be careful. **Part A** (Yellow Label) contains methylene diphenyldiisocyante. Vapors, which can be significant if heated or sprayed, may cause lung damage and sensitization. Use only with adequate ventilation. Contact with skin and eyes may cause severe irritation. Flush eyes with water for 15 minutes and get immediate medical attention. Remove from skin with soap and water.

Part B (Blue Label) is irritating to the eyes and skin. Avoid prolonged or repeated skin contact. If contaminated, flush eyes with water for 15 minutes and get immediate medical attention. Remove from skin with soap and water. When mixing with Part A, follow precautions for handling isocyanates. If machining cured FlexFoam-It!®, wear dust mask or other apparatus to prevent inhalation of residual particles.

Important: The information contained in this bulletin is considered accurate. However, no warranty is expressed or implied regarding the accuracy of the data, the results to be obtained from the use thereof, or that any such use will not infringe a copyright or patent. User shall determine suitability of the product for the intended application and assume all associated risks and liability whatsoever in connection therewith.

APPLYING A RELEASE AGENT...

These foams will stick to just about anything. A release agent is necessary to facilitate demolding when casting into or over most surfaces and will extend mold life. **Use a release agent made specifically for releasing urethane foams such as Ease Release® 2831** available from Smooth-On or your Smooth-On distributor. **Do not use silicone based release agent.** A liberal coat of release agent should be applied onto all surfaces that will contact the foam.

IMPORTANT: To ensure thorough coverage, lightly brush the release agent with a soft brush over all surfaces. Let the release agent dry for 30 minutes.

MEASURING & MIXING...

Liquid urethanes are **moisture sensitive** and will absorb atmospheric moisture. Mixing tools and containers should be clean and made of metal, glass or plastic. Materials should be stored and used in a warm environment (73°F/23°C).

Mixing can be done by hand or using a drill and a mixer attachment, such as a "squirrel" mixer. After dispensing required amounts of Parts A and B into mixing container, **mix thoroughly for 30 seconds.** Stir quickly and deliberately, making sure you scrape the sides and bottom of the mixing container several times. Be careful not to splash low-viscosity material out of the container. **Remember, these products cure quickly.** Do not delay between mixing and pouring.

POURING, CURING & PERFORMANCE...

Pouring & Curing **-** For best results, pour your mixture in a single spot at the lowest point of the containment field and let the mixture seek its level. Allow space in the containment field for the foam to grow as it expands to its ultimate volume. Allow foam to cure for at least 30 minutes before handling.

Improving Surface Finish & Minimizing Voids With Back Pressure **-** Use a board that will completely cover the mold opening. Using a 3/4" (2 cm) drill bit, drill 3 holes in the board spaced a few inches/cm apart. Make sure that when the board is placed over the mold opening the holes are over the mold cavity and rising foam will be able to make it through. Apply Ease Release® 2831 thoroughly to both sides of the board and into the drilled holes. Mix and pour FlexFoam-iT!® into mold cavity and place board over mold opening. Secure board firmly in place (mold straps may be necessary). As foam rises in the mold cavity, some foam will grow out of the drilled holes. After the foam stops growing, you can let go of the board. Do not handle for at least 30 minutes. After 30 minutes, you can then cut excess material that came through holes and gently remove board and casting.

Is Your Foam Collapsing? **-** This is a common phenomenon associated with cold temperatures, inadequate mixing or both. **Environment or material too cold?** Warm it up. **Inadequate mixing?** You must thoroughly pre-mix both parts A and B. After combining A and B, mix thoroughly. If using a mechanical mixer, mix for 15 seconds and then hand mix for 15 seconds. When hand mixing, mix quickly and aggressively, almost whipping the material.

SMOOTH-ON

Call Us Anytime With Questions About Your Application

Toll-free: **(800) 762-0744** Fax: **(610) 252-6200**

The new www.smooth-on.com is loaded with information about mold making, casting and more.

091312-JR

Figure 57. Page two of data sheet Flex Foam iT X

Appendix C. Data sheet of Body Double® Skin-Safe silicone rubber

Body Double®

"Apply to Skin" Platinum Silicone Rubber

Certified Skin Safe!

www.smooth-on.com

PRODUCT OVERVIEW

Body Double® is a long lasting platinum-cure silicone rubber that can be applied directly to the skin to make molds of the face, hands and other body parts. The rubber cures quickly and will reproduce perfect detail from any original model – far better detail than any alginate!

One Casting or Many . . . For About The Same Price: unlike alginates, which are good for one only casting, **Body Double®** will last for many castings of almost any material including plaster, Matrix® Neo®, wax, resins (Smooth-Cast urethanes, polyester, etc.), low-temperature melt metal alloys, etc. The amount of **Body Double®** used per mold is less than most alginates, so the cost per mold is about the same. **Body Double®** is odorless and is ACMI rated non-toxic and skin safe. Adding **HYPER-FOLIC® release additive** to **Body Double®** silicone will create a self-releasing silicone which is easily removed from hair-covered body areas.

Body Double® "Standard Set" for larger surface areas. Working time of 5 minutes and a demold time of 30 minutes*.

Body Double® "Fast Set" for fast turnaround. Working time of 90 seconds and a demold time of 5 minutes*.

*Depending on material temperature, ambient temperature and body temperature – see "Preparation" below for details.

TECHNICAL OVERVIEW

*All values measured after 7 days at 73°F/23°C

	A:B Mix Ratio by Volume or Weight	Mixed Viscosity (ASTM D-2393)	Specific Gravity (g/cc) (ASTM D-1475)	Specific Volume (cu. in./lb.) (ASTM D-1475)	Pot Life (ASTM D-2471)	Cure Time	Color	Shore A Hardness (ASTM D-2240)	Tensile Strength (ASTM D-412)	Die C Tear Strength (ASTM D-624)	Elongation At Break (ASTM D-412):	Shrinkage (in./in.) (ASTM D-2566):
Body Double® Fast Set	1A:1B	Brushable	1.17	23.7	90 sec.	5 min.	Aqua Green	25A	450 psi	40 pli	500%	<0.001
Body Double® Standard Set	1A:1B	Brushable	1.17	23.7	5 min.	30 min.	Purple	25A	525 psi	40 pli	500%	<0.001

PROCESSING RECOMMENDATIONS

PREPARATION... **Store and use Body Double® at room temperature (73°F / 23°C).** Warmer temperatures will drastically reduce working time and cure time. Storing material at warmer temperatures will also reduce the usable shelf life of unused material. This product has a limited shelf life and should be used as soon as possible. Wear safety glasses, long sleeves and rubber gloves to minimize contamination risk.

Safety - **We recommend that you do a small scale test on the back of your hand** to ensure that you have no allergic reaction to the release preparations or mold rubber. If you notice any type of skin reaction, do not use this product. Body Double® is safe for skin application only – it should not be ingested. Do not use to make molds of the inside of the mouth. You can make molds of a smile - parted lips with teeth exposed, but closed together.

Life casting is best done with at least three people. You will be working with materials that set up quickly. One person is the designated model and the others will mix and apply mold rubber and support shell.

Cure Inhibition - Contaminants on the skin will cause inhibition. Prior to applying Body Double® Release Cream, skin should be clean and free of make-up, cosmetics, skin creams, oils perfumes, etc. Do not apply rubber over skin coated with an aloe-based product, as this will cause cure inhibition. **Do not use latex gloves.** If using a bald cap, make sure it is latex free.

Because no two applications are quite the same, a small test application to determine suitability for your project is recommended if performance of this material is in question.

RELEASING BODY DOUBLE®... Body Double® will not stick to skin but it will "mechanically lock" onto skin hair including facial hair, eyebrows, eyelashes etc. **Body Double® Release Cream** or **HYPER-FOLIC® release additive** (see below) will minimize mechanical lock. Also, you can shave the intended molding area prior to applying Body Double®.

Body Double® Release Cream (available from Smooth-On) is a non-toxic skin conditioner that will aid in releasing Body Double® mold rubber from skin surfaces with or without hair. It washes off with soap and water. It is highly concentrated, so a little goes a long way. To use, wash intended body section with soap and water and dry thoroughly. Liberally apply Body Double® Release Cream to all skin surfaces

Figure 58. Page one of data sheet Body Double Skin-Safe silicon rubber

Safety First!

The Material Safety Data Sheet (MSDS) for this or any Smooth-On product should be read prior to use and is available upon request from Smooth-On. All Smooth-On products are safe to use if directions are read and followed carefully.

BE CAREFUL - Use only with adequate ventilation. Contact with skin and eyes may cause irritation. Flush eyes with soap and water for 15 minutes and seek immediate medical attention. Remove from skin with waterless hand cleaner followed by soap and water.

IMPORTANT - The information contained in this bulletin is considered accurate. However, no warranty is expressed or implied regarding the accuracy of the data, the results to be obtained from the use thereof, or that any such use will not infringe upon a patent. User shall determine the suitability of the product for the intended application and assume all risk and liability whatsoever in connection therewith.

(bare and hair covered) that will contact mold rubber. **Take special care to aggressively massage and work the cream into and over body hair.** Body hair not thoroughly coated with release cream will become encapsulated and stuck in rubber which will be difficult & painful to remove.

HYPER-FOLIC® Release Additive is a non-toxic, skin conditioning liquid that is mixed with Body Double® silicone mold rubber prior to applying rubber to the skin. HYPER-FOLIC® will not only aid in releasing cured rubber from the skin but will also release cured rubber from hair-covered skin surfaces (closely cropped beards, moustaches, eye-brows, pubic hair, etc.) See the HYPER-FOLIC® Technical Bulletin (available at www.smooth-on.com) for more information.

MEASURING & MIXING...

Body Double® "Fast Set" is best dispensed through its pre-measured **400 ml. cartridge tube system with static mixing tube** (1/2" – 18 elements). Cartridge dispensing guns and static mixing tubes are available from Smooth-On distributors. On cartridge tube set (A+B), remove clear cap from cartridge end and Twist / break off end-cap. Screw on static mixing tube and place cartridge in dispensing gun.

Do not squeeze trigger until you are ready to apply rubber. After squeezing trigger, Parts A & B will quickly be mixed through the static mixing tube and dispensed through the tip in a uniform color. Dispense directly onto skin and immediately spread mixture over all surfaces to be molded using a soft bristle brush.

Note: If you stop dispensing, product may cure in static mixing tube. If this happens, replace static mixing tube.

Storage Of Unused Material – Leave static mixing tube with cured material attached to cartridge. To use again, simply replace static mixing tube.

Body Double® "Standard Set" is available in larger units (quarts, gallons, etc.). Mix ratio is 1A:1B by volume. Dispense equal amounts into a mixing container and aggressively hand mix, making sure that you scrape the sides and bottom of your mixing container to attain a uniform color and eliminate any color streaks. Apply to skin with soft bristle brush.

Optional: For initial layer or "detail coat", rubber can be thinned for easier application with Smooth-On's Silicone Thinner. Apply to skin with soft bristle brush. Subsequent layers can be applied without thinner.

Add material as necessary – Body Double® sticks to itself, so adding more rubber is not a problem. Add new material as soon as possible. Be careful when adding new material to cured material - carefully "marry" sections to minimize seam lines. Final mold thickness should be ¼" – ½" (1 cm). Let material cure fully before applying support shell.

APPLYING A SUPPORT SHELL, DEMOLDING & CASTING...

Gypsona® Plaster Bandages (available from Smooth-On) remain the industry standard for making a fast, strong support shell. After Body Double® rubber has cured, brush a thin layer of petroleum jelly onto rubber mold surface to minimize chances of suction or mechanical locking of rigid support shell. Wet and apply bandages over rubber mold surface, following contours. Bandages dry in 15 minutes and can be removed from rubber surface.

Demold Rubber From Body - Slowly peel rubber away from skin surface. If you encounter encapsulated hair that is stuck (did not get enough release agent), you may have to slowly cut the hair with scissors. Be careful not to cut your skin or the mold rubber.

Removing Body Double® Release Cream – **Make-Up Remover will work well**. Apply to skin and then wash area with soap and water. **Baby oil will also work**, but may leave a residue on the skin.

Casting - Seat rubber mold into support shell before casting. A release agent is not necessary when casting most materials. **If casting another platinum-cure silicone rubber**, use Ease Release® 200. **If casting resins**, let rubber cure at least 60 minutes before casting. Store cured Body Double® rubber mold in support shell for best results.

SMOOTH-ON SINCE 1995

Call Us Anytime With Questions About Your Application.

Toll-free: **(800) 762-0744** Fax: **(610) 252-6200**

The new www.smooth-on.com is loaded with information about mold making, casting and more.

051910 - JR

Figure 59. Page two of data sheet Body Double Skin-Safe silicon rubber

Appendix D. Complex wave number for phantom model materials

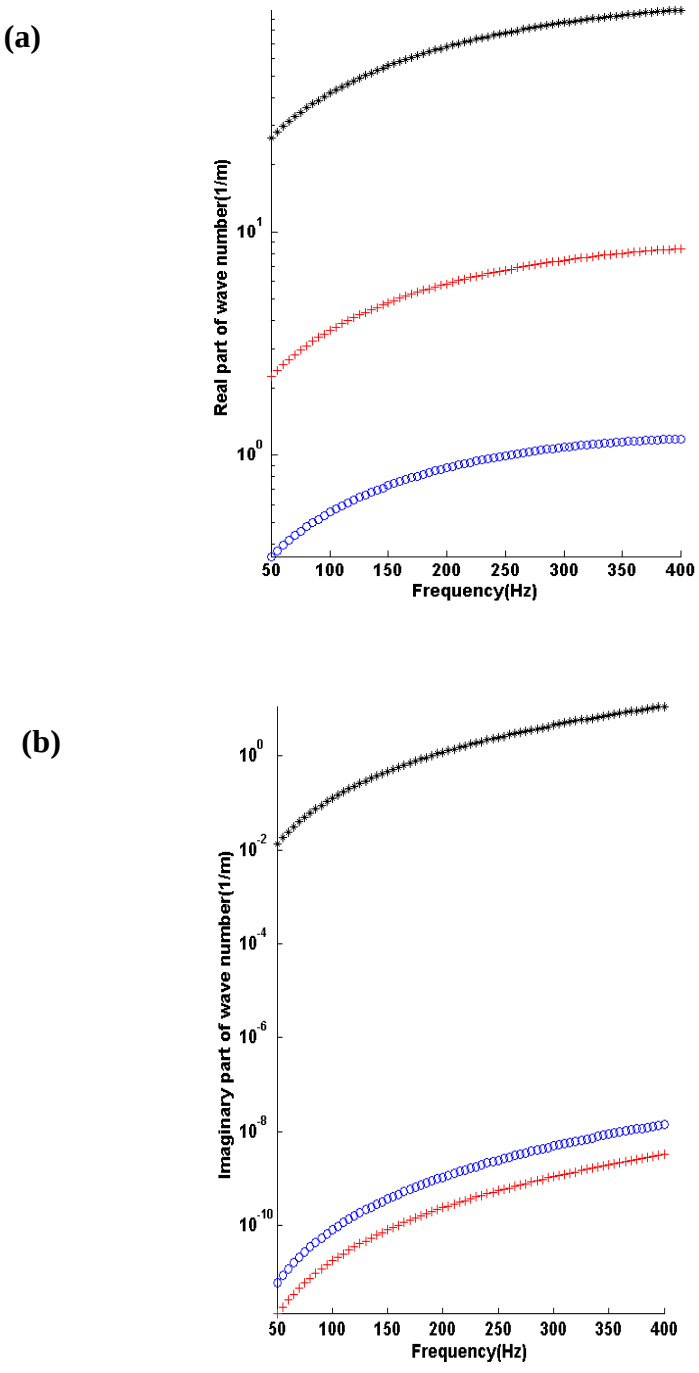

Figure 60. (a) Real part and (b) imaginary part of complex wave number for lung parenchyma(*), soft tissue (O) and air (×) [65]

Appendix E. The results of frequency responses of healthy model

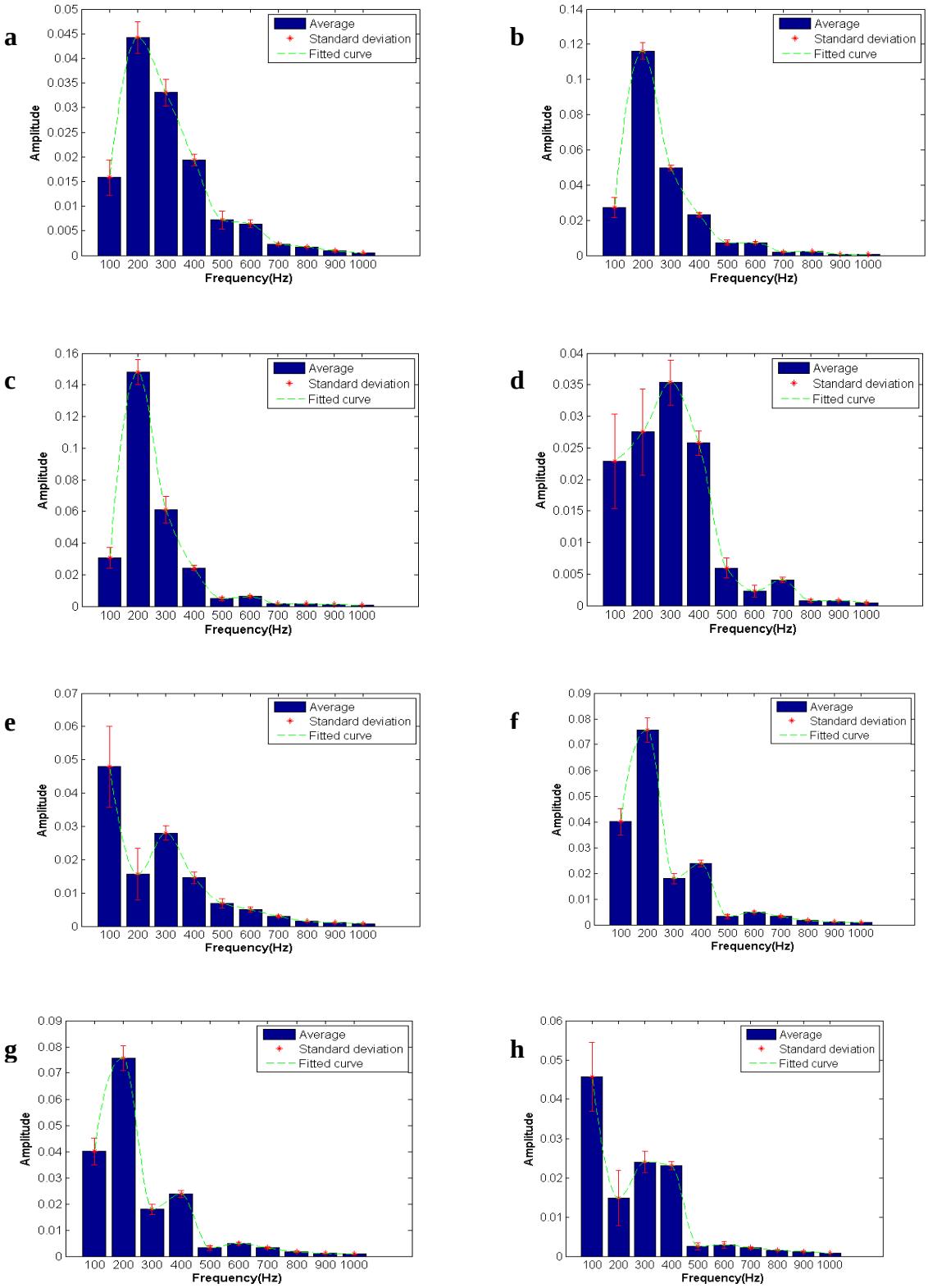

Figure 61. Frequency response of the healthy model at the axial position 175 mm and axial positions of 40 (a), 80(b), 120(c), 160(d),200(e), 240(f),280(g) and 320 degrees(h)

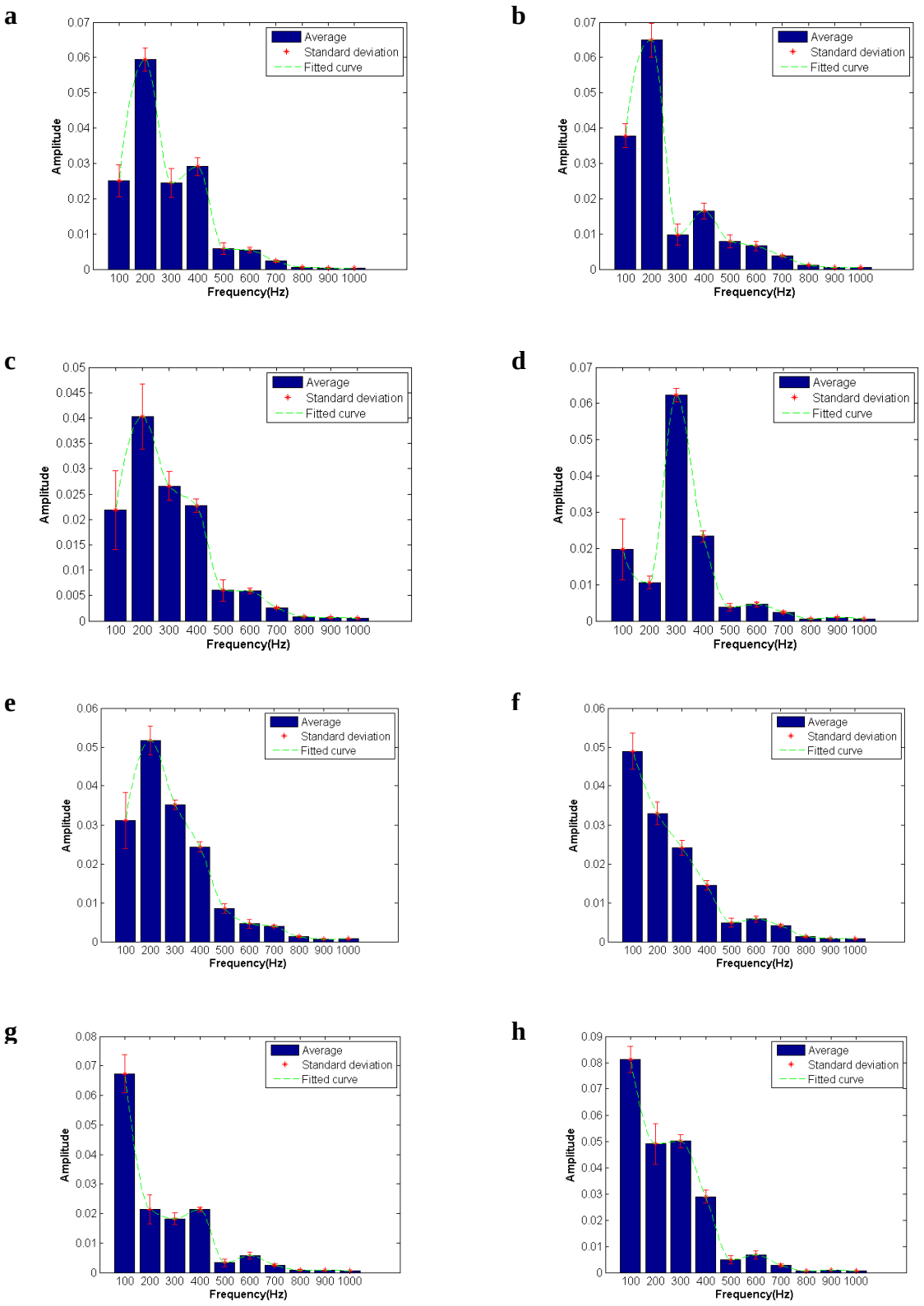

Figure 62. Frequency response of the healthy model at the axial position 105 mm and axial positions of 40 (a), 80(b), 120(c), 160(d),200(e), 240(f),280(g) and 320 degrees(h)

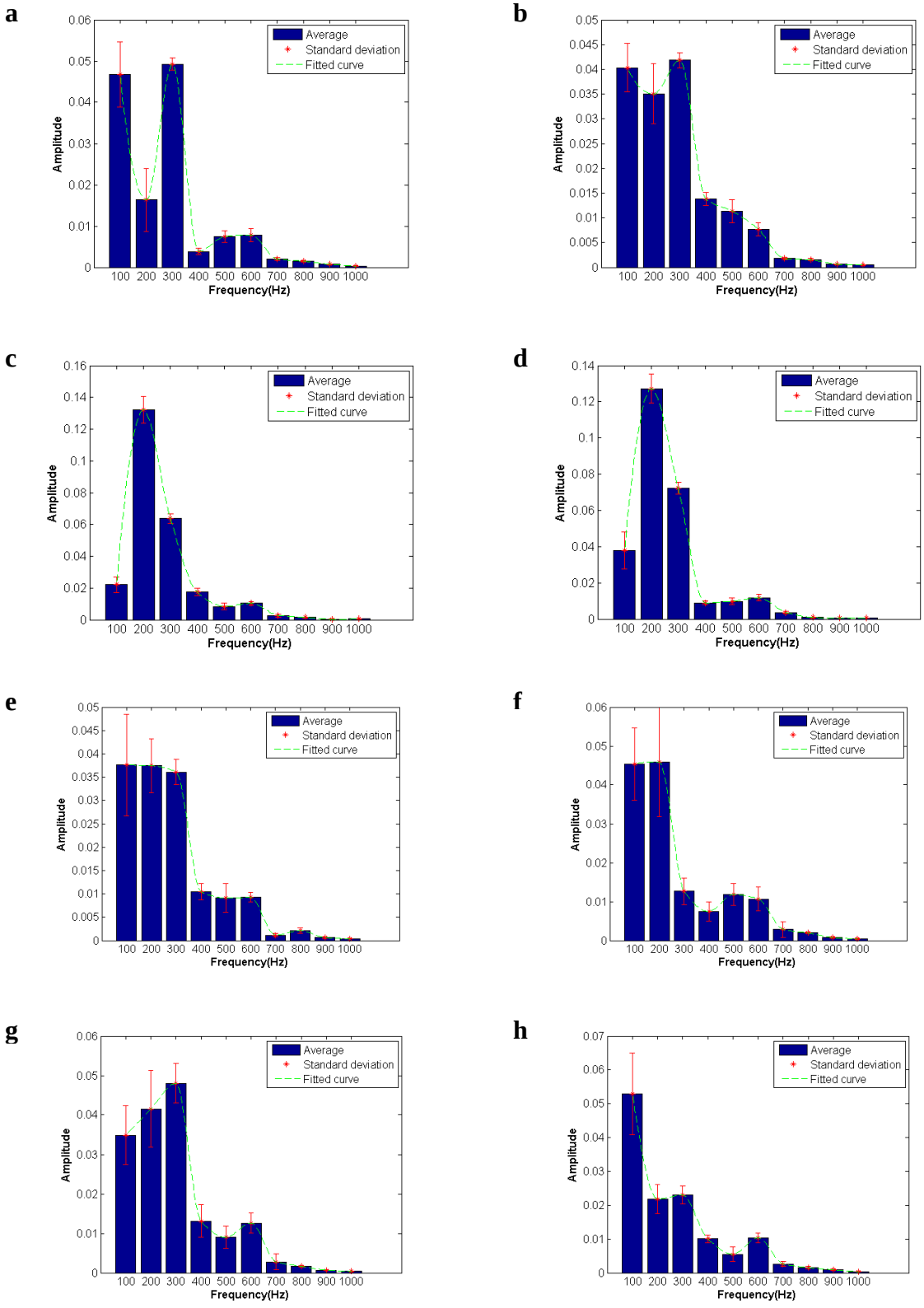

Figure 63. Frequency response of the healthy model at the axial position 35 mm and axial positions of 40 (a), 80(b), 120(c), 160(d),200(e), 240(f),280(g) and 320 degrees(h)

Appendix F. The results of frequency responses of pleural effusion model

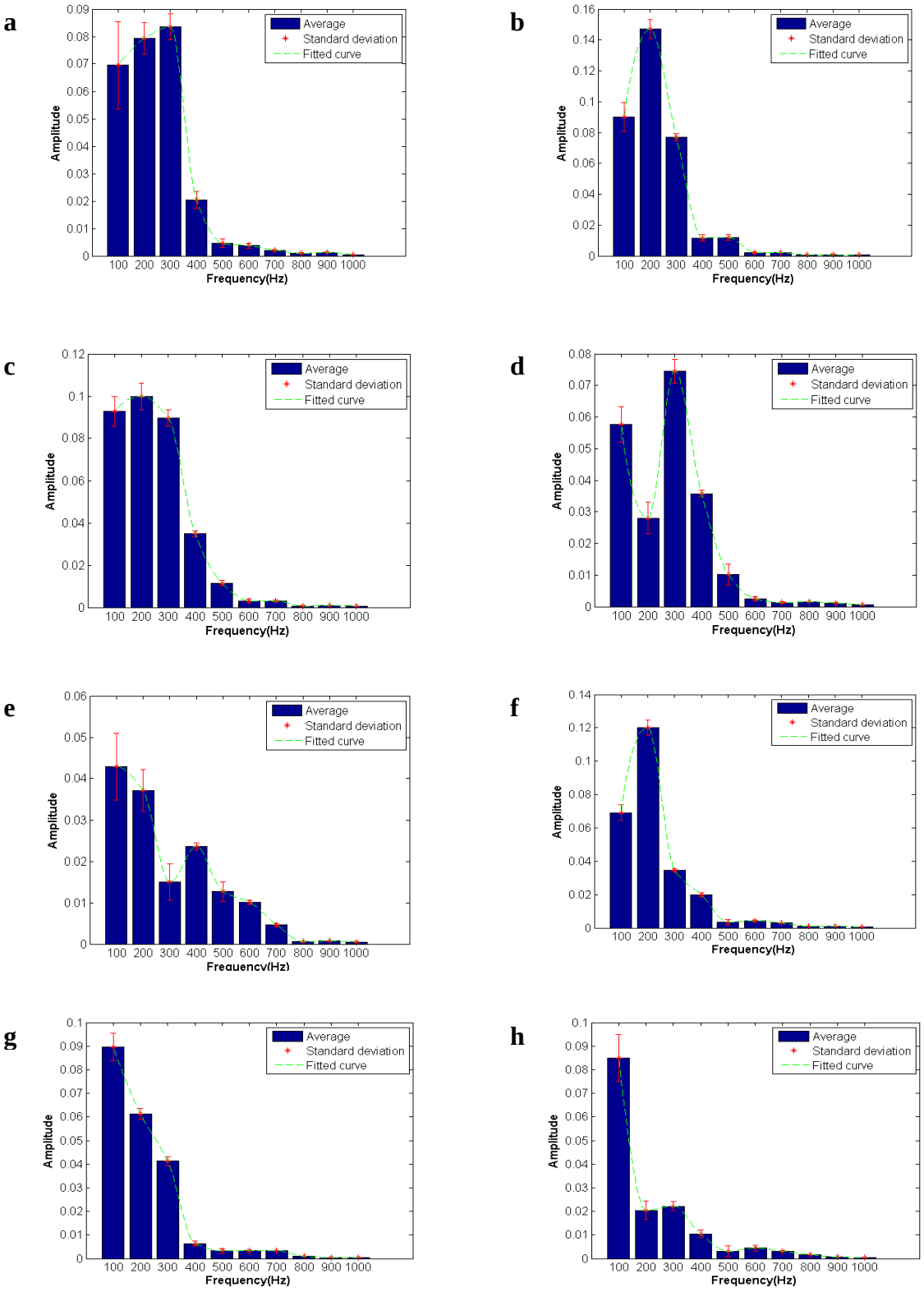

Figure 64. Frequency response of the pleural effusion model at the axial position 175 mm and axial positions of 40 (a), 80(b), 120(c), 160(d),200(e), 240(f),280(g) and 320 degrees(h)

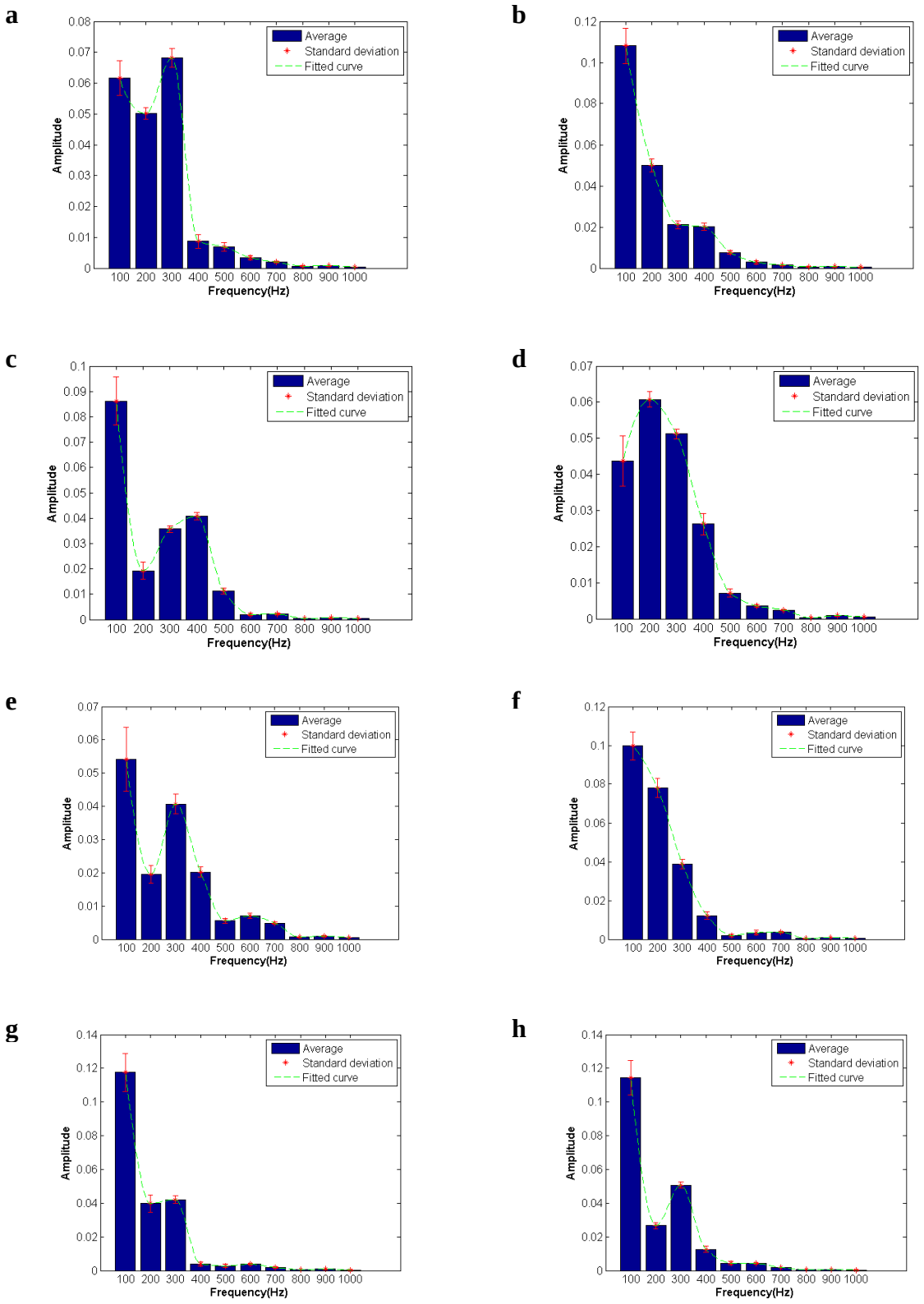

Figure 65. Frequency response of the pleural effusion model at the axial position 105 mm and axial positions of 40 (a), 80(b), 120(c), 160(d),200(e), 240(f),280(g) and 320 degrees(h)

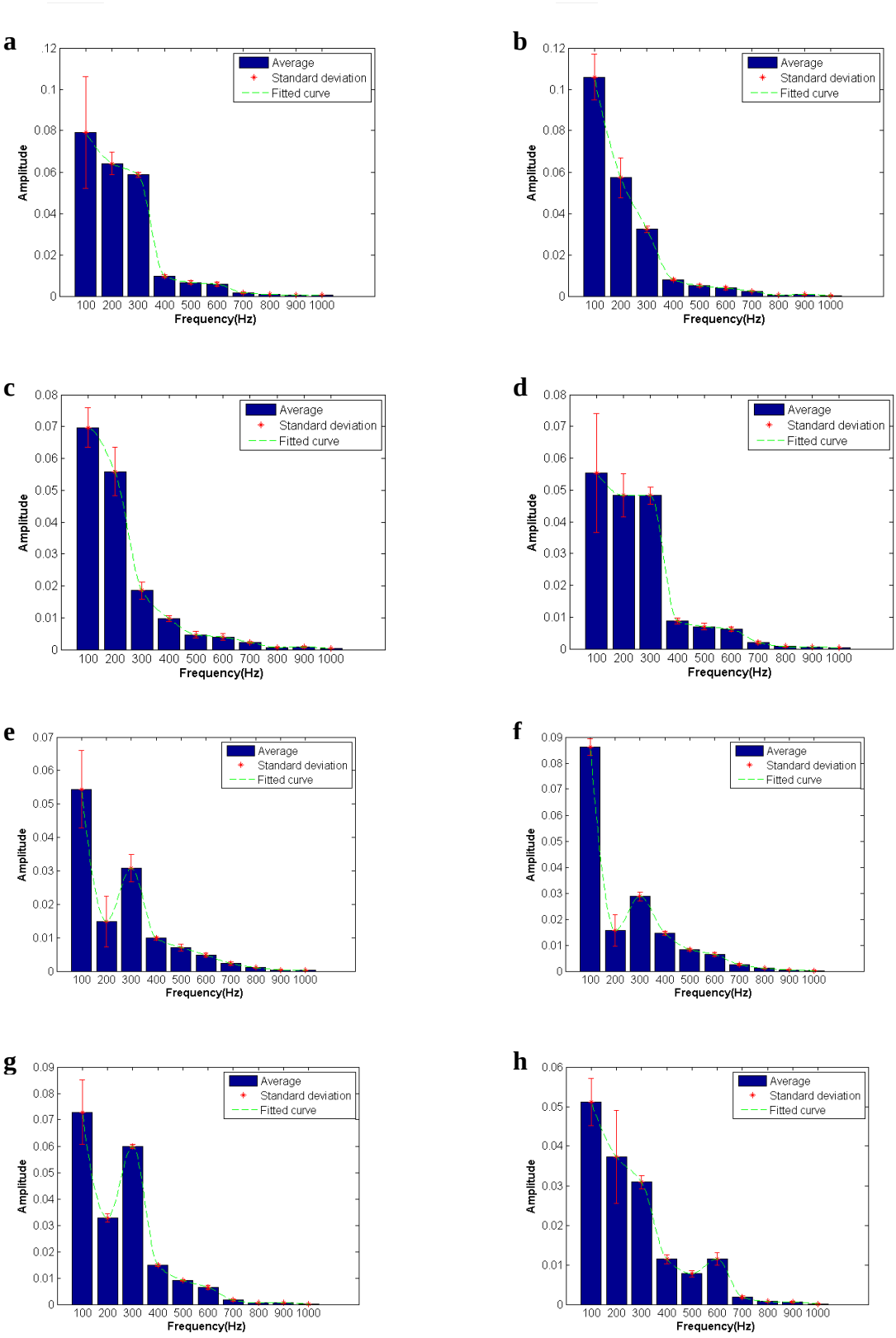

Figure 66. Frequency response of the pleural effusion model at the axial position 175 mm and axial positions of 40 (a), 80(b), 120(c), 160(d),200(e), 240(f),280(g) and 320 degrees(h)

Appendix G. The calculated time delay for the model

Table 16. Time delay calculated in the phantom model of the lungs with two water bags, one on either side.

Axial position	Angular position							
	θ=40°	**θ=80°**	**θ=120°**	**θ=160°**	**θ=200°**	**θ=240°**	**θ=280°**	**θ=320°**
175 mm	0.0017	0.0012	0.0020	0.0018	0.0019	0.0010	0.0011	0.0011
105 mm	0.0022	0.0011	0.0021	0.0021	0.0024	0.0009	0.0014	0.0013
35 mm	0.0025	0.0017	0.0021	0.0021	0.0025	0.0017	0.0014	0.0016

Table 17. Time delay calculated in the healthy phantom model of the lungs (without water inside)

Axial position	Angular position							
	θ=40°	**θ=80°**	**θ=120°**	**θ=160°**	**θ=200°**	**θ=240°**	**θ=280°**	**θ=320°**
175 mm	0.0017	0.0013	0.0020	0.0018	0.0014	0.0012	0.0012	0.0012
105 mm	0.0022	0.0011	0.0021	0.0021	0.0016	0.0010	0.0012	0.0013
35 mm	0.0025	0.0017	0.0021	0.0021	0.0023	0.0014	0.0015	0.0016

Appendix H. Stethoscope design

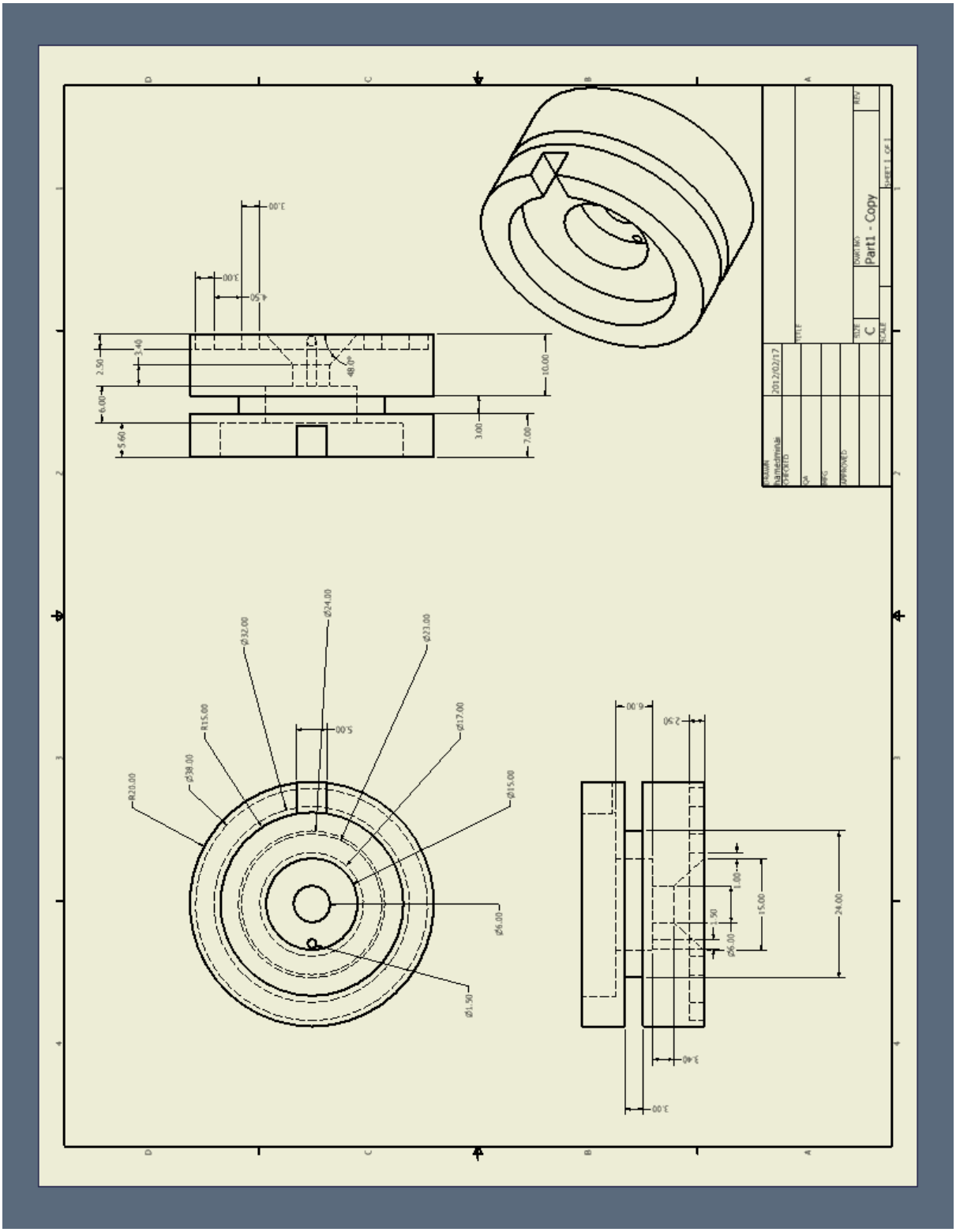

Figure 67. Stethoscope housing

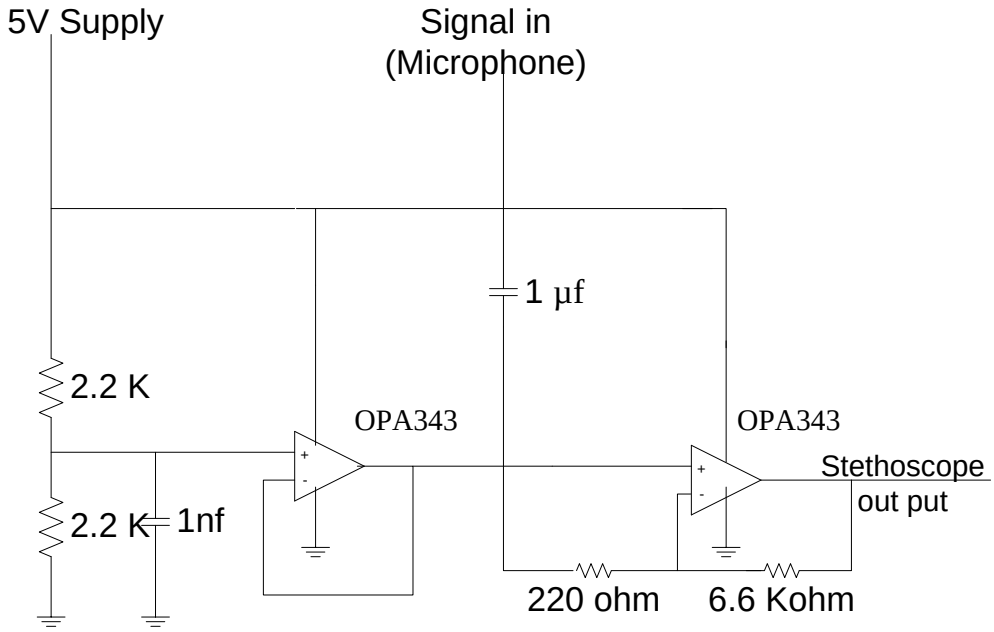

Figure 68. The circuit of the stethoscope

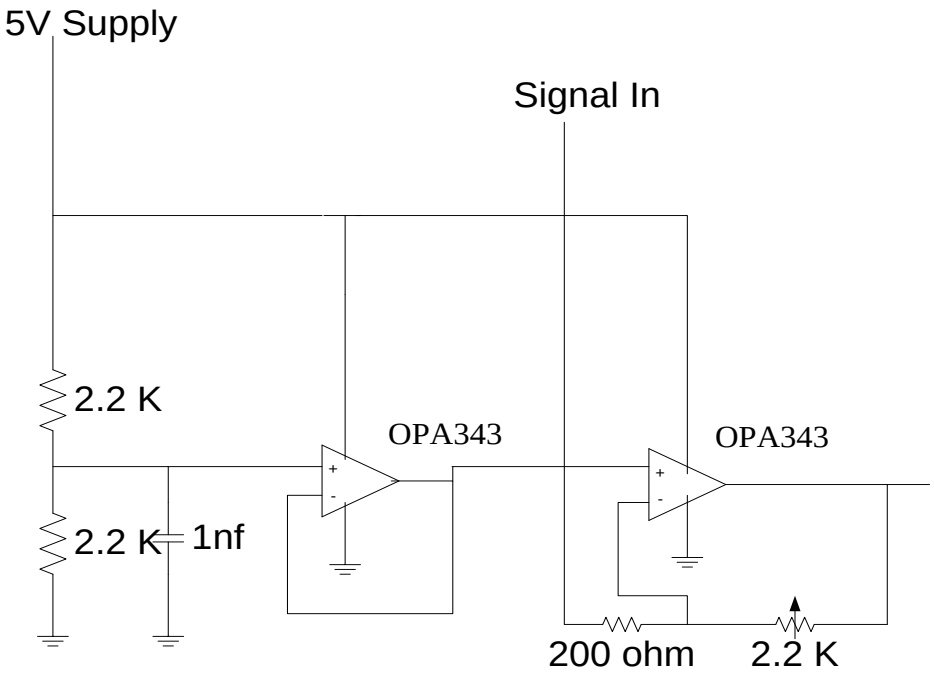

Figure 69. The circuit of the amplifier

Panasonic Microphone Cartridges

Omnidirectional Back Electret Condenser Microphone Cartridge

Series: **WM-61A**
WM-61 B (pin type)

■ **Features**

- Small microphones for general use
- Back electret type designed for high resistance to vibrations, high signal-to-noise ratio
- High sensitivity type
- Microphone with pins for flexible PCB (WM-61B type)

■ **Sensitivity**

Vs = 2.0V RL = 2.2kΩ	–35 ± 4dB

■ **Specifications**

Sensitivity	–35±4dB (0db = 1V/pa, 1kHz)
Impedance	Less than 2.2 kΩ
Directivity	Omnidirectional
Frequency	20–20,000 Hz
Max. operation voltage	10V
Standard operation voltage	2V
Current consumption	Max. 0.5 mA
Sensitivity reduction	Within –3 dB at 1.5V
S/N ratio	More than 62 dB

■ **Typical Frequency Response Curve**

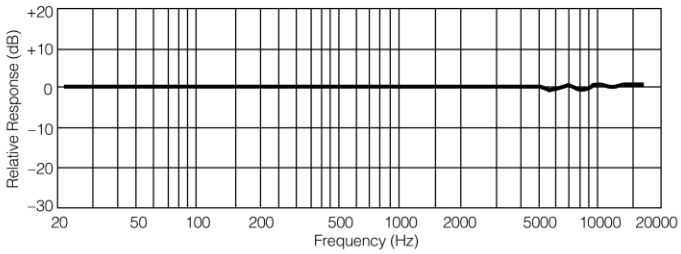

■ **Dimensions in mm** (not to scale)

WM-61A

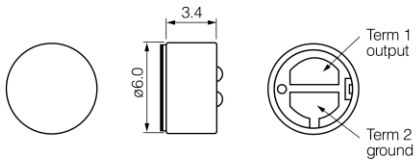

WM-61B

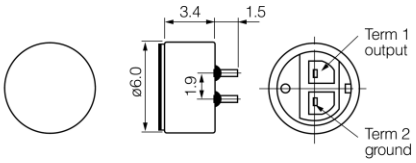

Design and specifications are subject to change without notice. Ask factory for technical specifications before purchase and/or use.
Whenever a doubt about safety arises from this product, please contact us immediately for technical consultation.

Figure 70. Data sheet of the microphone

Appendix I. Funnels design

(a)

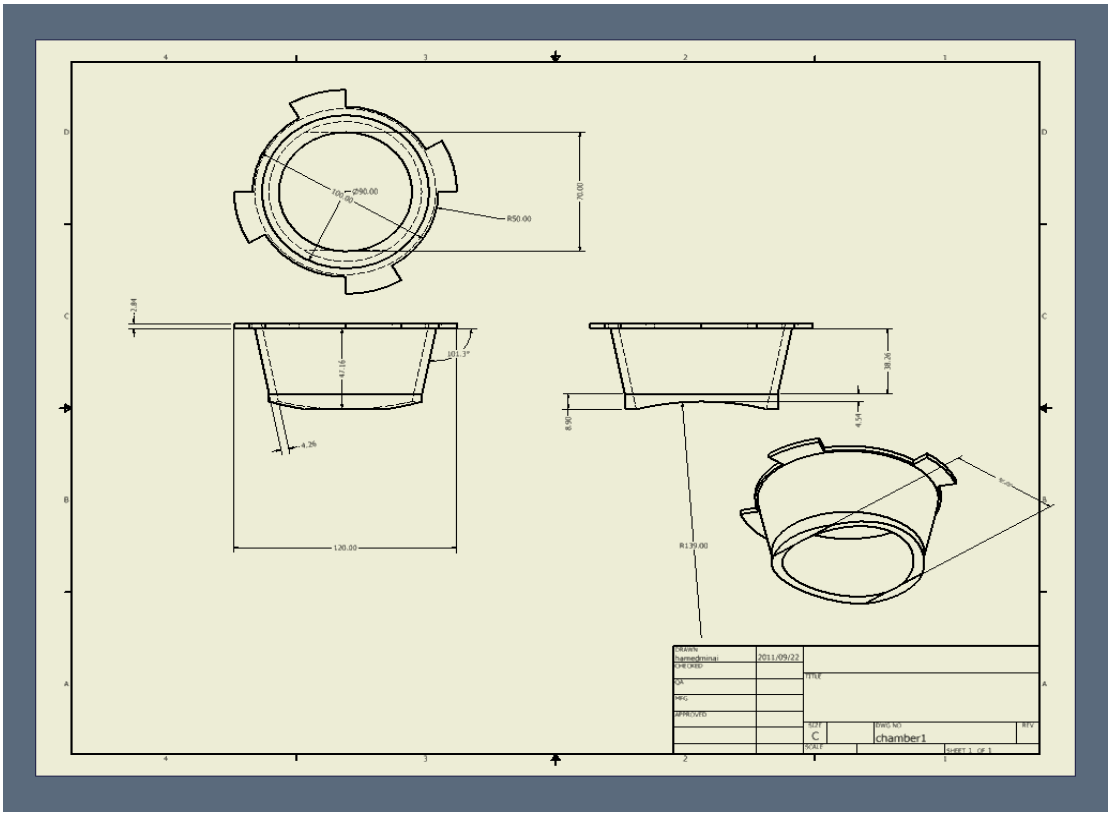

(b)

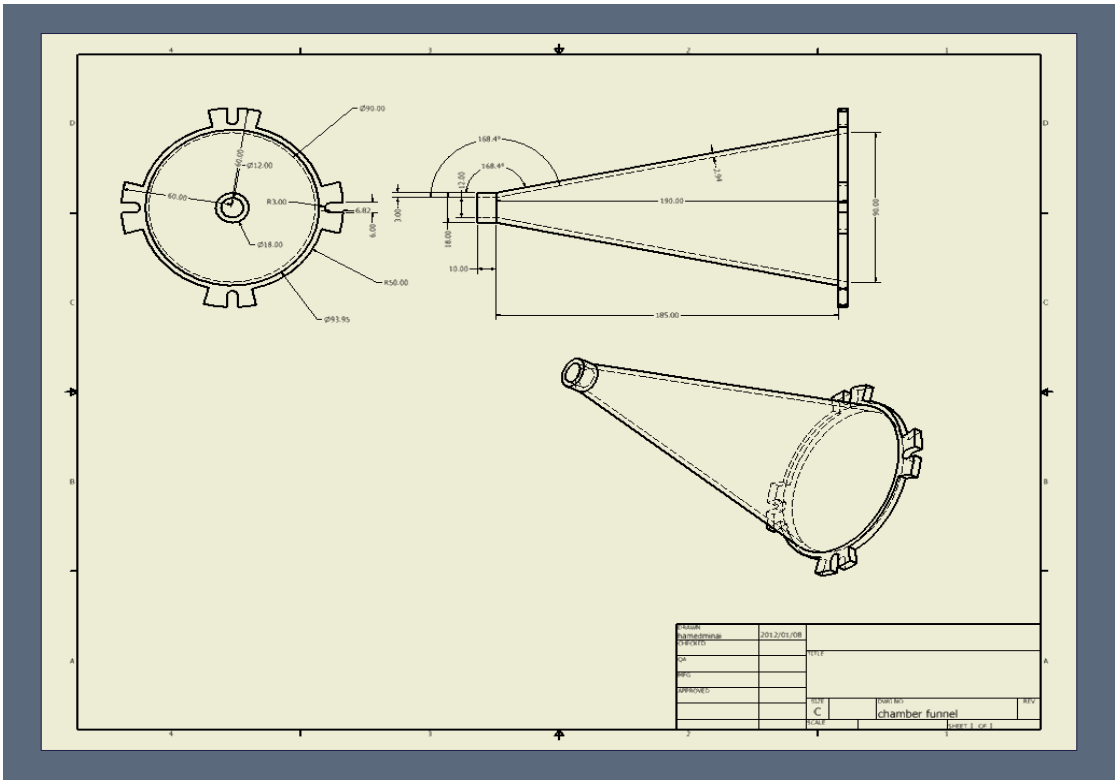

Figure 71. (a) Funnel design for transmission of sound from the chest of the model, (b) funnel design for transmission of sound from the trachea of the model

Appendix J. Calculated time delay for healthy subjects

Table 18. Calculated time delay for healthy subject by transmission of complex chirp sound

Subject number	Trial number	Location of microphones							
		UFR	UFL	RL	LL	URB	ULB	LRB	LLB
1	1	1.6	1.6	3.6	Nan	1.2	1.2	14.7	13.2
1	2	1.62	1.63	3.8	4.2	1.3	1.2	12.7	13.0
1	3	1.61	1.6	3.5	4.2	1.1	1	12.2	13.0
2	1	2.3	2.3	5.2	4.6	2.2	2.2	12.8	12
2	2	2.1	2.1	5.3	4.8	2.1	2.1	12.63	11.9
2	3	2.2	2.2	5.2	4.8	2.1	2.1	12	11
3	1	1.4	1.3	4.1	4	1.4	1.7	7.4	7.1
3	2	1.5	1.3	5.9	5.2	1.3	1.7	7.2	7.1
3	3	1.5	1.5	4.1	4.2	1.2	1.7	7.31	7.1
4	1	2.8	2.4	5.7	5	2.6	2.7	9.6	9.3
4	2	2.5	2.1	5.9	5.2	2.3	2.2	10	9.5
4	3	2.7	2.1	5.8	5.1	2.4	2.3	9.8	9.2
5	1	1.7	1.5	10	7	1.3	1.2	12.1	8.6
5	2	1.4	1.3	Nan	8	1.1	1	12.5	8.6
5	3	1.4	1.4	9.6	Nan	1	1	Nan	Nan
6	1	2.8	2.7	9	Nan	1.9	2	16	15
6	2	2.8	2.5	9.2	6.7	1.9	1.9	16.1	15.1
6	3	2.8	2.6	9	6.8	1.9	1.9	16.2	15.2
7	1	2.5	2	6.4	Nan	2.7	2.1	8.7	8.5
7	2	2.2	1.8	7.5	6.3	2.2	2.0	8.6	8.3
7	3	2.1	1.8	6.1	6.8	2.1	1.8	8.6	8.3
8	1	2.8	2.5	6	7.2	3.1	3.1	13.5	14.2
8	2	2.4	2.3	6.7	7.1	3.1	3.2	13.4	14.1
8	3	2.5	2.5	6.1	7.2	3.3	3.8	13.8	14
9	1	1	1.4	7.3	Nan	2.3	2.3	Nan	Nan
9	2	1	1	Nan	7.8	1.1	1	10.2	9.4
9	3	1	1.2	7.8	6.4	1.3	1	10	Nan
10	1	2.5	1.8	11.6	4.8	1.8	1.3	Nan	14.8
10	2	2.4	1.8	11.2	4	1.7	1.3	Nan	14.6
10	3	2.5	1.8	11.3	5	1.8	1.4	13.6	14.6
11	1	2.1	2.0	Nan	Nan	2.2	1.8	14.1	13.9
11	2	2.9	2.4	12	Nan	2.7	2.5	14.1	13.2
11	3	2.8	2.8	12	7.4	2.5	Nan	Nan	14.2
12	1	3.05	2.5	3.8	2.9	3.2	3.5	7.5	6.4
12	2	2.4	2.1	3.6	3.2	2.9	2.6	7.1	6.3

12	3	2.7	2.4	3.5	3.1	2.7	Nan	7.6	6.3
13	1	2.4	2.5	Nan	Nan	2.1	2.3	9.2	9.4
13	2	2.4	2.5	4	3.5	2.3	2.3	10	9.4
13	3	3.2	2.2	4.3	4.2	2.6	2.5	10	9.9
14	1	0.6	0.6	4	3.5	0.5	0.5	6.3	6.4
14	2	0.6	0.6	4.3	3.6	1	0.7	6.2	6.1
14	3	0.5	0.6	4.6	3.5	0.7	6	Nan	6.3
15	1	1.5	1.5	Nan	Nan	1.1	1	Nan	Nan
15	2	1.3	1.3	6.2	Nan	Nan	Nan	7.3	7.9
15	3	1.4	1.4	6	7.3	1	0.9	7.6	7.8
16	1	1.2	1.4	3.1	Nan	Nan	Nan	Nan	Nan
16	2	1.8	2.2	3.4	4.6	1.8	2.4	5.6	3.3
16	3	1.5	1.8	3.4	Non	1.4	2.3	5.4	3.5
17	1	2.3	3.9	4	3.5	1.2	1	13	14
17	2	2	3.9	4.2	3.5	1	1	13.6	14.1
17	3	2	3.5	4.2	3.5	1	1	13.5	14
18	1	2.1	2.4	7.7	8.8	2.8	2.4	9.6	8.1
18	2	2.1	2.3	7.7	8.6	2.1	2.1	9.8	8.1
18	3	1.8	1.8	6.8	7.2	2.1	2	10	8.5
19	1	1.7	1.5	3.5	4	1.8	1.8	9.3	8.6
19	2	1.5	1.3	3.5	3.8	2.1	2.1	9.3	8.7
19	3	1.6	1.3	3.8	3.0	1.9	1.8	9	8.4
20	1	1	1	4.2	3	1	1.2	6	6.1
21	1	2.2	2.3	9.2	8.3	1.8	1.7	15.3	12.7
21	2	1.5	1.3	3.5	3.8	2.1	2.1	9.3	8.7
21	3	2.1	2.1	9.6	8.4	2.1	2.6	15.3	15.3
22	1	Nan	Nan	7.2	8.1	1.8	1.8	8.3	8.8
22	2	1	1.2	Nan	Nan	1.8	1.4	8.2	8.5
22	3	2.1	2.1	Nan	Nan	2.6	2.9	9.2	9.2

Table 19. Calculated time delay for healthy subject by transmission of polyphonic sound

Subject number	Trial number	Location of microphones							
		UFR	UFL	RL	LL	URB	ULB	LRB	LLB
1	1	0.7	0.3	3.5	Nan	0.3	0.3	12	Nan
1	2	Nan	0.7	3.4	3.0	0.4	Nan	12	Nan
2	1	2.1	2.1	5.2	4.1	2.5	3.5	Nan	Nan
2	2	2	2	4.8	3.7	2.3	Nan	Nan	Nan
3	1	1.6	1.5	4.6	4.4	1.8	1.5	7.6	7.1
3	2	1.4	1.3	4.2	4.2	1.3	1.7	7.2	7.8
4	1	2.8	2.1	5.4	4.8	3.1	Nan	Nan	10
4	2	3.2	2.5	5.7	5	3.2	2.4	Nan	Nan

5	1	1.5	1.4	11	8	1	1	Nan	8.3
5	2	1.2	1.2	11	Nan	0.8	1	Nan	8.5
6	1	1.9	1.7	Nan	Nan	1.8	1.9	15.6	14.8
6	2	1.7	1.7	Nan	Nan	1.7	1.6	Nan	13.1
7	1	1.9	1.8	3.5	2.1	2	2.1	Nan	8.7
7	2	1.7	1.7	Nan	Nan	1.8	1.8	Nan	7.7
8	1	3.8	3.8	5.7	6.5	3.5	3.4	Nan	Nan
8	2	3.1	3.5	6.3	7.5	3.5	3.6	Nan	4.3
9	1	1	0.9	Nan	7.2	0.9	0.8	7.1	7.5
9	2	1	1	7	Nan	0.9	0.8	Nan	Nan
10	1	2.5	1.7	12	Nan	2.1	2	Nan	14.0
10	2	2.4	1.7	11	4	1.9	2	Nan	14.0
11	1	1.9	1.7	Nan	Nan	1.7	1.4	13.9	13.8
11	2	2.2	1.4	4.8	Nan	1.6	1.6	Nan	14
12	1	3.2	Nan	2.3	4.3	3.6	3.2	6.8	Nan
12	2	3.2	3.1	3	4.4	2.8	2.5	7.1	4.6
13	1	2.3	2.1	2.7	2.6	2.8	2.8	Nan	Nan
13	2	2.4	2.2	4.8	3.3	3.2	3	4.2	3.3
14	1	0.6	0.7	6.9	6.5	0.6	0.6	Nan	6.7
14	2	0.7	0.6	Nan	Non	0.6	0.6	Nan	7.1
15	1	1.4	1.4	6.5	Nan	1	1	4	3.2
15	2	1	1	6.4	Nan	0.8	0.8	7.5	8
16	1	1.2	1.4	3.1	2	1.7	2.1	4	3
16	2	1.8	1.5	3.3	2.1	1.8	2	Non	2.8
17	1	1.1	1.4	3.2	2.0	6.8	6.3	7	7.5
17	2	1.6	1.4	3.5	3.2	1.8	2	Nan	Nan
18	1	Nan	Nan	Nan	6.0	2.9	2.5	10	6.9
18	2	Nan	Nan	Nan	Nan	2.2	2.2	9.8	Nan
19	1	1.9	2	3.2	3.9	2.3	2.3	Nan	Nan
19	2	1.8	1.8	3.2	3.5	2	1.8	Nan	Nan
20	1								
21	1	2.0	2.1	9.2	Non	1.8	1.7	9.3	8.9
21	2	1.8	1.7	6	Non	2.1	2.1	Non	9.1
22	1	2.1	2.3	2.1	3	2.5	Non	9.6	9.2
22	2	2	2.1	2.5	3.5	2.5	3.9	Non	Non

Appendix K. Ethics approval of research

Approval Notice

New Application

04-Jun-2012
Minai Zaeim, Hamed H

Ethics Reference #: S12/03/069

Title: **Evaluation of an active and passive acoustic methodology in diagnosis of pleural effusion**

Dear Mr. Hamed Minai Zaeim,

The **New Application** received on **08-Mar-2012**, was reviewed by members of **Health Research Ethics Committee 1** via Expedited review procedures on
01-Jun-2012 and was approved.

Please note the following information about your approved research protocol:

Protocol Approval Period: **01-Jun-2012 -01-Jun-2013**

Please remember to use your **protocol number** (**S12/03/069**) on any documents or correspondence with the REC concerning your research protocol.

Please note that the REC has the prerogative and authority to ask further questions, seek additional information, require further modifications, or monitor the conduct of your research and the consent process.

After Ethical Review:

Please note a template of the progress report is obtainable on www.sun.ac.za/rds and should be submitted to the Committee before the year has expired.
The Committee will then consider the continuation of the project for a further year (if necessary). Annually a number projects may be selected randomly for an external audit.

Translation of the consent document in the language applicable to the study participants should be submitted.
Federal Wide Assurance Number:
00001372 Institutional Review Board
(IRB) Number: IRB0005239

The Health Research Ethics Committee complies with the SA National Health Act No.61 2003 as it pertains to health research and the United States Code of Federal Regulations Title 45 Part 46. This committee abides by the ethical norms and principles for research, established by the Declaration of Helsinki, the South African Medical Research Council Guidelines as well as the Guidelines for Ethical Research: Principles Structures and Processes 2004 (Department of Health).

Provincial and City of Cape Town Approval

Please note that for research at a primary or secondary healthcare facility permission must still be obtained from the relevant authorities (Western Cape Department of Health and/or City Health) to conduct the research as stated in the protocol. Contact persons are Ms Claudette Abrahams at Western Cape Department of Health (healthres@pgwc.gov.za Tel: +27 21 483 9907) and Dr Helene Visser at City Health (Helene.Visser@capetown.gov.za Tel: +27 21 400 3981). Research that will be conducted at any tertiary academic institution requires approval from the relevant hospital manager. Ethics approval is required BEFORE approval can be obtained from these health authorities.
We wish you the best as you conduct your research.
For standard REC forms and documents please visit: www.sun.ac.za/rds

If you have any questions or need further help, please contact the REC office at 0219389657.